Characterization of New RSV-F-Mutants Using BAC Technology Reflecting Their Impact on Viral Growth and Palivizumab Susceptibility

Dissertation

der Mathematisch-Naturwissenschaftlichen Fakultät

der Eberhard Karls Universität Tübingen

zur Erlangung des Grades eines

Doktors der Naturwissenschaften

(Dr. rer. nat.)

vorgelegt von

Huu Kim Trinh Weitbrecht

aus Ho Chi Minh Stadt/Vietnam

Tübingen

2018

Gedruckt mit Genehmigung der Mathematisch-Naturwissenschaftlichen Fakultät der Eberhard Karls Universität Tübingen.

Tag der mündlichen Qualifikation:	22.02.2019
Dekan:	Prof. Dr. Wolfgang Rosenstiel
1. Berichterstatter:	Prof. Dr. Gerhard Jahn
2. Berichterstatter:	Prof. Dr. Hans-Georg Rammensee

Acknowledgments

*"I know you are there and I am happy"*_ Thich Nhat Hanh_

First of all, I would like to express my sincere appreciation to Prof. Dr. med. Gerhard Jahn and Prof. Dr. med. Dr. rer. nat. Klaus Hamprecht for providing me the opportunity to start and finish my doctoral studies. I am grateful for their teaching and workshops that aroused my interest in the whole field of virology. I cherish the chance they have given me to attend national and international congresses. A special thanks also goes to Prof. Dr. rer. nat. Georg Rammensee for reading this thesis and preparing the second assessment, as well as for the fast and simple communication that allowed me to complete my work even when I was abroad.

My sincere thanks goes to my supervisor Dr. Katharina Göhring for putting faith in me and for her teaching that brought me to the world of virology. I appreciate her sincerity, patience for explaining me all of my questions as well as for her generosity taking her free time correcting my written works. Without help from her precious support it would not be possible for me to finish this thesis. I am also grateful to Dr. rer.nat. Kevin Dennehy for helping me with the FACS facility, for supporting me with all the buffers/solutions I needed for flow cytometry, and for his suggestions to improve this thesis.

I thank my labmates and colleges for the stimulating discussions, for the helps and joint activities which made my Ph.D. become a memorable and beautiful time. In particular, I thank Anna and Katrin for the ladies nights that light up my working days, and my table-mate, Dr. Juliane Hädicke-Jarboui, for the coffee breaks and for the pleasure time sharing the office with her. My thanks also goes to the colleges in the Diagnostic Department for supporting me with viral isolates, material for cell cultures, and PCR as my storage was blank. I am grateful for all the unconditional help, the time and the talks that we had.

Last but not the least, I would like to thank my parents and my friends for their presence on my site and for supporting me spiritually throughout my life.

Abbreviations

BAC	Bacterial artificial chromosome
BAL	Broncho alveolar lavage
BHK	Baby hamster kidney
BRSV	Bovine respiratory syncytial virus
bp	Base pairs
CMV	Cytomegalovirus
Cp	Crossing point
CPE	Cytopathic effect
CT	Cytoplasmic tail
DMEM	Dulbecco's modified eagle medium
DMSO	Dimethylsulfoxid
dNTP	Deoxynucleoside triphosphate
ds	Double stranded
EIA	Enzyme immunoassay
HRA, HRB, HRC	Heptad-repeat sequence A, B, C
HFF	Human foreskin fibroblasts
IC_{50}	Inhibitory concentration 50
IC	Immunochromatography
FACS	Fluorescence-activated cell sorting
FDA	Fluorescein diacetate
FCS	Fetal calf serum
FFU	Fluorescence-forming unit
g	Gravitational acceleration (9,81m/s^2)

GE	Gene end
GMEM	Glasgow minimum essential medium
GS	Gene start
HPLC	High performance liquid chromatography
hpi	Hour post infection
kbp	Kilobase pairs
LB	Luria broth
LRTI	Lower respiratory tract infection
M	Mol
MCC	Microcrystalline cellulose
MEM	Minimal essential medium
MOI	Multiplicity of infection
NaCMC	Sodium carboxymethylcellulose
nm	Nanometer
nt	Nucleotide
PCR	Polymerase chain reaction
PFA	Paraformaldehyde
PRNA	Plaque-reduction neutralization assay
rcf	Relative centrifugal force
RSV	Respiratory syncytial virus
SOC	Super optimal broth with catabolic repressor
SP	Signal peptide
TBE	Tris-borate-EDTA
$TCID_{50}$	Tissue culture infective dose 50
TM	Transmembrane domain
TPB	Tryptose phosphate broth

URTI	Upper respiratory tract infection
VE	german: “Vollentsalztes”, english “fully demineralized”
VLBW	Very low birth weight

Contents

1. Introduction 1

1.1 Background 1

1.2 Respiratory syncytial virus (RSV) 2

1.2.1 The virion 2

1.2.2 Viral genome 3

1.2.3 Viral surface glycoproteins 4

1.2.3.1 The attachment (G) protein 4

1.2.3.2 The small hydrophobic (SH) protein 5

1.2.3.3 The fusion (F) glycoprotein 6

1.2.4 Neutralizing epitopes on the RSV fusion glycoprotein 9

1.2.5 Viral replication cycle 11

1.3 Pathogenesis and disease burden 13

1.3.1. Viral tropism 13

1.3.2 The infant and the elderly as main target 14

1.3.3 RSV pathology and its long-term sequel 15

1.4 Therapy and antiviral drugs 18

1.4.1 Therapy options 18

1.4.2 Vaccines and small molecule antiviral drugs under development 18

1.4.3 Passive immunization with palivizumab 20

1.4.4 Palivizumab cost-benefit relation 22

1.4.5 Detection of palivizumab resistance-associated mutation 23

1.5 Marker transfer analysis 24

2. Aim of the study 26

3. Material and Methods 28

3.1 Material 28

3.1.1 Patients 28

3.1.2 Cells 30

3.1.3 BAC and plasmid 30

3.1.4 Viruses 31

3.1.5 Bacteria 31

3.1.7 Reagents for cell culture 32

3.1.8 Reagents for bacterial culture 33

3.1.9 Reagents for PCR and sequencing 34

3.1.10 Primers for mutagenesis and sequencing 35

3.1.11 Reagents for gel electrophoresis 39

3.1.12 Reagents for transfection 40

3.1.13 Reagents for immunofluorescence and flow cytometry 40

3.1.14 Consumables 41

3.1.15 Kits 42

3.1.16 Small appliances 43

3.1.17 Large equipment 43

3.2 Methods 44

3.2.1 Cell culture 44

3.2.2 Generation of recombinant RSV mutants using en passant mutagenesis 44

3.2.2.1 Generation of PCR-products with defined point-mutations 45

3.2.2.2 Gel electrophoresis 47

3.2.2.3 Purification of PCR-products and DpnI digestion 48

3.2.2.4 Generation of electrocompetent *E.coli* GS1783 for transformation and BAC-mutagenesis 49

3.2.2.5 Removal of the positive selection marker 52

3.2.2.6 Extraction of BAC-DNA by mini-preparation 54

3.2.2.7 Control of successful mutagenesis by sequencing 55

3.2.2.8 Midi-preparation for transfection 55

3.2.2.9 Transfection of the BAC-DNA into BSR T7/5 cells and virus growth..... 56

3.2.3 Phenotypic characterization of recombinant RSV mutants 58

3.2.3.1 Determination of virus titer as fluorescence-forming units/ml (FFU/ml) ... 58

3.2.3.2 Determination of virus titer as $TCID_{50}$ by end-point dilution assay 59

3.2.3.3 Characterization of viral growth by multi-step growth curves..... 60

3.2.3.5 Characterization of viral growth by flow cytometry 61

3.2.3.4 Phenotypic characterization of recombinant RSV by PRNA 65

4 Results 69

4.1 Generation of recombinant RSV with defined mutations 69

4.1.1 Generation of PCR-products with defined point-mutations 69

4.1.2 BAC-mutagenesis and sequencing of the respective regions on the fusion (F) gene 71

4.1.2.1 Generation of *E.coli* GS1783/pSynkRSV-l19F 71

4.1.2.2 BAC-mutagenesis of pSynkRSV-l19F with defined point mutation 71

4.1.3 Transfection of RSV BAC DNA into BSR T7/5 and recovery of recombinant RSV 75

4.2 Phenotypic characterization 76

4.2.1 Characterization of viral growth by multi-step growth curves 76

4.2.3 Characterization of viral growth by flow cytometry 81

4.2.2 Characterization of palivizumab susceptibility by plaque-reduction neutralization assays (PRNA)..... 86

4.2.2.1 IC_{50} values (µg/ml) determined by PRNA 86

4.2.2.2 Test of a new overlay with colloidal microcrystalline cellulose (MCC)..... 91

5 Discussion 93

5.1 Generation of mutated RSV by en passant mutagenesis 93

5.2 Phenotypic characterization 96

5.2.1 Characterization of viral growth by multi-step growth curves..... 96

5.2.1.1 Multi-step growth curves of RSV strain A2 and recombinant strain RSV A2-K-line19F 97

5.2.1.2 Multi-step growth curves of recombinant strains harboring mutations..... 98

5.2.2 Phenotypic characterization of viral growth by flow cytometry 99

5.2.3 Comparison between growth curves determining with end-point dilution assays and flow cytometry..... 101

5.2.4 Palivizumab susceptibility by plaque-reduction neutralization assays (PRNA) . 103

6. Summary 107

7. Zusammenfassung 109

8. References..... 111

1. Introduction

1.1 Background

In 1956, respiratory syncytial virus (RSV) was recovered from “normal” chimpanzees during an outbreak of coryza (acute upper respiratory illness characterized by coughing, sneezing and mucopurulent nasal discharge) at the Walter Reed Army Institute of Research in Washington, D.C., and it was termed as chimpanzee coryza agent (Morris et al. 1956, Ellis 2013). In 1957, this agent was linked with a virus that was isolated from infants with respiratory illness in Johns Hopkins University Hospital in Baltimore, Maryland (Chanock and Finberg 1957, Chanock et al. 1957). Chanock et al. described the property of this virus to form syncytia in infected cell culture and thus the virus was renamed as respiratory syncytial virus (Chanock et al. 1962). A short time later, a formalin-inactivated (FI) RS vaccine was tested. Unfortunately, it not only failed to protect vaccinated infants and children against natural RSV infection, but also caused vaccine enhanced disease (Kapikian et al. 1969, Kim et al. 1969). In the clinical trial with infants, 80% (16/20) of the vaccinees required hospitalization and two of them died after getting naturally infected with RSV (Kim et al. 1969). After this notable vaccine failure in the 1960s, there is no licensed vaccine for RSV until now. In 1998, a RSV-neutralizing antibody, palivizumab (Synagis®) that targets the fusion protein F on the surface of the RSV virions, was approved for passive immunization in high-risk children (Romero 2003). Monthly administrations of palivizumab (15mg/kg) were shown to be able to reduce RSV associated hospitalizations by 55% (The IMpact-RSV Study Group 1998). However, this RSV immunoprophylaxis therapy is too expensive and inconvenient for broader applications especially for low-income countries (Collins and Murphy 2007). As a result, palivizumab recommendations respecting cost-benefit are still under debate (Geskey et al. 2007, Olchanski et al. 2018). In addition, a range of resistance-associated mutations have already been identified and reported in several studies (Boivin et al. 2008, Bates et al. 2014). To date, RSV remains globally a serious pathogen that causes high mortality in children under 5 years with up to 118 000 deaths/year (2015) (Shi et al. 2017).

1.2 Respiratory syncytial virus (RSV)

The human respiratory syncytial virus (HRSV) was formerly a member of the subfamily *Pneumovirinae* within the family *Paramyxoviridae*. In 2016, this subfamily was then reclassified as the family *Pneumoviridea* with two genera, *Metapneumovirus* and *Orthopneumovirus* to which HRSV now belongs (Rima et al. 2017). Other viruses in this genus are: bovine orthopneumovirus (BRSV) and murine pneumovirus (MPV).

1.2.1 The virion

Observing under electron microscopy, RS virions are heterogeneous in size and shape (Melero 2007). When produced in Vero cells, RSV particles consist of predominantly filamentous forms with lengths of up to 10µm, and round or kidney-shaped particles of 150-250 nm in diameter (Bachi and Howe 1973). In cell culture, 95% of the progeny virus couldn't bud fully and remains associated with the cell surface. Hence, while preparation of virus stocks, infected cells are typically subjected to freeze-thawing to release attached viruses (Collins et al. 2013).

RSV particles are surrounded by a lipid bilayer, on which 3 structural proteins are presented: the attachment (G), the fusion (F) and the small hydrophobic (SH) glycoproteins (Figure 1). The matrix (M) protein interacts on one hand with the envelope glycoproteins and on the other hand with the nucleocapsid (Ghildyal et al. 2006). The virus nucleocapsid is found inside the virion and consists of the negative-sense viral RNA, the nucleoprotein (N), the RNA-dependent RNA polymerase (L), the phosphoprotein (P) and the transcription elongation factor M2-1 (Melero 2007, Collins et al. 2013). There are 2 regulatory M2 proteins: M2-1, an antitermination protein and M2-2, a transcription/replication regulatory protein, both are encoded on the M2 gene (Griffiths et al. 2017). RSV encodes further 2 non-structural proteins, NS-1 and NS-2, which are involved in evasion of the innate immune response (Griffiths et al. 2017).

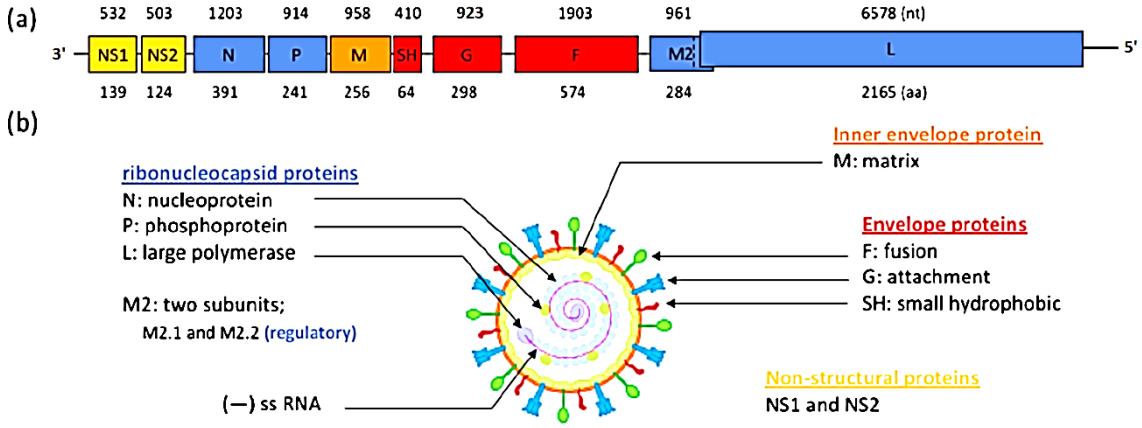

Figure 1: Human Respiratory Syncytial Virus genome and proteins. (a) Map of negative-sense RNA genome of strain RSV A2 with respective lengths of genes given as nucleotides (nt, upper row) and lengths of the primary, unmodified proteins given as amino acids (aa, lower row). (b) Illustration of RS virion and its proteins (modified from Taleb et al. 2018).

1.2.2 Viral genome

RSV is an enveloped virus with non-segmented negative sense RNA that is made-up of approx. 15,200 nucleotides and encodes 11 proteins: 2 non-structural and 9 structural proteins (Taleb et al. 2018) (Figure 1). The genome has 10 genes arranged in the order 3'-NS1-NS2-N-P-M-SH-G-F-M2-L. Each gene encodes a corresponding mRNA and each mRNA a single major protein except for M2, which encodes for both the M2-1 and M2-2 (Collins et al. 2013).

The 3' end of the genome represents the extragenic leader region that consists of 44 nt and the 5' end the extragenic trailer region with 155-nt. The first 24-26 nt of the leader and trailer region are by 88% complementary (antiparallel), representing conserved promoter elements (Collins et al. 2013). Each gene begins with a highly conserved 9-nt gene-start (GS) and is terminated by a moderately conserved 12-14-nt gene-end (GE). From NS1 to M2, genes are separated by intergenic regions which differ in length. The GS sequence of L is located upstream the GE sequence of M2, thus between M2 and L there is no intergenic region (Collins et al. 2013). It is reported that recombinant RSV could tolerate intergenic region of up to 160 nt in length with minimal influence on gene expression and viral replication (Bukreyev et al. 2000).

RSV is classified in two subtypes, RSV A and B, which can co-circulate during annual RSV season and cause different disease severity (Vandini et al. 2017). Classification of these subtypes was previously based on antigenic reactivity to monoclonal antibodies (Anderson et al. 1985). Lately, the greatest inter-subgroup diversity was shown to be associated with variations in the attachment (G) glycoprotein with only 53% homology between subtypes A and B (Johnson et al. 1987). Thus nowadays, based on phylogenic analysis of the hypervariable region of the G protein, viral strains within each subgroup could be divided furthermore into clades, which were named from GA1 to GA5 for subtype A, and GB1 to GB4 for subtype B (Peret et al. 1998). Novel RSV genotype emerging expands the list of existing clades for both subgroups A and B (Eshaghi et al. 2012, Schobel et al. 2016). Most recently, it is suspected that RSV serotype and genotype variability might have an influence on the clinical course of infection regarding pathogenesis, disease severity and host immune response (Melero and Moore 2013, Vandini et al. 2017, Pangesti et al. 2018).

1.2.3 Viral surface glycoproteins

Since this work addresses newly identified mutations on the F gene, one of the three genes encoding the RSV viral surface glycoproteins. Thus, these proteins and their potential functions relating to RSV infection will be briefly described in this section.

Among the structural proteins, 3 are present on the surface of the virus: the attachment (G) protein, the fusion (F) protein and the small hydrophobic (SH) protein, whereby F and G are the only two proteins that can elicit neutralizing antibodies (Sastre et al. 2005). In contrast, SH is poorly immunogenic and did not elicit a significant neutralizing antibody response for protection upon natural infection (Connors et al. 1991). Surprisingly, unlike F, RSV SH and G proteins were shown to be not essential for viral replication in vitro (Karron et al. 1997). As shown, recombinant virus that has F as it only surface glycoprotein can still infect cells in culture (Techaarpornkul et al. 2001, Techaarpornkul et al. 2002).

1.2.3.1 The attachment (G) protein

G is a large glycoprotein that is made of 289-299 amino acid (aa) depending on strains and is vastly glycosylated (Collins and Mottet 1992, McLellan et al. 2013). G is a type

II transmembrane protein that has a membrane anchor near to its N-terminus and an extracellular C-terminus (Collins et al. 2013). The extracellular extending ectodomain of G consist two large highly variable mucin-like domains flanking a central region that comprises of a highly conserved domain, a cysteine nose domain and a highly basic heparin-binding domain (McLellan et al. 2013). Several studies demonstrate that interactions between the viral surface proteins G and F with cell surface heparan sulfate proteoglycans (HSPGs) elicit attachment and binding of RSV to the cell membrane, and that peptides that bind HSPG could inhibit RSV infection (Hallak et al. 2000, Hallak et al. 2007, Donalisio et al. 2012). Furthermore, binding of G to the fractalkine (Fkn) receptor (CX3CR1) could facilitate RSV infection of cells and alter Fkn-mediated immune response associated with cell trafficking and cytokine and chemokine expression (Tripp et al. 2001). In addition, G is also produced as a secreted form that has been shown to interfere with antibody-mediated neutralization by acting as an antigen decoy for neutralizing antibody and thus helps RSV evade neutralization (Bukreyev et al. 2008). Several studies report about the immune modulation ability of G including mimicking the receptor for tumor necrosis factor alpha (TNF-α), interaction with DC-SIGN on human dendritic cells (DC) and inhibiting the production of inflammatory cytokines (Langedijk et al. 1998, Polack et al. 2005, Johnson et al. 2012).

1.2.3.2 The small hydrophobic (SH) protein

The small hydrophobic (SH) protein is 64-65 aa (depending on strains) transmembrane protein with an intracellular N-terminus and an extracellular C-terminus (Collins and Mottet 1993, McLellan et al. 2013). It exists several isoforms of SH but theirs significance is unclear (McLellan et al. 2013). Bukreyev reported that recombinant RSV that lacks SH gene could grow efficiently in vitro but attenuated in mice (Bukreyev et al. 1997). Several studies pointed to the function of SH as pentameric ion channels that probably act as viroporin and enhance membrane permeability in the host (Carter et al. 2010, Gan et al. 2012). Furthermore, SH was also reported to inhibit TNF-α signaling and prevent infected cells from undergoing apoptosis (Fuentes et al. 2007).

1.2.3.3 The fusion (F) glycoprotein

The fusion glycoprotein F is an important target for neutralizing antibodies and is highly conserved with only 25 aa differences in the F ectodomain of the two subgroups A and B (Graham et al. 2015) . RSV F protein belongs to the class I fusion protein. Three inactive precursors F_0, each consists of 574 aa, assemble into a trimer. As passing through the Golgi apparat during the protein secretion pathway, the monomers are activated by furin-like host protease resulting in the F2, F1 subunits and a 27 aa peptide, of which the function is still unknown (Collins et al. 1984, Collins and Mottet 1991, Bolt et al. 2000). These two subunits F2 and F1 are covalently linked by two disulfide bonds between aa70 and aa212, and between aa37 and aa439 (Graham et al. 2015) (Figure 2). There are two N-linked glycans on F2 at aa27 and aa70, and only one on F1 at aa500, which unlike others is required for an efficient syncytium formation (Zimmer et al. 2001).

The functional F protein is present on the virion surface in two forms, a metastable pre-fusion and a stable post-fusion conformation (Liljeroos et al. 2013, McLellan et al. 2013). F Protein must remain in the metastable pre-fusion form to enable appropriate refolding into the stable post-fusion form during the membrane fusion process (Hicks et al. 2018). It has been shown that this conformational change from the pre- to post-fusion state is triggered by low-molarity buffer (e.g. 10 mM HEPES), heat and freeze-thaw cycles (Gupta et al. 1996, Yunus et al. 2010, Chaiwatpongsakorn et al. 2011). Binding F in the pre-fusion conformation can interact with the refolding process and thus disrupt the membrane fusion and prevent virus entry (Rossey et al. 2018).

McLellan's group was the first group that was able to reveal the post-fusion structure of F by X-ray crystallography (McLellan et al. 2011, Swanson et al. 2011). The structure reveals that F2 and F1 subunits are deeply intertwined and all previously identified antigenic sites are present on the post-fusion conformation (McLellan 2015). Due to the energetically unstable property, the pre-F conformation is more difficult for structure determining. Fortunately, McLellan's group again was able to reveal the X-ray structured of the pre-fusion conformation by prior stabilizing this metastable state with a pre-fusion specific antibody (McLellan et al. 2013). These structures disclosed that appx. 300 aa in the ectodomain are in similar positions in both pre- and post-fusion

conformation and the most dramatic rearrangements are located in the N- and the C-terminus of the F1 subunit (McLellan 2015).

In contrast to the F1 subunit that bears multiple antigenic site and thus is intensively investigated, the F2 subunit remains mostly uncharacterized but it has gained more and more attention from researchers in the last several years. This subunit is believed to determine the species specificity of RSV infection, as it is shown that virus containing the F1 and G from BRSV with only F2 from HRSV could infected human cells and vice versa (Schlender et al. 2003). Lawlor reported in 2013 about a single mutation at amino acid 66 within the F2 subunit, that was identified in a live attenuated vaccine strains, could alter virus growth and cell fusiogenicity in vitro (Lawlor et al. 2013). Recently, a comprehensive mutagenesis-based study of the heptad repeat C domain (aa 75-97) within F2 subunit revealed that this region plays an important role in membrane fusion by affecting the stability of the pre-fusion form (Bermingham et al. 2018). Newly, five residues in the apical loop (residues 62-75) of the F2 subunit were reported to be critical for the fusion activity (Hicks et al. 2018).

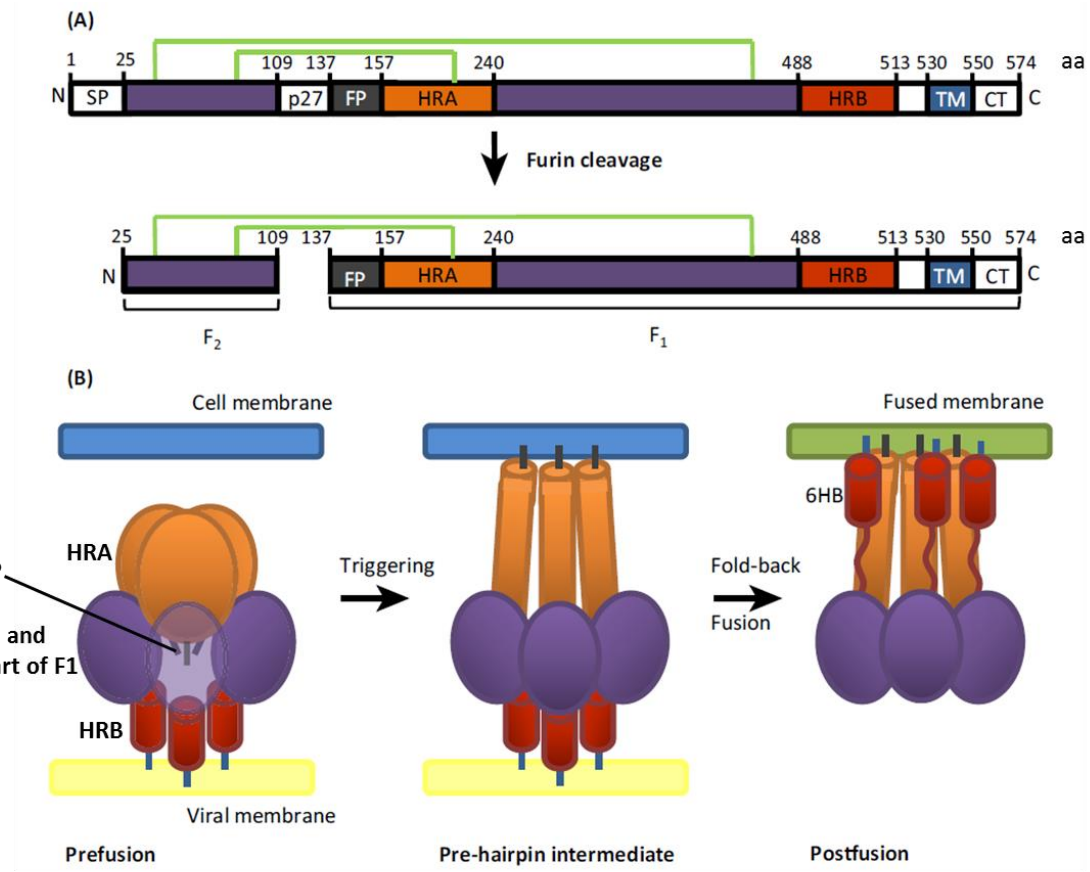

Figure 2: The fusion protein of RSV. (A) Primary structure of RSV F, before (upper) and after (lower) furin cleavage. The precursor F0 consists of following domains in the order: SP (signal peptide); F2 subunit; p27 (peptide 27); FP (fusion peptide); HRA (heptad repeat A); an unnamed region containing several antigenic sites (complete or partial); HRB (heptad repeat B); TM (transmembrane domain); CT (cytoplasmic tail). The precursor is activated after furin cleavage at position 109 and 137 resulting in subunit F2 at N-terminus, F1 subunit at C-terminus as well as the separated peptide 27. These two subunits are linked by two disulfide bonds between aa70 and aa212, and between aa37 and aa439. (B) Illustration of the membrane fusion process and the conformational rearrangement of F protein from its pre- to post-fusion constitution. In the pre-fusion form, the fusion peptides (dark grey sticks) are buried in the middle of the homotrimer protein. After triggering, refolding of HRA results in insertion of the fusion peptides into the host membrane. This constitution is called pre-hairpin intermediate. In the next refolding step, HRA and HRB are combined to form a stable 6-helix bundle (6HB) resulting in membrane fusion. The in purple indicated central region (F2 and part of F1) of F remains mostly unchanged during the refolding process. Adopted and modified from Rossey et al. 2018.

1.2.4 Neutralizing epitopes on the RSV fusion glycoprotein

Several antigenic sites on pre- and post-F conformation were identified and characterized in the last three decades along with their significance on antibody responses and virus neutralizing activity. Of those, site Ø to V are depicted in Figure 3. Site I is a post-fusion specific epitope and antibodies that bind to this site have marginal effect in virus neutralization (Lopez et al. 1998, Widjaja et al. 2015). Antigenic site II (aa 254-277) and IV (aa 422-471) are major neutralizing epitopes that present on both pre- and post-fusion conformations of RSV F (McLellan 2015). Neutralizing antibodies that target these sites could neutralize infection and inhibit cell-cell fusion but do not inhibit virus attachment (Magro et al. 2010). However, it was shown that neutralizing antibodies that specifically target pre-fusion epitopes account the majority of neutralizing activity compared to those that target post-fusion epitopes (Magro et al. 2012). Pre-fusion specific antibodies bind to regions at the N-terminus or C-terminus of the F1 subunit, that undergo dramatic conformational change at the fusion event (McLellan 2015). First pre-fusion specific antibodies were described by the Beaumont's group in 2010 and their binding epitope was disclosed by McLellan and named as site Ø (zero) (Kwakkenbos et al. 2010, McLellan et al. 2013). The antigenic site Ø comprises an unstructured region in F2 and a region within the HRA in F1(McLellan 2015). Several pre-fusion specific antibodies that recognized multiple antigenic sites were identified (Flynn et al. 2016). For example, the human monoclonal antibody MPE8 binds primarily to site III and parts of site II, IV and V; another human monoclonal antibody hRSV90 binds to sites II, V and Ø; or AM14 that was isolates from pool of immortalized human B cell interacts with site IV and V (Gilman et al. 2015, Rossey et al. 2018). More recently, further antigenic sites VI, VII and VIII were identified and described (Lopez et al. 1998, Wu et al. 2007, Mousa et al. 2016, Mousa et al. 2017).

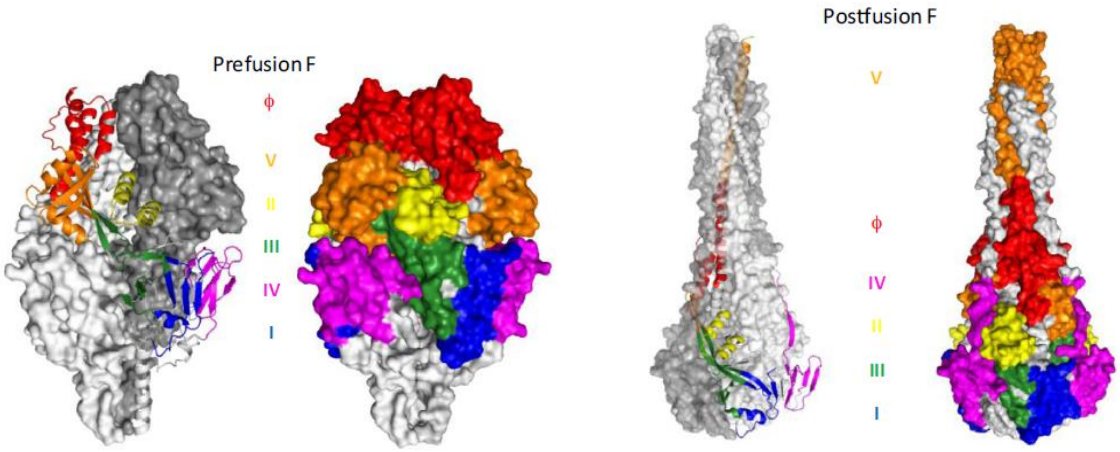

Figure 3: Structure of pre-fusion (left) and post-fusion F (right). In each conformation, one protomer is depicted as ribbon and colored by sites. Shown are 6 antigenic sites Ø (red), I (blue), II (yellow), III (green), IV (magenta), V (orange) on the homotrimer (Rossey et al. 2018).

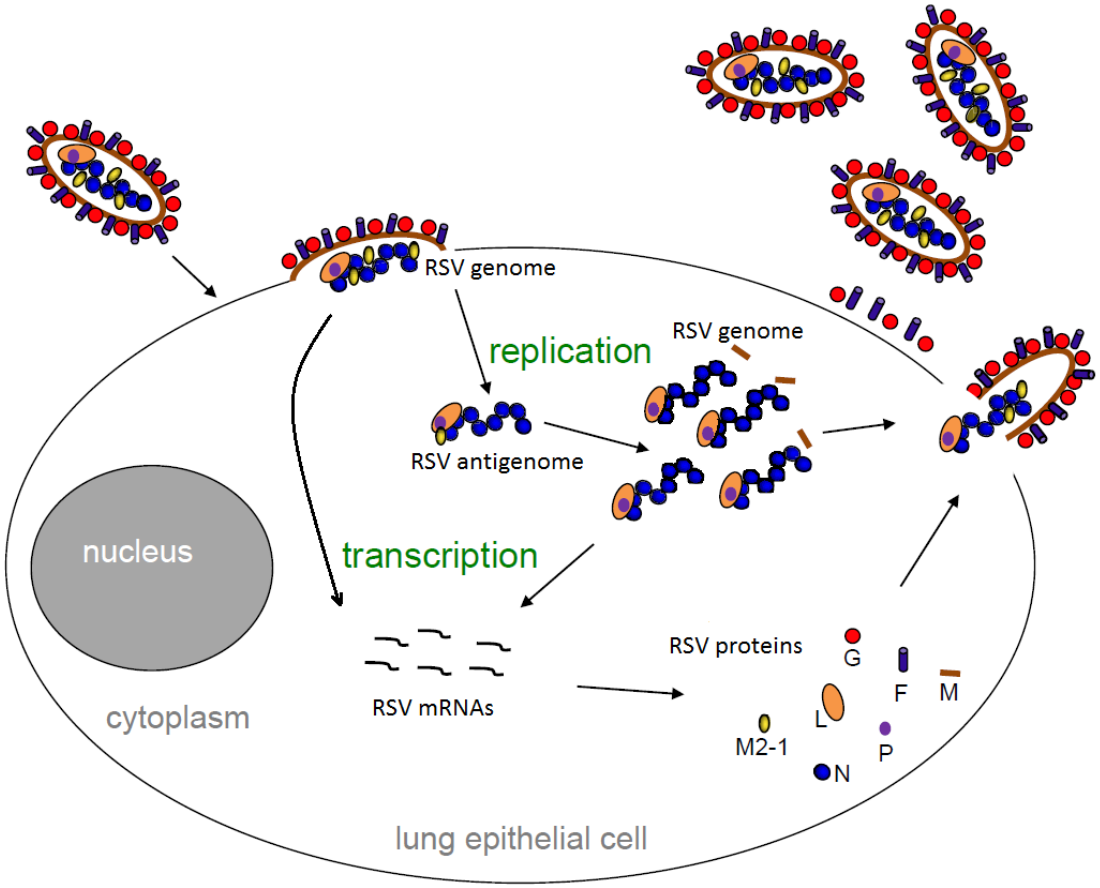

Figure 4: RSV replication cycle in the cytoplasm. Transcription and replication of the viral genome take place in the cytoplasm and are conducted by the viral RNA polymerase L. Translation of viral mRNA is carried out by cellular ribosome. Upon translation, viral proteins are transport towards the apical plasma membrane, where RSV assembly and budding occur. Adopted and modified from Fearns and Deval 2016.

1.2.5 Viral replication cycle

The infection cycle is starting with attachment and binding of the virus to the host membrane, that are mediated by the RSV attachment G and fusion F protein (Collins et al. 2013). For the attachment and binding event, several cell receptor candidates have been described as potential targets for G including heparin sulfate proteoglycans (HSPG) (Hallak et al. 2000, Donalisio et al. 2012), CX3 chemokine receptor 1 (CX3CR1) (Tripp et al. 2001), annexin II (Malhotra et al. 2003). More recently, nucleolin and toll-like receptor 4 (TLR4) have been reported as a cellular receptor for F (Tayyari et al. 2011, Marr and Turvey 2012). After the attachment event, conformational rearrangement from the pre- into the post-fusion state of F is triggered, which leads to insertion of the fusion peptide into the host membrane. This state is called pre-hairpin intermediate (Rossey et al. 2018) (Figure 2). As the viral and host membrane are fused, the viral nucleocapsid is released into the cell cytoplasm and transcription of the viral genome is activated. The viral nucleocapsid consists of the viral RNA and the nucleoprotein N to form a left-handed helical structure (Bakker et al. 2013), that further associates with the RNA-dependent RNA polymerase complex formed by the polymerase (L), the phosphoprotein (P) and the transcription factor M2-1 (Fearns and Deval 2016). Transcription of the negative-sense RNA into to mRNA as well as into a positive-sense RNA takes place in the cytoplasm and is conducted by the viral RNA polymerase L (Collins and Melero 2011). The full length anti-genome RNA acts as a template for further genome synthesis. Both newly synthetized genome and anti-genome become encapsidated and have been detected in virions (Collins et al. 2013, Fearns and Deval 2016). A set of mRNA is generated in a polar gradient with the most abundant mRNAs for the NS1 and NS2 and the lowest for the L protein. This occurs because some of the transcribing polymerase dissociate irreversibly from the genome at various gene junctions while others remain template bound and continue transcribing at the next GS signal (Fearns et al. 2002, Collins et al. 2013). Most recently, RNA synthesis is suggested to take place in so called inclusion bodies (IBs), that appear around the same time as the protein synthesis begins (6 hpi) (Lifland et al. 2012, Collins et al. 2013). All components required for the viral RNA polymerase complex (genomic RSV-RNA, -N, -M2-1, -L and -P protein) are co-localized in IBs, whereby newly synthesized viral mRNA and the viral transcription anti-terminator M2-1 were found in a sub-compartment, termed “IB-associated granules” (Garcia et al.

1993, Lifland et al. 2012, Rincheval et al. 2017). The balance between RNA transcription and replication seems to be regulated by the M2-2 protein (Bermingham and Collins 1999, Cheng et al. 2005). Translation of viral mRNA is carried out by cellular ribosome as it would translate host mRNA (Griffiths et al. 2017). Upon translation, viral protein trafficking and RSV assembly and budding occur in a poorly understood manner at the apical plasma membrane (Roberts et al. 1995, Zhang et al. 2002). In absence of the viral matrix (M) protein, viral filaments do not form and M is found to be co-localized with IBs, thus M was suggested to be important for trafficking of nucleocapsids from IBs to the cell surface (Ghildyal et al. 2002, Mitra et al. 2012, Shaikh and Crowe 2013). Most recently, the viral matrix (M) protein was shown to interact with a host protein, the cellular adaptor protein complex 3, which is also assumed as a critical interaction for trafficking (Ghildyal et al. 2006, Ward et al. 2017).

1.3 Pathogenesis and disease burden

1.3.1. Viral tropism

HRSV, BRSV and MPV infect human, bovine and murine in a species-specific manner (Rima et al. 2017, ICTV 2018). This makes development of a suitable animal model for HRSV to a challenge. Different animal models have been investigated to study the pathogenesis and immune responses to RSV infections (Sudo et al. 1999, Openshaw 2013). Nevertheless, all reported animal models of human RSV are semi-permissive except for chimpanzee that develops upper respiratory infection most nearly an RSV infection in human (Prince et al. 1979, Collins et al. 2013). In older BALB/c mice, higher titer and larger volume inoculum are required for development of clinical manifestations of illness such as ruffled fur, reduced activity, weight loss, and infiltration of immune cells into the lung (Graham et al. 1988). Recently, a chimeric strain RSV A2-line19F was shown to recapitulate in mice key features of RSV pathogenesis with higher viral load, interleukin-13 (IL-13) induction, greater mucus induction and airway dysfunction (Moore et al. 2009, Hotard et al. 2012). In this chimeric strain, sequence for the fusion F protein originates form RSV Line 19, while other proteins from RSV A2. Both RSV A2 and Line 19 are human strains. Moore and his group developed subsequently a RSV recovery system based on a bacterial artificial chromosome (BAC) that encodes the anti-genomic DNA of this chimeric strain RSV A2-line19F and an additional fluorescence reporter gene mKate2, called RSV-BAC pSynkRSV-line19F. This is the first BAC-based reverse genetic system that stably enables mutagenesis and efficient recovery of recombinant RSV. This BAC plays an important role in this work to establish marker transfer analysis for newly detected mutations in the fusion (F) gene of RSV.

In vivo, RSV replication is mainly limited in the apical ciliated epithelial cells and basal epithelial cells are spared from RSV infection (Roberts et al. 1995, Zhang et al. 2002, Collins et al. 2013). RSV antigens have also been detected in macrophages and circulating mononuclear leukocytes, but all of this evidence is thought not to be associated with replication or an extrapulmonary infection (Domurat et al. 1985, Franke et al. 1994, Collins et al. 2013). In context with severe RSV infection, a few studies reported systemic dissemination of RSV to the heart, liver and cerebral fluid which may associate with sudden infant death in some cases (Eisenhut 2006). Paradoxically, in

vitro, RSV could infect a wide variety of cell types derived from different tissues including Vero, HEp-2, HeLa, BHK-21, HFF etc. but with different efficiency.

All these observations lead to the suggestion that there are factor that determine the tropism of the virus such as presence of receptors for viral attachment and entry, host structures that may be exploited by the virus for its replication, host dependent ability to counter antiviral response or other innate and immune defence mechanism (Collins et al. 2013).

1.3.2 The infant and the elderly as main target

In healthy patients, RSV infection are mild, self-limited and are treated in outpatient settings (Wright and Piedimonte 2011). Generally, RSV infects all age groups but patients at the age extremity are at higher risk for developing a severe RSV infection (Falsey et al. 2005, van Drunen Littel-van den Hurk and Watkiss 2012). Infants who at high-risk for severe RSV infection are those under 6 months of age, premature born, or those with bronchopulmonary dysplasia, congenital heart disease, immunodeficiency, cystic fibrosis and neuromuscular disease (Resch 2012). For this high-risk population, the mortality rates associated with RSV infection increase significantly from below 1% for the healthy children up to 37% depending on study reports and comorbidity (Welliver et al. 2010). This review summarized 36 studies and reported case fatality rates of 3.5%-23% for infants with chronic lung disease, 2-37% for infants with congenital heart disease and 0-6.1% for premature infants. A global observation in 2005 estimated that children in developing countries are at higher risk for acute lower respiratory infection (ALRI) with >93% of all RSV-ALRI episodes and 99% of RSV-ALRI mortality (Nair et al. 2010). More recently for 2015, 33.1 million episodes of RSV-ALRI with about 3.2 million hospital admissions were estimated in children younger than 5 years, of which the overall mortality could be as high as 118200 cases (Shi et al. 2017).

Even in adults with high-risk cardiopulmonary diseases, the elderly and immunocompromised individuals, the impact of RSV are comparable to that of non-pandemic influenza (Haber 2018). Since 1980s, the significance of RSV on morbidity and mortality for those over 65 years old has been recognized through several observed outbreaks (Morales et al. 1983, Sorvillo et al. 1984, Agius et al. 1990, Han et al. 1999).

More recent studies describe the clinical importance of RSV in older adults and emphasized the increasing global burden of RSV in developed nations with aging populations (Falsey et al. 2014, Branche and Falsey 2015). A study from Korea compared the risk of mortality associated with RSV and influenza infection in adults reported that adult patients were less likely diagnosed with RSV compared to influenza, but RSV infection showed significant higher risk of death compared to the seasonal influenza with a hazard ratio of 2.32 (RSV vs. influenza) (Kwon et al. 2017). Comorbidities such as COPD, hematological diseases and immunodeficiency are also a risk factor for RSV associated hospital stay and intensive care for adults (Khanna et al. 2008, Mehta et al. 2013). As well as for the younger target of RSV, there is also a need for development of RSV prophylaxis, vaccine and treatment for adults (Volling et al. 2014).

1.3.3 RSV pathology and its long-term sequel

RSV is transmitted from person to person via droplet. After an incubation period from 2-8 days, the virus spreads rapidly in the respiratory tract, where it preferably targets the apical ciliated epithelial cells. Binding and fusion between the virus and host membrane facilitating insertion of the viral nucleocapsid into the host cells are mediated by the surface glycoprotein G and F. Thereupon, the virus start to replicate in the host cytoplasm. Necrosis of the respiratory epithelial cells is caused by both viral cytotoxicity and host's cytotoxic response (Schweitzer and Justice 2018). Shedding and sloughing of infected epithelial cells from upper to lower respiratory tract enable on one hand virus spread, on the other hand aggravate the infection with small airway obstruction. For neonates, obstruction of their small airway with mucus and cell debris is a major problem in RSV associated bronchiolitis (Ruckwardt et al. 2016).

Observing an infection as interplaying between the virus, the host within a given environment, each of them has a special impact on the RSV pathogenesis and will be discussed briefly below.

Several studies could verify the general expectation about a clearly correlation between disease severity and viral load (DeVincenzo et al. 2010, Utokaparch et al. 2011). RSV manipulates the cell cycle by arresting infected cells in G0/G1 or downgrading apoptosis, and thus makes them more favorable for virus production (Bitko et al. 2007,

Wu et al. 2011). Several mechanism facilitating RSV infection have been discussed : (1) location-related infectivity, (2) evasion of neutralizing antibody by conformational changes and (3) functional modification of the host immune responses (Taleb et al. 2018). That RSV almost exclusively infects the superficial ciliated epithelial cells might protect the virus from getting in contact with dendritic cells (DC) and thus interrupts or delays the immune reaction (Taleb et al. 2018). Further observation pointed to the ability of RSV in inhibiting the trafficking of human DCs from the lung to the draining lymph nodes and preventing a robust T-cell response (Varga and Braciale 2013). Neutralizing antibodies are thought to be circumvented by the contemporary presence of both pre- and post-fusion conformation of F on the viral surface as well was by the existing of an antibody decoy, the secreted form of the G protein (Bukreyev et al. 2008, Liljeroos et al. 2013). Functional modifications of host immune response by RSV were reported. For example, NS1 and NS2 inhibit type I IFN signal transduction (Barik 2013); interactions between RSV G and DC/L-SIGN diminish DC activation, and might limit induction of RSV-specific immunity (Johnson et al. 2012).

At point of host, many factors could affect the severity of an RSV infection. Generally, an RSV infection are mild or moderate for healthy adults but it can become a severe life threatening infection for those at high-risk such as premature infants with bronchopulmonary dysplasia and the elderly with comorbidities or those with immune suppression (Falsey 2007). It has been reported that vitamin D deficiency in healthy neonates is associated with higher risk for RSV lower respiratory tract infection (LRTI) in the first year of life (Belderbos et al. 2011). Additionally, association between severe RSV infection in healthy infants and genetics polymorphisms of host that may alter the innate immune response in controlling RSV infection has been reported, but their statistical significance still remains unclear (Miyairi and DeVincenzo 2008).

Several epidemiological factors that involve in the severity of a RSV infection have been identified including pollution (Karr et al. 2009, Evangelisti et al. 2015), expose to cigarette smoke (Bradley et al. 2005, Groskreutz et al. 2009), crowding and nutrition status of the child (Okiro et al. 2008), evidence of asthma in the mother (Weber et al. 1999, Carroll et al. 2012) as well as low socioeconomic status and parental education (Sommer et al. 2011). In addition, a few studies reviewed the influence of climate parameters such as temperature and humidity on the RSV epidemic. It appears that low

temperature and low ambient relative humidity are the optimal condition for RSV transmission (Lapena et al. 2005, Noyola and Mandeville 2008, Zhang et al. 2013). Whereby, the low temperature might have a greater impact on the RSV incidence (du Prel et al. 2009, Sirimi et al. 2016). According to this observation, in Germany RSV infections occur in the winter months spanning from November to April (RSV season) (Tabatabai et al. 2014).

Compared to other respiratory virus, RSV cause less cytopathic effects in vitro on human primary airway epithelial cell cultures (Zhang et al. 2002), but there is evidence for significant pathology in vivo. For example in hamster model, it was observed, that sloughing of RSV infected ciliated cell into the narrow–diameter bronchiolar airway lumens caused acute distal airway obstruction marked with accumulation of detached, pleomorphic epithelial cells (Liesman et al. 2014). This effect is believed to be associated with one of the two RSV nonstructural proteins, the NS-2 (Liesman et al. 2014) and offer an explanation, how a less cytopathic virus like RSV can cause more severe lower respiratory tract infection (LRTI) than influenza virus LRTI (Welliver et al. 2008). In addition, airway obstruction during RSV infections is caused furthermore by DNA-rich viscous mucus and inflammatory cell debris (Johnson et al. 2007), whereby neutrophil contribute the highest number of infiltrated cells (~ 80%) in the airway of pediatric patients with RSV–induced bronchiolitis (Geerdink et al. 2015). On one hand, neutrophils can limit the viral replication and viral spread; on the other hand neutrophilic inflammation might injure the lung and disrupt the delicate lung development in infancy with lasting consequence that might promote other chronic disease such as asthma (Geerdink et al. 2015). Inversely, RSV is also a major cause of exacerbation of chronic obstructive pulmonary disease (COPD) and asthma, but the mechanism is still unclear (Ramaswamy et al. 2009, Hewitt et al. 2016).

1.4 Therapy and antiviral drugs

1.4.1 Therapy options

Despites relentless effort to develop pharmacological therapies against RSV, the most effective therapy remains supportive care including fluid replacement, oxygen supplement, decongestant nose drops and ventilation support (Resch 2017). Currently, only two antivirals for RSV are available, palivizumab for prevention and ribavirin for treatment of an active RSV infection (Griffiths et al. 2017). The routine use of ribavirin, a broad antiviral synthetic nucleoside analogue, is controversial due to its high cost, difficulties in administration route, and the possibility to be a teratogen (Wright and Piedimonte 2011). In context of safe handling hazardous drugs, the hazard of aerosol ribavirin for health care workers caused by environmental exposure during therapy has been intensively investigated (Bradley et al. 1990, Linn et al. 1995). Considering drug safety and effectiveness, ribavirin is limitedly used in complicated cases such as in immunocompromised individuals in combination with intravenous immune globulin (Khanna et al. 2008, Wright and Piedimonte 2011, Turner et al. 2014).

RespiGam (MedImmune Inc, Maryland) was an RSV immune globulin intravenous (RSV-IGIV) that contained high titres of human neutralizing antibody against RSV (Oertel 1996). This product was shown to be able to neutralize 62 different clinical RSV strains including both subgroups A and B in vitro (Tan 1998). However, its cost-effective was only proved for infants at highest risk for severe RSV infection (Barton et al. 2001, Fuller and Del Mar 2006). Several years after the introduction of a higher potential (50x) monoclonal antibody, palivizumab, RespiGam was taken from the market (Turner et al. 2014). As there is still a lack in RSV therapy, further IGIV preparations (RI-001, RI-002) are still under developing for RSV prevention and treatment in primary immunodeficiency disease and other immune compromised populations (Wasserman et al. 2016, Wasserman et al. 2017).

1.4.2 Vaccines and small molecule antiviral drugs under development

Vast efforts have been putting in development of a vaccine for RSV but there is still no licensed vaccine to date. 18 vaccine candidates are now reaching clinical trials phase I-III tested on 3 major target indications: pediatric, maternal and elderly (Mazur et al.

2018, PATH 2018). These candidates could be divided in 5 vaccine strategies: particle-based, vector-based, protein subunit, live-attenuated/chimeric vaccines, and monoclonal antibodies. Among the 18 candidates, the RSV F nanoparticle vaccine from Novavax addressing maternal immunization, an option to increase maternal antibodies in infants, is the farthest (phase III) along in clinical development (Blanco et al. 2018, Mazur et al. 2018). These promising new approaches in RSV vaccine development aroused optimism for new medication that helps to control and reduce the public health burden of RSV infection.

Several small molecules are now also under clinical development for treatment of RSV infection. Two major drug classes are RNA polymerase and fusion inhibitor. Inhibiting the RNA polymerase is a good strategy to interrupt the virus replication cycle, since RSV belongs to the group of non-segmented, negative-sense RNA viruses and relies on its RNA-dependent RNA polymerase for transcription and replication of its genome (Fearns and Deval 2016). ALS-8112 is a small molecule that was shown to be able to inhibit viral polymerase activity by the intracellular formation of its 5'-triphosphate metabolite working as a nucleoside analogue. However, ALS-8112 has a low oral bioavailability (Deval et al. 2015). To improve its pharmacokinetic properties, a prodrug was developed, ALS-8176 (Wang et al. 2015). This first-in-class nucleoside analog ALS-8176, or called lumicitabine, is now in phase II clinical trial for treatment of hospitalized RSV infected infants (Deval et al. 2015, ClinicalTrials.gov 2018c). Besides, several promising fusion inhibitors are developed and tested in clinical trials on both infants and adults. AK0529 is now in testing on infants between 1 months and 24 months of age who are hospitalized due to RSV infection (ClinicalTrials.gov 2018b). Presatovir (previously GS-5806) was shown to be safe with proven antiviral efficacy in preclinical and clinical studies. However, this drug has a complex pharmacology as being a substrate of several efflux transporters such as P-glycoprotein, breast cancer resistance protein and as being a substrate of cytochrome P450 (Xin et al. 2018). Phase II study of JNJ-53718678 on healthy adult volunteers has also been completed with positive results and is now followed by phase II testing on non-hospitalized adults with RSV infection (Israel et al. 2016, Stevens et al. 2018, ClinicalTrials.gov 2018a). Note, emergence of resistant viruses against ALS 8112, ALS 8176, AK0529 and JNJ-

53718678 were already detected during development (Fearns and Deval 2016, Roymans et al. 2017, McKimm-Breschkin et al. 2018).

Table 1: Overview of RSV vaccines, monoclonal antibodies (mAbs) and small molecules. Listed examples are in clinical development.

mAbs and vaccines
• Particle-based: RSV F nanoparticle, bacterium-like particles (BLP) carrying F proteins • Vector-based: antigens expressed in attenuated modified vaccinia Ankara virus, adeno virus vectors • Protein subunit: pre-F subunit, extracellular domain of SH • Live-attenuated/chimeric vaccines: Attenuation via RSV genome modification e.g. ΔM2-2 or ΔNS2 deletion, HRSV N gene expressing Bacillus Calmette-Guerin (BCG) vaccine • Monoclonal antibodies: MEDI8897 (nirsevimab) target antigenic site Ø on pre-F
Small molecules
• RNA polymerase inhibitor: ALS-8112, ALS-8176 (lumicitabine) • Fusion inhibitor: AK0529, GS-5806 (presatorvir), JNJ-53718678

1.4.3 Passive immunization with palivizumab

As mention above, only palivizumab (Synagis®, MedImmune Inc.), a monoclonal antibody against the RSV-F-protein, that has been approved since 1998 remains available for RSV prevention in high-risk infants (Turner et al. 2014). This antibody is by 95% comparable to any human antibody and only 5% of it originates from the mouse (Resch 2017). Palivizumab went through a 10-year period of developing an antibody that prevents cellular infection by preventing the viral membrane from fusion with the target cell and the virus cell-to-cell spread by syncytia formation. Since F-protein is essential for membrane fusion and well-conserved between subgroups A and B, it becomes the most suitable target for developing such an antibody. From an extensive

library of monoclonal antibodies against RSV, palivizumab was than selected as the one with the strongest binding affinity against the F-protein and most effective neutralizing activity (Young 2002). Palivizumab neutralized a broader panel of 57 RSV clinical isolates of both RSV A and B subtypes (Johnson et al. 1997). The mode of action of palivizumab wasn't clear at the time. After a while, as its binding epitope, the antigenic site II, was identified and as the structure of pre- and post-fusion conformation of F were revealed, it appears that the neutralizing activity of palivizumab results from steric hindrance of the membrane fusion event (Rossey et al. 2018). Because the antigenic site II is present on both pre- and post-fusion F and remains largely intact after the conformational transition from pre- to post-fusion, it is per se not expected to prevent refolding of F (Rossey et al. 2018).

Before 2014, most guidelines recommended palivizumab for preterm infants ≤32weeks gestational age (wGA), those under 35 weeks gestational ages with additional risk factors, and infants with congenital heart disease (Resch 2014). In 2014, the American Academy of Pediatrics (AAP) updated its guidance for management of RSV patients and narrowed the high-risk subpopulation of preterm infants to those ≤28 wGA (AAP 2014, Olchanski et al. 2018). For the immune prophylaxis, palivizumab is given as monthly intramuscular injection at dose of 15mg/kg throughout the RSV season (4-5 doses). With this application regime, palivizumab can reduce hospitalizations by 55% (10.6% placebo vs 4.8% palivizumab) (The IMpact-RSV Study Group 1998). In cotton rat, serum concentration of ≥ 40 μg/ml was linked with a significant reduction of RSV titer in the lung (99% reduction) and this concentration is well maintained in the majority of patient with the monthly dose of 15 mg/kg (Forbes et al. 2014). That palivizumab is needed to be administrated monthly is a consequence of a mean haft life of 20 days (Subramanian et al. 1998). Optimization of new F specific RSV-neutralizing monoclonal antibodies with better neutralizing capacity and extended half-live is now also one of the vaccine strategies that are followed by many researchers. For example, MEDI8897 is a monoclonal antibody that targets the pre-fusion of F. This antibody is reported to have a 50-fold higher neutralizing activity and 3-fold longer half-life than palivizumab (Zhu et al. 2017). There is also interesting achievement in developing an antiviral antibody for RSV treatment, which could directly administered to the site of infection via inhalation, e.g. ALX-0171 (Larios Mora et al. 2018) and F-VHH-4

(Rossey et al. 2017). ALX-0171 and F-VHH-4 are both single-domain antibodies that correspond to the variable region of a heavy chain of a camelid antibody (VHH). Due to their single-domain nature, these antibodies are very small and stable against physical stress during nebulization (Rossey et al. 2018). Local delivery at side of infection required lower dose compared systemic administration, even though it would ensure a more rapid onset of action with fewer potential side effects, which offers many advantage for treatment of lung diseases (Van Heeke et al. 2017).

1.4.4 Palivizumab cost-benefit relation

Since, palivizumab administration is weight dependent, the cost of immunoprophylaxis varies. A single course of palivizumab ranges from $1500-$4300 and calculating for a whole RSV season with 4-5 doses results in a cost of $6000-$20000 for a child (Olchanski et al. 2018). To optimize the cost-benefit ratio, it is indispensable to have a better understanding of the foundation epidemiology and outcomes associated with RSV diseases. The most important point seems to be the definition of correct subgroups of children who are at high-risk for RSV infection. This led to the consequence that the RSV patient management guidance of the American Academy of Pediatrics has been changed 4 times since the approval of palivizumab (1998). According to the most recent update in 2014, palivizumab is recommended for preterm infants with ≤28 weeks of gestation age (wGA) and those ≤12 months with chronic lung disease and/or with non-cyanotic heart disease (Olchanski et al. 2018). In addition, palivizumab is also recommended for older children (12-24 months) with chronic lung disease who required medical therapy within 6 months of RSV season start (Olchanski et al. 2018). However, results from an Italian study pointed to a need of re-evaluation of this guidance relating to a conceivable palivizumab prophylaxis for the preterm subpopulation with ≥29 wGA (Capizzi et al. 2017). On the other hand, several studies showed that shorter application regimes with 3-4 doses could result in an adequate protection compared to a 5 doses regime, and thus they propose a shorter application regime along with a broader target indication (Gutfraind et al. 2015, Weinberger et al. 2015, Lavoie et al. 2016). It can be seen clearly that palivizumab recommendation is a still ongoing debate between different points of view from providers, payers and the child parents.

1.4.5 Detection of palivizumab resistance-associated mutation

As the RNA-dependent RNA polymerase of RNA virus lacks proofreading-repair function, RSV is highly mutated (nucleotide substitution rate 10^{-3} to 10^{-4}), which is also an advantage for the virus to adapt to selective pressure (Domingo et al. 1997, Zhao et al. 2004, Collins et al. 2013). Several antibodies resistance-conferring mutations have been identified in vitro, cotton rats and in vivo (Beeler and van Wyke Coelingh 1989, Crowe et al. 1998, Zhao et al. 2004, Zhu et al. 2011, Bates et al. 2013). These mutation are showed to be located with thin the palivizumab binding site between the amino acid positions 262-276 and with a frequency of 5% in children with breakthrough RSV infection during immunoprophylaxis therapy (Zhu et al. 2011, AAP 2014). However, these breakthrough RSV infections consisted of only RSV hospitalisations (1.4%) and outpatient medically attended lower respiratory tract infections (3.9%) (Carbonell-Estrany et al. 2010). Following amino acid variations at positions 262, 268, 272, 275, 276 were described associating with palivizumab resistance (Beeler and van Wyke Coelingh 1989, Zhu et al. 2011). Another study determined higher occurrence frequency of resistance conferring mutations, namely 8.7% in palivizumab recipients (Papenburg et al. 2012). For the palivizumab naïve subjects, only a few studies report about the frequency of natural polymorphisms in the RSV F gene and in these, antigenic site II mutation conferring palivizumab resistance was reported to occur in a very low frequency <1% (Zhu et al. 2012). In addition, it was reported that these escape mutants initially do not grow in cell culture as isolate in the mixed population, but are selectable in the presence of palivizumab (Boivin et al. 2008, Zhu et al. 2011, Papenburg et al. 2012). Furthermore, these escape mutant are variously impaired in their fitness and could even disappear from the mixed population after passaging (Zhao et al. 2004, Zhao et al. 2006). Thus, characterization of complete recombinant infectious virus is the only way to determine palivizumab susceptibility for these virus variants.

1.5 Marker transfer analysis

As mentioned, RSV isolates with palivizumab resistance associated mutations do not grow in cell culture (Zhu et al. 2011). Hence, still unknown mutations have to be phenotypically characterized using recombinant technique, so called marker transfer analysis. In this method, the examined mutation is introduced into a genome of a drug sensitive parental strain. And subsequently, the complete recombinant infectious virus will be characterized concerning viral fitness and drug susceptibility.

Despite the clinical significance of RSV, there aren't many established platforms that allow stable and efficient mutagenesis of RSV genome. The first RSV revers genetic platform was established by Collins in 1995 (Collins et al. 1995, Collins et al. 1999). In this method, cDNA derived virus was recovered after co-transfection of cultured cells with a plasmid encoding the anti-genomic cDNA of RSV and four helper plasmids encoding the proteins of the nucleocapsid/polymerase complex, in particular N, P, M2-1 and L (Collins et al. 1995). In this method, recovery of infectious virus is not very efficient due to the genetic instability of cDNA (Stobart et al. 2016). Another platform was established by Hotard in 2012 by using bacterial artificial chromosome (BAC) encoding the anti-genome of RSV A2-line19F under the control of a T7 promoter and four helper plasmids encoding the optimized sequence for N, P, M2-1 and L genes (Hotard et al. 2012). All 4 helper plasmid are also under control of T7 promoter. This platform enables efficient recombinant-mediated mutagenesis and cloning in bacteria. Chosen cell culture for transfection is a BHK-21 cell line, BSRT7/5, that stably expresses T7 RNA polymerase (Buchholz et al. 1999). The BAC contains furthermore a gene encoding a far-red fluorescence gene, mKate2, which enables continuous tracking of infection through fluorescence.

BAC-mutagenesis is now widely used in molecular biology studies for variable approaches such as gene function examination, protein localization studies and genetic disease models. To facilitate these studies, various mutagenesis methods were developed. Among these, homologous recombination allows genetic engineering of large DNA even in the absence of restriction enzyme sites. These methods mostly exploit phage lambda-derived recombination system with three genes exo, beta and gam enzymes (Lai et al. 2015). In 2006, Tischer and colleagues developed a method called

"*en passant*" mutagenesis that enables a modification of BAC DNA without retention of any unintended sequence changes in the end product. In this method, BAC recombination is performed in an *E.coli* strain, GS1783, using Red-recombination system and a further enzymatic activity of the I-SceI endonuclease that is utilized not only for counterselection but also for generation of the substrate for the second Red recombination, by which the positive selection marker is scarless removed (Tischer et al. 2006) (detail will be described in 3.2.2). BAC-mutagenesis allows control of successful insertion by sequence analysis prior transfection of cell culture for virus recovery, and spared the time-consuming plaque purification of reconstituted viruses.

To date, this reverse genetic platform for RSV is the unique one that offers versatile, stable and efficient for generation of recombinant RSV (Stobart and Moore 2014). As many small molecules and mAbs are now under development for RSV prophylaxis and treatment, a functional marker transfer analysis would be one of the required technics in the future for study of antiviral resistance emerging phenomena.

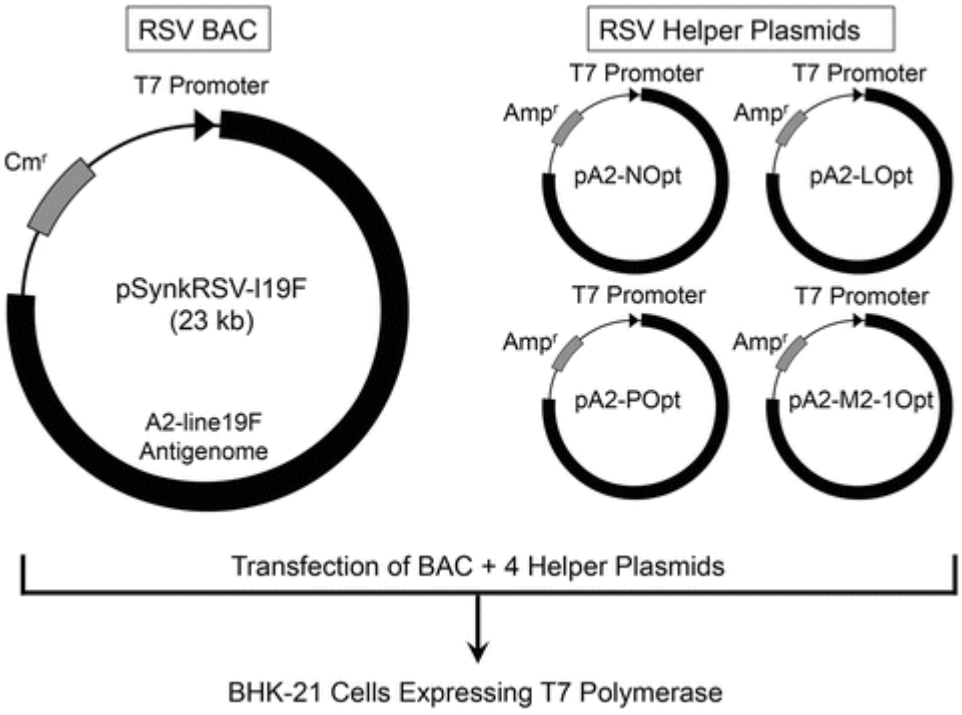

Figure 5: Revers genetic platform for RSV comprises a RSV BAC and 4 helper plasmids encoding sequence optimized genes for the N, M2-1, P and L proteins, respectively (Stobart et al. 2016).

2. Aim of the study

Due to the clinical significance of RSV, a lot of effort has been put into development of new antiviral drugs including mAbs and small molecules. Many promising candidates are now in clinical trials testing in both infants and adults. The natural ability to elicit and tolerate spontaneous mutations of a RNA virus would allow RSV to generate escape mutants during antiviral therapy. To date, RSV therapy options still remains modest with only two licenced therapeutics: ribavirin and palivizumab. Therefore, the context of antiviral resistance associated mutations for RSV did and do not gain much interest. Discovery of new potential antiviral drugs is likewise accompanied with emerging of its escape mutants and this phenomenon is confirmed in the case of palivizumab, the mAbs used in RSV immunoprophylaxis, as well as in cases of investigated small molecules in clinical development including ALS 8112, ALS 8176, AK0529 and JNJ-53718678 (Table 1).

In 2010, Adams et al. described mutation N276S in context of a RSV breakthrough in a child during palivizumab immunoprophylaxis therapy and thus suspected that this mutation is responsible for palivizumab resistance. Short after, Zhu et al. could deny this statement by phenotypical characterization of recombinant RSV harboring this mutation. Note, another mutation K272E which is clearly known to confer palivizumab resistance also was found in this isolate after several passages selecting with palivizumab. Hence, a valid marker transfer analysis that allows reliable phenotypical characterization of newly detected mutation associating with antiviral resistance is indispensable in such a case. This is also the main subject of this study to establish maker transfer analysis for antiviral resistance-conferring mutations in RSV, a field that is still only available to a limited extent.

The instability nature of RNA virus makes this proposal to a challenging goal. This problem can be circumvented by using a bacterial artificial chromosome (BAC) RSV recovery platform (Hotard et al. 2012). On the other hand, at the Institute of Medical Virology in Tuebingen, there was a well-established mutagenesis technique applied for generation human cytomegalovirus (HCMV) mutants, namely "*en passant*" mutagenesis (Fischer et al. 2013). In this work, these two components should be

combined to establish marker transfer analysis for RSV. In the next step, reconstituted recombinant viruses would be phenotypic characterized regarding their fitness and antiviral susceptibility. Viral replication should be investigated using both multi-step growth curves and flow cytometry. Since, ribavirin is not the medication of first choice, proof of concept was firstly focused on palivizumab and mutations in F gene.

In this project, identified mutations on F gene of eight RSV A infected patients, who were randomly chosen independently of their age and their palivizumab status, were introduced into RSV BAC pSynkRSV-l19F (BEI Resources Nr-36460), respectively. Recombinant viruses that rescued from RSV-BAC pSynkRSV-l19F harboring the mutations were characterized by their growth kinetics to investigate influence of the mutation on the virus replication. The parental sensitive strain (RSV A2-K-line19F) rescued directly from RSV BAC pSynkRSV-l19F, that does not harbor any mutation, served as the reference strain in all phenotypic assays. Virus growth was detected by both the virus titers in the supernatants by end-point dilution assays and the cell-to-cell viral spread by flow cytometry. Susceptibility against palivizumab was analysed by plaque-reduction neutralization assays (PRNA). Recombinant viruses with mutation K272E and N276S were additionally generated and characterized. These two strains served as resistance and sensitive control to confirm the functionality of the assays used for susceptibility testing. Furthermore, using the same test methods, phenotypic differences between strain RSV A2-K-line19F and strain A2 (a clinical strain purchased from ATCC® VR-1540P) should also be investigated.

3. Material and Methods

3.1 Material

3.1.1 Patients

All mutations in this work originated from patient samples that were diagnosed as RSV positive in the Institute of Medical Virology and Epidemiology of Viral Diseases of the University of Tuebingen. Since only a restricted number of RSV isolates was available, adult as well as paediatric viral isolates were included in this study. However, as for prove of principle and establishment of new methods, there was no need to distinguish between children and adults.

Altogether there were 8 RSV A positive samples, from which virus was isolated, and subsequently the F protein gene was sequenced to look for mutations. These samples were randomly selected between 2008 and 2015. Three of these samples were from children under 2 years old, and five were from adults, among them three over the age of 50 years. One of the children (RSV isolate V361) was in the Neonatology Unit 2 of the Tuebingen Hospital, where neonates are under monitored intensive care. One child was in the intensive care unit of the Pediatric Cardiology (RSV isolate V391), and one in the Neurodevelopmental Care Unit (RSV isolate P6510). Only in one of these samples, mutations in the F gen were detected (RSV isolate P6510 with mutations C21G and R49K). According to a retrospective interview with the family physician, the child did not receive a prophylaxis with Synagis® since the parents denied the prophylactic therapy recommended by the paediatric physician. In the adult group: two patients were diagnosed with bronchiectasis and recurrent respiratory infections, two were transplant patients and one was a multiple myeloma patient with bronchopneumonia. Three of these 8 patients were co-infected with bacteria or other viruses.

The Department of Clinical Virology offers different validated methods for detection of viral infection. For detection of RSV, both a cell culture based protocol in combination with antigen detection and a PCR are available. Further details concerning clinical conditions and diagnostic results are listed in Table 2.

RSV Isolates	Age	Samples	Clinical features	Virological Diagnostic	New (non-silence) mutations
V361	3 m/o	Oral throat wash	Respiratory deterioration, oxygen desaturation, dyspnea, nosocomial infection	RSV positive [a,b]	-
V391	11 m/o	Tracheal secretion	Rhabdomyosarcoma, RSV pneumonia	RSV positive [a,b], syncytia formation 4 dpi	-
P6510	19 m/o	Throat swab	Aspiration pneumonia (RSV, *E.coli, Pseudomonas)*	RSV positive [d], Cp 10,97	C21G (SP) R49K (F2)
V144	74 y/o	Tracheal secretion	Bronchiectasis, resection of the left lung, pneumonia (RSV, *Pseudomonas*)	RSV positive [a,d], strongly marked syncytia formation 5dpi in Vero, Cp 11.78	A103P (F2)
V349	62 y/o	Tracheal secretion	Multiple myeloma, general reactivation of Herpes virus, bronchopneumonia	Co-infection: RSV[a,d], HSV[d], CMV[d], EBV[d]. RSV A: CPE formation 8dpi, Cp 12,89	T100S (F2) A518V (F1)
V907	47 y/o	Bronchoalveolar lavage	Bronchiectasis, recurrent infection	RSV positive [a,d], CPE in HFF und Vero 5dpi, Cp 19,33	-
V1312	55 y/o	Oral throat wash	Stem cell transplant patient	RSV positive [a,b], CPE detected 8dpi	-
V1772	37 y/o	Bronchoalveolar lavage	Transplant patient, aplasia after chemotherapy	Co-infection CMV[c,d] and RSV[a,b,d]. RSV A: CPE formation 4dpi, Cp 26,38	C550Y (F1) Q34R (F2)

Table 2: Collected patient samples in this study and their characteristics in clinical features and virological diagnostic. Laboratory methods for detection of RSV infection: Cytopathic effect (CPE) formation in cell culture with human foreskin fibroblasts (HFF) and/or African green monkey kidney cells (Vero) (a), immunochromatography- enzyme immunoassay (IC-EIA) (b), enzyme immunoassay (EIA) (c) and molecular diagnostic using polymerase chain reaction (PCR) (d).

3.1.2 Cells

Kidney cells of African green monkeys (Vero) were purchased from ATCC and used up to passage 100.

BSR T7/5 cells were kindly provided by Prof. Conzelmann, Munich. BSR T7/5 is a baby hamster kidney (BHK) cell clone that continuously expresses T7 RNA polymerase under selection of Geneticin G418 (Buchholz et al. 1999).

3.1.3 BAC and plasmid

The RSV BAC rescue system containing the following bacterial artificial chromosome (BAC) and four helper plasmids were kindly provided by Biodefense and Emerging Infections Research Resources Repository (BEI Resources): pSynkRSV-l19F, pA2-Lopt, pA2-Nopt, pA2-Popt, pA2-M2opt (Hotard et al. 2012).

pSynkRSV-l19F (BEI Resources Nr-36460) is a BAC plasmid encoding RSV A2-line19F antigenomic DNA and an additional gene for the far-red fluorescent protein monomeric Katushka 2 (mKate2) that allows detection of infection through fluorescence. In this BAC, sequence for the F protein of strain A2 was substitute with that of Line 19 (Herlocher et al. 1999) while other proteins are identical to that of the RSV A2. The chosen genotype RSV A2-line19F was previously shown to be able to induce key features of RSV pathogenesis in mice (Moore et al. 2009).

pA2-Lopt, pA2-Nopt, pA2-Popt, pA2-M2-1opt (BEI Resources Nr- 36461, 36462, 36463, 36464) are helper plasmids containing four sequence-optimized genes from RSV strain A2, respectively: large polymerase (L), nucleoprotein (N), phosphoprotein (P) and matrix 2-1 protein (M2-1).

The RSV-BAC and helper plasmids contain the gene under control of a T7 promotor.

For this study, these plasmids were propagated in One Shot™ TOP 10 Chemically Competent *E.coli* under antibiotic selection with ampicillin. Plasmid extraction was performed using NucleoBond®Xtra Midi Kit (Macherey-Nagel).

In addition, plasmid pEP-kanS, that contains gene for I-SceI recognition site and the kanamycin-resistance gene (KanR) (Tischer et al. 2006), was used as template for

mutagenesis PCR. This plasmid was a gift from Nikolaus Osterrieder (Addgene plasmid # 41017)

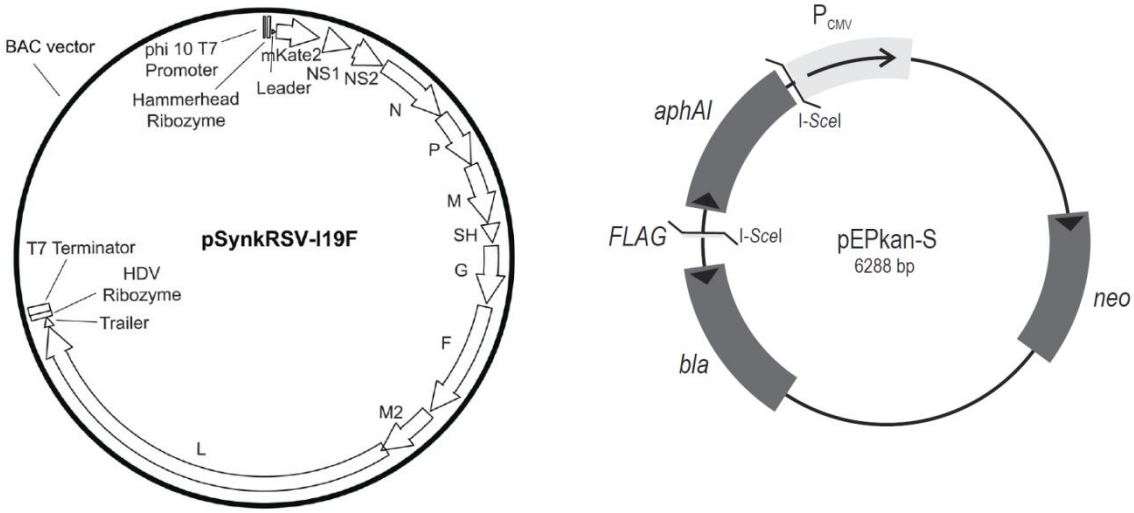

Figure 6: Map of recombinant RSV-BAC pSynkRSV-l19F and plasmid pEPkan-S. In the RSV-BAC pSynkRSV-l19F, the gene encoding the red fluorescent protein mKate2 is located right after the RSV leader sequence and followed by genes encoding for the RSV proteins. The plasmid pEPkans- S is constructed to harbor the kanamycin resistance gene *aphAI* and the I-SceI restriction site (Tischer et al. 2006, Hotard et al. 2012).

3.1.4 Viruses

Respiratory syncytial virus strain A2 that was first isolated in 1961 from a sick infant with bronchiolitis and bronchopneumonia in Melbourne, Australia was purchased at ATCC (ATCC®VR-1540P™). ATCC®VR-1540P™ is a purified virus from original isolate to remove contaminating adenovirus type 1(Lewis FA et al. 1961, Cameron et al. 2003).

RSV-VI-1447 is a RSV isolate, which was a gift from Ortwin Adams, Duesseldorf, Germany. He detected in this isolate mutation N276S and mutation K272E. These mutation serve as palivizumab sensitive and resistant control in this work.

3.1.5 Bacteria

One Shot™ TOP 10 Chemically Competent *E.coli* was purchased from Thermo Fisher (Catalog Nr: C404010) and was used for plasmid propagation. Transformation was performed according to recommended protocol from the manufacturer.

E.coli GS1783 was kindly provided by Gregory Smith (Northwestern University, Chicago) and was used as host cells for performing "*en passant"* mutagenesis, a two steps "scarless" recombination method. This *E.coli* strain contains in its genome the Red genes to enable homologous recombination. Expressing of Red proteins is controlled by a temperature-inducible promotor. A successful application of *en passant* mutagenesis requires furthermore a transient expression of the endonuclease I-SceI enzyme. Therefore a gene encoding for the I-SceI is also integrated in the genome of *E.coli* GS 1783 (Tischer et al. 2010).

3.1.7 Reagents for cell culture

Dulbecco's Modified Eagle Medium (DMEM)	(Gibco)
Glasgow Minimum Essential Medium (GMEM)	(Gibco)
Fetal calf serum (FCS), heat inactivated 56°C, 1h	(Gibco)
Dulbecco's phosphate buffered saline (DPBS)	(Gibco)
TrypLE Express	(Gibco)
Penicillin/streptomycin	(Gibco)
Bambanker™, Serum-Free Cell Freezing Medium	(Nippon Genetics)
Minimal Essential Medium (MEM) Amino (50x)	(Gibco)
Tryptose Phosphate Broth (TPB) (1x)	(Gibco)
Geneticin™ (G418 Sulfate) (50mg/ml)	(Gibco)
Trypan blue	(Sigma)
Methylcellulose (MC)	(Sigma)
Colloidal microcrystalline cellulose (435244) (colloidal MCC)	(Aldrich)

Formula of growth medium for maintenance of cell culture:

For Vero cells: DMEM, 5% FCS, 1% penicillin/streptomycin

For BSR T7/5: GMEM, 5% FCS, 0.5% penicillin/streptomycin, 2% MEM amino acid (50x), 1% tryptose phosphate broth, additionally with 1mg/ml geneticin every other passage

2% MC stock: 5 g MC in 250 ml PBS, disperse slowly, stir for 1 h, autoclaved and rehydration by stirring for several hours

3% colloidal MCC: 3g colloidal MCC in 90 ml ddH_2O, disperse slowly, stir for 1h. Add 10 ml 10xPBS, autoclaved and rehydration by stirring for 1h.

3.1.8 Reagents for bacterial culture

Luria Broth (LB) medium	(Carl Roth)
Luria Broth (LB) agar	(Carl Roth)
Super Optimal Broth with Catabolic repressor (SOC) medium	(Carl Roth)
Kanamycin	(Genaxxon)
Chloramphenicol	(BIO101)
Ampicillin	(Sigma)
Glycerol	(AppliChem)
L-(+)-Arabinose	(Sigma)
Ampuwa	(Fresenius)

Formula of medium for maintenance of bacteria culture

LB medium: 25 g LB granulate in 1 liter fully demineralized (VE) water

pH 7.0± 0.2

Composition:

Trypton	10g/l
Yeast extracts	5g/l
Natrium chloride	10g/l

LB agar: 40 g LB granulate in 1 liter VE water, pH 7.0± 0.2

Composition:

Trypton	10g/l

Yeast extracts	5g/l
Natrium chloride	10g/l
Agar agar	15g/l

Antibiotics stock solution and working solution

Kanamycin: 50 mg/ml in ddH_20 (aliquot storage at -20°C)

Working solution: 50 µg/ml ≙ 85.8 µM (1:1000 dilution)

Chloramphenicol: 10 mg/ml in methanol (storage at -20°C)

Working solution: 25 µg/ml ≙ 77.4 µM (1:400 dilution)

Ampicillin: 100mg/ml in ddH_20 (aliquot storage at -20°C)

Working solution: 100 µg/ml ≙ 286.2 µM (1:1000 dilution)

Glycerol stock for long-term storage of bacteria

700µl overnight culture

300µl glycerol

3.1.9 Reagents for PCR and sequencing

Pwo Master	(Roche)
Compositons:	25U Pwo Super Yiel DNA polymerase
	4 mM $MgCl_2$
	1.6 mM dNTPs
	∑250µl
Primer (50pm)	(Biomers)
pEP-kanS (Addgene plasmid # 41017)	(Addgene)
ExactRun-DNA Polymerase (2U/µl)	(Genaxxon)
ExactRun buffer 5x (with $MgCl_2$)	(Genaxxon)
Set of dATP, dCTP, dGTP, dTTP (each 400µl, 100 mM)	(Promega)
ddH_20, BioScience grade water	(Carl Roth)

DpnI 20000U/ml (NEBiolabs)

10x Cutsmart® buffer (NEBiolabs)

3.1.10 Primers for mutagenesis and sequencing

All by HPLC purified primers were ordered from Biomers (Ulm, Germany). In addition to a universal KAN *reverse* primer (a gift from Prof. Sinzger, Ulm) , for each mutation three specific primers were required to construct the suitable PCR fragments for *en passant* mutagenesis: a *forward long*, *forward short* and a *reverse* primer. How to construct these primers will be descried in 3.2.1.1. In Table 3 all used primers for *en passant* mutagenesis are listed, and in Table 4 primers for sequencing. Note, primers 1F, 4F, 5F and 2R are taken from previous publication (Xia et al. 2014).

Table 3: Primers used for *en passant* mutagenesis

Mutation	Codon change	Sequence 5'→3'
C21G	TGC→GGT	*forward long:* A GCA AAT GCA ATT ACC ACA ATC CTC GCT GCA GTC ACA TTT **GGT** TTT GCT TCT AGT CAA AAC ATaggatgacgacgataagtaggg *forward short:* AGCAAATGCAATTACCACAA *reverse:* A TTG ATA AAA TTC TTC AGT GAT GTT TTG ACT AGA AGC AAA **ACC** AAA TGT GAC TGC AGC GAG GAcaaccaattaaccaattctgattag
Q34R	CAA→CGA	*forward long:* TGC TTT GCT TCT AGT CAA AAC ATC ACT GAA GAA TTT TAT **CGA** TCA ACA TGC AGT GCA GTT Aaggatgacgacgataagtaggg *forward short:* TGC TTT GCT TCT AGT CAA AA *reverse:* AGC ACT AAG ATA GCC TTT GCT AAC TGC ACT GCA TGT TGA **TCG** ATA AAA TTC TTC AGT GAT G caaccaattaaccaattctgattag

R49K	AGA→AAA	*forward long:* ACA TGC AGT GCA GTT AGC AAA GGC TAT CTT AGT GCT CTA **AAA** ACT GGT TGG TAT ACT AGT Gaggatgacgacgataagtaggg *forward short:* ACA TGC AGT GCA GTT AGC AA *reverse:* ACT TAA TTC TAT AGT TAT AAC ACT AGT ATA CCA ACC AGT **TTT** TAG AGC ACT AAG ATA GCC Tcaaccaattaaccaattctgattag
T100S	ACA→TCA	*forward long:* T AAA AAT GCT GTA ACA GAA TTG CAG TTG CTC ATG CAA AGC **TCA** CCA GCA GCA AAC AAT CGAaggatgacgacgataagtaggg *forward short:* T AAA AAT GCT GTA ACA GAA T *reverse:* CT TGG TAG TTC TCT TCT GGC TCG ATT GTT TGC TGC TGG **TGA** GCT TTG CAT GAG CAA CTG CA caaccaattaaccaattctgattag
A103P	GCA→CCT	*forward long:* T GTA ACA GAA TTG CAG TTG CTC ATG CAA AGC ACA CCA GCA **CCT** AAC AAT CGA GCC AGA AGA GA aggatgacgacgataagtaggg *forward short:* T GTA ACA GAA TTG CAG TTG C *reverse:* A ATT CAT AAA CCT TGG TAG TTC TCT TCT GGC TCG ATT GTT **AGG** TGC TGG TGT GCT TTG CAT GAcaaccaattaaccaattctgattag

C550Y	TGT→TAC	*forward long:* A ATA TTG TTA TCA TTA ATT GCT GTT GGA CTG CTC CTA TAC **TAC** AAG GCC AGA AGC ACA CCA ATaggatgacgacgataagtaggg *forward short:* A ATA TTG TTA TCA TTA ATT G *reverse:* G TTG ATC CTT GCT TAG TGT GAT TGG TGT GCT TCT GGC CTT **GTA** GTA TAG GAG CAG TCC AAC AGcaaccaattaaccaattctgattag
A518V	GCT→GIT	*forward long:* TTT ATT CGT AAA TCC GAT GAA TTA TTA CAT AAT GTA AAT **GTT** GGT AAA TCA ACC ACA AAT Aaggatgacgacgataagtaggg *forward short:* TTT ATT CGT AAA TCC GAT GA *reverse:* AAT TAT AGT AGT TAT CAT GAT ATT TGT GGT TGA TTT ACC **AAC** ATT TAC ATT ATG TAA TAA Tcaaccaattaaccaattctgattag
K272E (positive control)	AAG→GAG	*forward long:* G TCA TTA ATC AAT GAT ATG CCT ATA ACA AAT GAT CAG AAA **GAG** TTA ATG TCC AAC AAT GTT CAaggatgacgacgataagtaggg *forward short:* G TCA TTA ATC AAT GAT ATG C *reverse:* A ACT TTG CTG TCT AAC TAT TTG AAC ATT GTT GGA CAT TAA **CTC** TTT CTG ATC ATT TGT TAT AGcaaccaattaaccaattctgattag

N276S (negative control)	AAC→AGC	*forward long:* T GAT ATG CCT ATA ACA AAT GAT CAG AAA AAG TTA ATG TCC **AGC** AAT GTT CAA ATA GTT AGA CAaggatgacgacgataagtaggg *forward short:* T GAT ATG CCT ATA ACA AAT G *reverse*: A CAT GAT AGA GTA ACT TTG CTG TCT AAC TAT TTG AAC ATT **GCT** GGA CAT TAA CTT TTT CTG ATcaaccaattaaccaattctgattag
universal KAN *reverse*		caaccaattaaccaattctga

Table 4: Primers used for sequencing of RSV-BAC and recombinant virus. Annealing positions of these primers are shown in Appendix 1.

Primer	Sequence 5'→ 3'
1F (forward)	GGGGCAAATAACAATGGAGTT (Xia et al. 2014)
4F(forward)	CAGCAAAGTGTTAGACCTCAA (Xia et al. 2014)
5F(forward)	TCAAAAACAGATGTAAGC (Xia et al. 2014)
190R(reverse)	CTGGTTAAGACACTAACTCC
2R(reverse)	CATTGTAAGAACATGATTAGGTGCT (Xia et al. 2014)

3.1.11 Reagents for gel electrophoresis

Rotiphorese ® 10x TBE Buffer (Carl Roth)

Composition: 1.0 M Tris-Borate
20 mM EDTA
in distilled, deionized water pH 8.3

SeaKemLE agarose (Lonza)

Midori Green Advance (Biozym)

100 bp Ladder (1,0 µg/ml) (Invitrogen)

Gel loading dye, purple (6x) (NEB biolabs)

Formula and working solution

1x TBE buffer: 1:10 dilution of 10x TBE buffer with VE water

Agarose gel 1%: 0.5 g SeaKemLE agarose, ad 50 ml 1x TBE buffer
Add 2µl Midori Green after boiling

100 bp Ladder 1:4 dilution with BioScience Grade water

Gel loading 10 µl DNA
2µl Gel loading dye

3.1.12 Reagents for transfection

Lipofectamin™ 2000 Transfection Reagent (1mg/ml)	(Invitrogen)
Opti-MEM Reduced Serum Medium	(Gibco)
pA2-Lopt helper plasmid (100µg/ml)	(Bei Resources)
pA2-Nopt helper plasmid (100µg/ml)	(Bei Resources)
pA2-Popt helper plasmid (100µg/ml)	(Bei Resources)
pA2-M2-1opt helper plasmid (100µg/ml)	(Bei Resources)

3.1.13 Reagents for immunofluorescence and flow cytometry

10x Phosphate buffered saline (PBS) pH 7.2	(Gibco)
Paraformaldehyde (PFA)	(Merck)
Acetone	(Applichem)
Dimethylsulfoxid (DMSO)	(Applichem)
Fluorescein diacetate (FDA)	(Sigma)
Primary antibody	(Merck)
-Mouse anti-RSV fusion protein monoclonal antibody MAB8599, clone 131-2A (1mg/ml)	
-Mouse anti-RSV nucleoprotein monoclonal antibody MAB858-3, clone 130/12H (1mg/ml)	
Secondary anibody	(Dianova)
-Cy3-labeled goat-anti-mouse antibody	

Formula of stock solution and working solution

1x PBS buffer	50 ml 10x PBS buffer
	450 ml aqua bidest
	2,5 ml FCS (0,5%) sterile filtrated
Primary antibody	1:1500 dilution in 1x PBS buffer

Secondary antibody	1:300 dilution in 1x PBS buffer
Acetone 80 %	400 ml Acetone
	100 ml aqua bidest
4% PFA solution	10g PFA
	Ad 250 ml 1x PBS buffer
	Heat in water bath at 50°C until completely dissolved storage at -20°C
	Working solution: 1:2 dilution in PBS (2% PFA)
FDA stock	1mg/ml FDA solution in DMSO
	Storage at -20°C
	Working solution 4:10000 dilution in 1x PBS (0,4µl in 1 ml)

3.1.14 Consumables

2mm electroporation cuvettes	(Biozym)
5 ml polystyrene round-bottom tubes	(Falcon)
6-well plates	(Greiner)
24-well plates	(Greiner)
96-well plates	(Greiner)
Cell culture flasks 25 cm^2	(Greiner)
Cell culture flasks 75 cm^2	(Greiner)
Cell culture flasks 175 cm^2	(Greiner)
Cryotubes 2 ml	(Greiner)
Drigalski spatula	(neoLab)
EASYstrainer® 40µm	(Greiner)
EASYstrainer® 70µm	(Greiner)
EASYstrainer® 100µm	(Greiner)

Falcon tubes 15 ml	(Falcon)
Falcon tubes 50ml	(Falcon)
TipOne® pipet tips with filter 10/20 µl	(Starlab)
TipOne® pipet tips with filter 100 µl	(Starlab)
TipOne® pipet tips with filter 1000 µl	(Starlab)
PCR reaction tubes 0.2 ml	(Sarstedt)
PCR reaction tubes 0.5 ml	(Sarstedt)
Petri dish	(Multimed Biotech)
Reaction tubes 1.5 ml	(Eppendorf)
Reaction tubes 2 ml	(Eppendorf)
Syringe 5 ml	(Becton-Dickinson)
Syringe 50 ml	(Becton-Dickinson)
Millex sterile filters 0.22 µm	(Merck)
Minisart sterile filters 0.45 µm	(Satorius)
Stripettes 5 ml	(Costar)
Stripettes 10 ml	(Costar)
Stripettes 25 ml	(Costar)
UVette® 220 nm-1600 nm	(Eppendorf)

3.1.15 Kits

NucleoSpin Gel and PCR cleanup	(Macherey-Nagel)
NucleoSpin Plasmid	(Macherey-Nagel)
NucleoBond Xtra Midi	(Macherey-Nagel)
QIAamp Viral RNA Mini kit	(Qiagen)
Transcriptor First Strand cDNA Synthesis Kit	(Roche)

3.1.16 Small appliances

Gel electrophoresis chamber	(Hybaid)
Heating block	(Heidolph)
Microwave oven	(AEG)
Photometer	(Eppendorf)
Thermomixer 5436, comfort	(Eppendorf)
Vortex	(Heidelph)

3.1.17 Large equipment

Axiovert200 fluorescence microscope	(Zeiss)
Centrifuges:	
-Eppendorf 5415D	(Eppendorf)
-Eppendorf 5417R	(Eppendorf)
-Megafuge 10R	(Heraeus)
-Rotina 48R	(Hettich)
Lamina flow	(BDK)
CO2-incubator	(Labotech, Heraeus)
Axiovert 25 microscope	(Zeiss)
Electroporator	(Biorad)
Peltier Thermal Cycle 200	(MJ Research)
Shaker	(B. Braun Biotech Intern.)
UV-transluminator	(Bachofer)
Water bath	(GFL)
FACSCalibur	(Becton-Dickinson)

3.2 Methods

3.2.1 Cell culture

African green monkey cells (Vero) that were used for all experiments involving respiratory syncytial virus were maintained in DMEM supplemented with 5% fetal calf serum (FCS) and 1% penicillin/streptomycin (P/S). Medium was renewed every 4 days and cells were splitted in ratio 1:6 after 7-10 days, when the monolayer became confluent. Cells were subcultivated as following procedure. After discarding the exhausted culture medium, the cell monolayer was briefly rinsed with DPBS and the appropriated amount of TrypLE Express was added to flask and incubated for 5 min (Table 5). The same amount of complete growth medium was added and cells were aspirated by gently pipetting. The appropriated aliquots of the cell suspension were transferred to new culture flask and filled to required volume with fresh growth medium (Table 5).

Table 5: Cell culture

	25 cm^2 flask	75cm^2 flask	175 cm^2 flask
TrypLE express	1 ml	3ml	7 ml
Total volume of growth medium	5 ml	15 ml	20 ml

BSR T7/5 cells are baby hamster kidney 21 (BHK-21) cells that constitutively express T7 RNA polymerase. This cell line was used for transfection of RSV-BAC DNA, and was cultured in GMEM supplemented with 5% fetal calf serum (FCS), 0.5% penicillin/streptomycin (P/S), 2% MEM amino acid and 1% tryptose phosphate broth. BSR T7/5 cells were subcultivated in ratio 1:3 once a week and growth medium was renewed after 3-4 days. Subcultivation was analogously to the described procedure for Vero. In addition, the growth medium was supplemented with 1 mg/ml Geneticin each other passage to maintain the expression of T7 polymerase.

3.2.2 Generation of recombinant RSV mutants using *en passant* mutagenesis

En passant mutagenesis is a recombination technique that was established by Tischer and his research group (Tischer et al. 2006, Tischer et al. 2010). This method consists of

two successive homologous recombination steps. In the first one, PCR product containing the viral target point mutation, the I-SceI recognition site, the positive selection marker and the required length of homologous sequences is introduced into the target gene. Recombination has been mediated by Red proteins. The positive selection marker contributes to distinguish bacteria in which the recombination with BAC has been successful. Subsequently, the I-SceI recognition site together with the gene for the positive selection marker will be removed. As result, the introduced point mutation is the only modification left in the target sequence. Following, this method will be described in details.

3.2.2.1 Generation of PCR-products with defined point-mutations

The first step in *en passant* mutagenesis was the amplification of positive selection marker KanR from the plasmid pEPkan-S. Furthermore, the resulted PCR-product had to contain following components. In particular, the I-SceI recognition site followed by the kanamycin-resistance gene was flanked in both directions upstream and downstream by homologous sequences harboring the new sequence of mutation (Figure 7). Thus, constructing appropriate primers for mutagenesis PCR played an important role. The *forward long* primer started at its 5'end with 2 homologous segments (I and II), each app. 20 bp in length, followed by sequence of the target mutation (red mark) and the third homologous segment (III). At its 3'end was the annealing sequence to the selection marker cassette. As using plasmid pEPkan-S to amplify the kanamycin-resistance gene, the 3' end of the *forward long* primer was represent by the sequence 5'-aggatgacgacgataag**taggg**-3', in which part of the I-SceI recognition site was implemented (marked in bold) (Tischer et al. 2006). The reverse primer containing the reverse complement sequence of the target gene with the modified nucleotide was constructed in the same way, and had in its 3'end the sequence 5'-caaccaattaaccaattctgattag-3'. The revers and forward long primers were both approximately 80 bp in length. The forward short primer had the identical sequence to the first homologous block (I) of the forward long primer. The universal KAN reverse primer contained reverse complement sequence to the kanamycin-resistance gene on plasmid pEPkan-S and was 21 bp long. All constructed primers are listed in 3.1.10, Table 3.

Appropriate PCR fragments for *en passant* mutagenesis were obtained after two successive PCRs. For the first PCR, only the forward long and the universal KAN revers primers were used, and for the second the forward short and the reverse primers. Purified product of the first PCR served as template for the second one. Components and their amounts used for mutagenesis PCR are listed in Table 6.

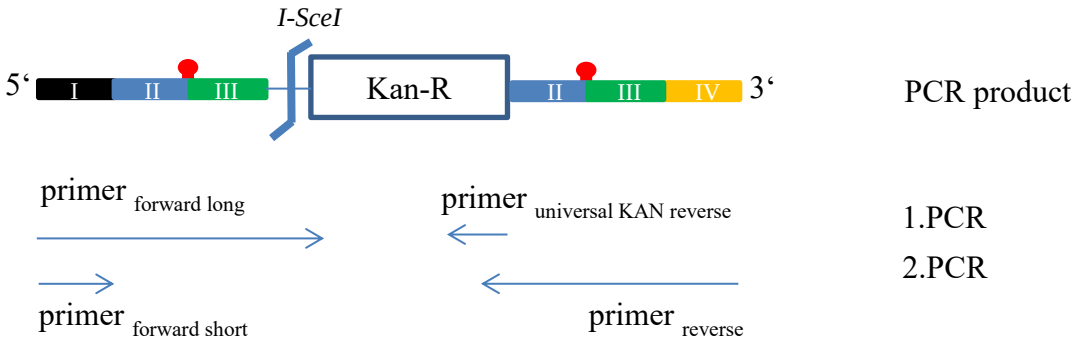

Figure 7: Construction of PCR fragments for en passant mutagenesis and illustration of required primer sequence for PCR. Each colors block (black, blue, green, orange) represents a homologous segment on the target gene and is app. 20 bp in length. The red mark stays for the to be introduced mutation.

Table 6: Mutagenesis PCR reaction components

1. PCR		**2. PCR**	
Components	Volume	Components	Volume
Primer forward long (50pm)	0,5 µl	Primer forward short (50pm)	1 µl
Primer uni. KAN reverse (50pm)	0,5 µl	Primer reverse (50pm)	1µl
Pwo Master (2x concentrated)	25 µl	Pwo Master (2x concentrated)	50 µl
pEPkan-S (1ng/µl)	0,5 µl	Purified 1. PCR product	1 µl
ddH_20	23,5 µl	ddH_20	47 µl
Total	**50 µl**	**Total**	**100 µl**
Purified and eluate in ddH_20	25 µl	Purified and eluate in ddH_20	50 µl

The thermal cycle for mutagenesis PCR contains two successive cycling phases with different annealing temperatures. In the first cycling phase, primers were allowed to bind template DNA at 51°C and in the second at 60°C. The first phase was programmed to run for 9 cycles and the second one for 24 cycles. Details of the PCR thermal cycler are shown in Table 7.

Table 7: PCR condition (Thermal cycler)

Cycle step	Temperature	Time	Cycle
Initial denaturation	95°C	5 min	1
Denaturation	95°C	45 s	9
Annealing	51°C	2 min	
Elongation	68°C	2 min	
Denaturation	95°C	45s	24
Annealing	60°C	2 min	
Elongation	68°C	2 min	
Final elongation	68°C	10 min	1

3.2.2.2 Gel electrophoresis

Success of mutagenesis PCR was than checked by gel electrophoresis on 1% Agarose-gels. 0,5g of Agarose were suspended in 50 ml 1x TBE buffer and boiled in a microwave until completely dissolved. After supplement of 2 µl Midori Green, the solution was allowed for gelation at room temperature in a suitable gel-chamber. Before loading onto the agarose-gel, 10µl of the PCR product were mixed with 2 µl of the loading dye. Lengths of PCR products were compared with a 100 bp DNA ladder, which was treated in the same way with loading dye and loaded on the first lane of each gel. Gel electrophoresis was run at 100 Volt and for 30 to 45 min.

3.2.2.3 Purification of PCR-products and DpnI digestion

After each PCR, the reaction mixtures were purified using the kit "NucleoSpin Gel and PCR clean up" by Macherey-Nagel. In brief, PCR products were allowed to react with a double amount of binding buffer. Subsequently, the mixture was loaded onto the NucleoSpin column, and centrifuged at 11000 rpm for 1 min. This was followed by a wash with 600 µl washing buffer, and centrifuged at 11000 rpm for 1 min. Silica-membrane was then dried by a centrifugation at 11000 rpm for 2 min. Instead of NE buffer as recommended by Macherey-Nagel, PCR products were eluted in ddH_20 (Table 6) and stored at 4°C until further use.

In addition to a standard clean-up, the end PCR products need to be digested by DpnI to remove the pEPkan-S plasmid before transformation. Because of encoding of the kanamycin-resistance gene, this plasmid was used as template in the first mutagenesis PCR for amplification of the positive selection marker, the kanamycin resistance gene KanR. Presence of this plasmid as contamination in bacterial cells will lead to an unintended expression of kanamycin-resistance gene and yield a false positive selection of bacterial colony with the correct incorporated PCR-products. Hence, this template plasmid needs to be completely clarified out of the PCR-product bevor electroporation. DpnI is a methylation-sensitive restriction enzyme, which digests only methylated DNA (Figure 8). As a consequence, only the template DNA is cleaved and the PCR products remained unaffected.

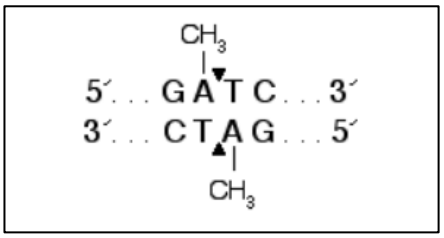

Figure 8: Recognition site of DpnI restriction enzyme. Picture taken from the NEB website

DpnI digestion was performed in a total volume of 50 µl (Table 8) and incubated at 37°C for 2-2,5h. Afterwards, the digested mixture was purified using the kit "NucleoSpin Gel and PCR clean up" and eluted in 15 µl ddH_2O. If transformation into *E.coli* GS1783 would be performed on the same day, this product would be stored on ice, otherwise at 4°C.

Table 8: DpnI digestion

Components	**Volume**
PCR product	40µl
10x Cutsmart buffer NEB	5 µl
DpnI	3 µl
ddH_2O	2 µl
Total	**50 µl**

3.2.2.4 Generation of electrocompetent *E.coli* GS1783 for transformation and BAC-mutagenesis

To enable RSV-BAC-mutagenesis within *E.coli* GS1783, the RSV-BAC had to be transformed firstly into *E.coli* GS1783. This resulted in the *E.coli* GS 1783/pSynkRSV-l19F strain, that gained the chloramphenicol resistance phenotype caused by newly harbored BAC. Transformation was performed by electroporation as described below.

3.2.2.4.1 Generation of *E.coli* GS 1783/pSynkRSV-l19F

An overnight culture of *E.coli* GS1783 was prepared a day before performing electroporation by inoculating a small amount of the bacteria glycerol stock in 10 ml LB- medium. On the day of experiment, 1 ml of the overnight culture was reinoculated in 50 ml LB-medium and grown at 32°C, 200 rpm for 3h. The suspension was than cooled down on ice for at least 20 min. In the following steps, the bacteria were kept preferably cooled on ice. Likewise, all consumables e.g. pipets, electroporation cuvettes, and all reagents e.g. ddH_20 (Ampuwa), PCR products were pre-cooled on ice. After chilling, bacteria were pelleted by centrifugation at 4000 rpm, 4°C for 10 min. The supernatant was discarded and the pellet was resuspended in the residual liquid by shaking the falcon in an ice-cold water bath before adding ddH_20 to a total volume of 50 ml. Bacteria were then again pelleted by centrifugation at 4000 rpm, 4°C for 5 min. This washing step was repeated for at least three times to remove as much as possible salt left-over from the growth medium to prevent an electrical “bang” during electroporation. After discarding of the supernatant in the last washing step, the bacteria were resuspended in the remaining water and keep cold on ice. These bacteria became electrocompetent after this preparation procedure and were ready for electroporation.

A mixture of 2µl pSynkRSV-l19F plasmid DNA and 100 µl bacteria was then transferred into a chilled 2 mm electroporation cuvette and immediately electroporated according to a pre-set protocol of Bio-Rad for *E.coli* with 2500 V, 25 µF and 200Ω. Straightway after pulsing, 1 ml 32°C pre-warmed SOC-medium was added to the bacteria, mixed by pipetting up and down once. The mixture was transfer to a 1.5 ml Eppendorf tube and shaken at 32°C, 200 rpm for 2 h. In this time, the chloramphenicol resistance gene on plasmid pSynkRSV-l19F is expressed and allowed growth of

successfully transformed *E.coli* GS1783/pSynkRSV-l19F on agar plate in the presence of chloramphenicol (25µg/ml). After 2h incubation, the bacteria were pelleted at 6000 x g for 30 s, 800µl of the supernatant were discarded. Pellet was then resuspended in the residual growth medium and plated on 2 LB-agar plates with 25µg/ml chloramphenicol, each with 100 µl of the bacteria suspension. These plates were than incubated overnight at 32°C. Success of transformation of pSynkRSV-l19F into *E.coli* GS1783 was checked additionally by PCR and sequencing. Several glycerol stocks of this E.coli GS 1783/pSynkRSV-l19F strain were aliquoted and stored at -80°C.

3.2.2.4.2 BAC-mutagenesis: Generation of *E.coli* GS 1783/pSynkRSV-l19F with defined point mutation

PCR products were than electroporated into *E.coli* GS1783/pSynkRSV-l19F for mutagenesis. Preparation of electrocompetent *E.coli* GS1783/pSynkRSV-l19F for transformation was performed with the same procedures as describe above, with following changes.

-*E.coli* GS 1783/pSynkRSV-l19F was grown in presence of 25 µg/ml chloramphenicol: overnight culture was prepared in 10 ml LB- medium with 25 µl chloramphenicol stock solution and likewise, on the next day in 50 ml LB-medium with 125 µl chloramphenicol stock solution.

- After the 3h incubation time on the next morning, the flask was transferred to a pre-heated water bath at 42°C, and shaken for exactly 15 min. In this time, expression of the Red recombinase proteins for homologous recombination is induced.

- For electroporation, 5µl of purified PCR-product were mixed with 100 µl of electrocompetent bacteria. As transformation of PCR-product into *E.coli* GS1783/pSynkRSV-l19F happened, the PCR-products were incorporated in to the plasmid pSynkRSV-l19F through homologous recombination carried out by the previously induced Red proteins (Figure 9). By means of the expression of the kanamycin-resistance gene encoded on the PCR-product, the bacteria became resistant to kanamycin. Thus, selection of successful transformed bacteria now took place on LB-agar plates containing both chloramphenicol and kanamycin. Therefore, after 2 h incubation following electroporation the bacteria were pelleted, 800 µl of supernatant were discarded. Bacteria were resuspended and plated on 2 LB-agar plates with

25µg/ml chloramphenicol and 50 µg/ml kanamycin, each with 100 µl of the bacteria suspension and incubated overnight at 32°C.

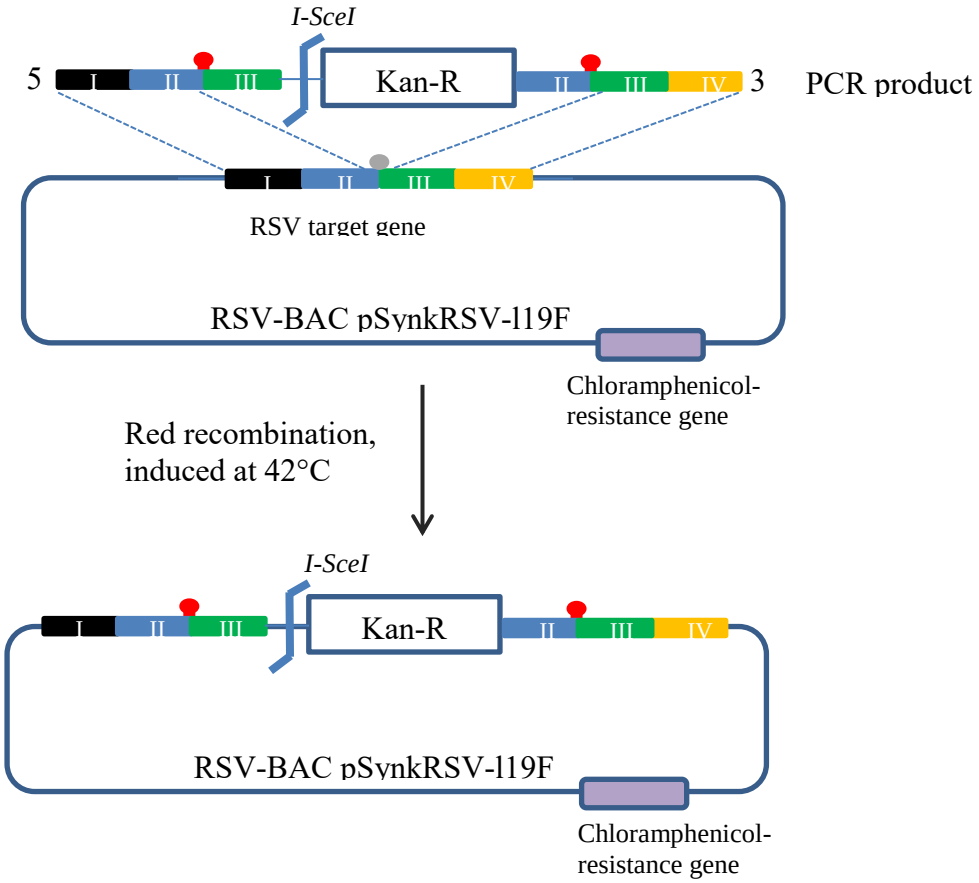

Figure 9: First recombination step in *en passant* mutagenesis. Expression of Red proteins was induced in water bath at 42°C for 15 min. By means of electroporation, the PCR-products were transferred into *E.coli* GS1783/pSynRSV-l19F. Afterwards, a homologous recombination between the PCR-products and RSV target gene were mediated by the transient expressed Red proteins. As result, the PCR-product with its kanamycin-resistance gene was incorporated into the RSV-BAC and *E.coli* GS1783/pSynRSV-l119F became resistant to kanamycin.

3.2.2.5 Removal of the positive selection marker

In the second recombination of *en passant* mutagenesis, the positive selection marker cassette would be removed completely. Three to four colonies of *E.coli* with the mutated BAC were selected and inoculated respectively in 1 ml LB-medium with 2.5 µl chloramphenicol stock solution overnight at 32°C, 200 rpm. On the next day, 100 µl of each overnight culture were transferred into 2 ml LB-medium containing 5 µl chloramphenicol stock solution and incubated for 2 h. Afterwards, 2 ml pre-warmed LB-medium containing 2% arabinose and 5 µl chloramphenicol were added into the bacteria culture and incubated for another 1 hour. By supplement the growth medium with arabinose, the expression of I-SceI enzyme will be induced. The gene encoding for the I-SceI enzyme is already integrated in the genome of *E.coli* GS1783 and its expression is controlled by an arabinose-induced promotor. The endonuclease I-SceI bound and cleaved at its recognition site on the previously constructed PCR segment that was now incorporated in the RSV-BAC. By this restriction, the RSV- BAC was linearized (Figure 11). I-SceI recognition site (Figure 10) on the PCR-product is the unique one in this system. After 1h incubation period, bacteria cultures were moved to a 42°C pre-heated water bath and shake at 100 rpm for 30 min. During this time, expression of Red recombinase proteins were induced and it led to the second homologous recombination, which was mediated between the identical sequence segments II and III on both ends of the linearized RSV-BAC. In that way, the RSV-BAC is recirculated, and the point mutation remained as the only modification on the RSV-BAC. After induction at 42°C, bacteria cultured were shaken again at 32°C, 200 rpm for further 2 h. Then, 0.5 µl of bacteria culture were diluted in 5 ml LB-medium, and 100 µl from this suspension was plated on a freshly prepared LB-agar plate supplemented with 1% arabinose and 25 µg/ml chloramphenicol. Plates were incubated overnight at 32°C.

5'…TAGGGATAA▼CAGGGTAAT…3'

3'…ATCCC ▲TAT TGTCCCATTA…5'

Figure 10: I-SceI recognition site.

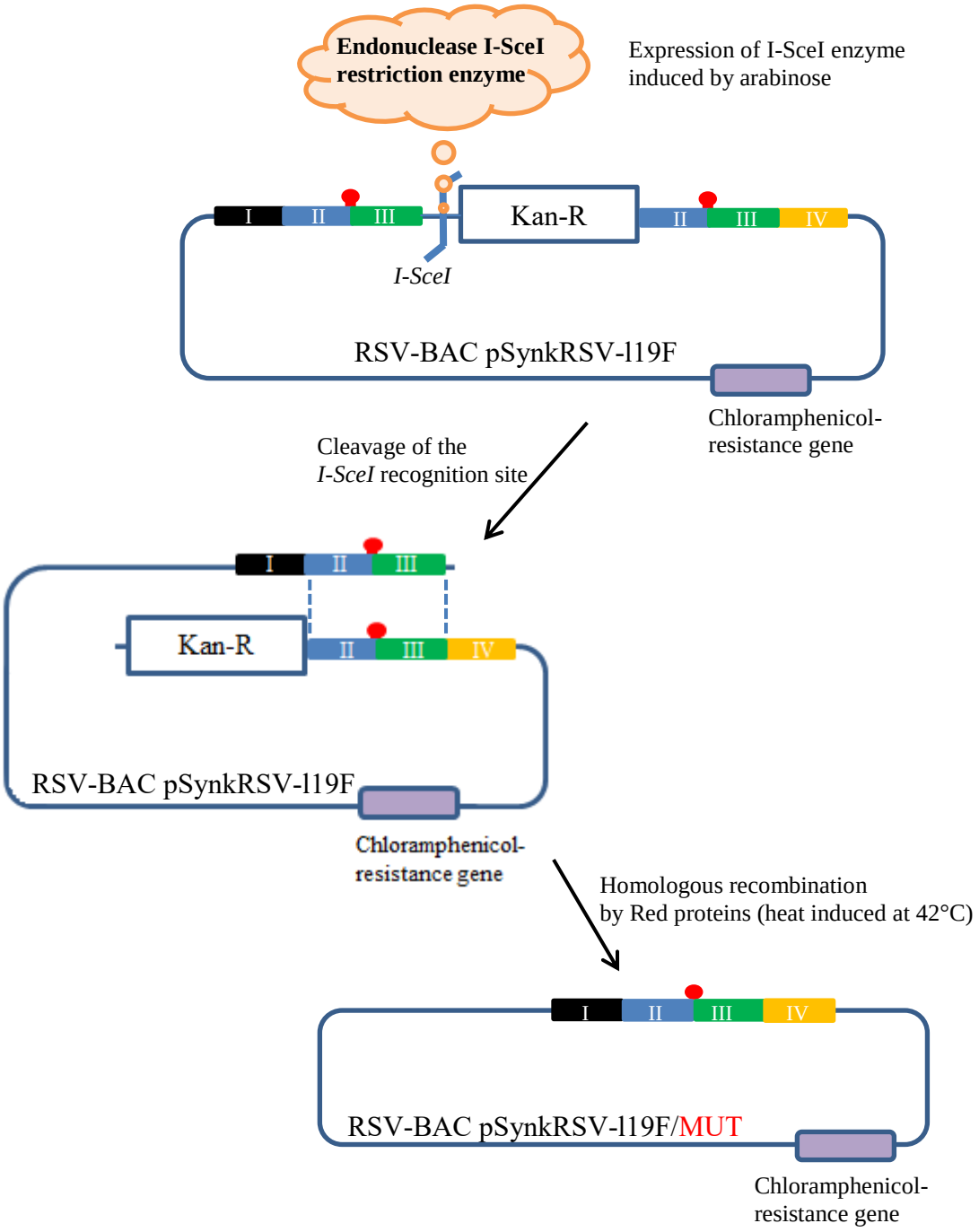

Figure 11: The second homologous recombination in *en passant* mutagenesis. In this step the selection marker was removed completely, leaving the point mutation as the only modification on the RSV-BAC pSynKRSV-l19F. Expression of the I-SceI endonuclease was induced by adding arabinose into the growth medium. RSV-BAC was than cleaved by the I-SceI with in its recognition site on the PCR fragment that was incorporated into the RSV-BAC previously. Thereby, the RSV-BAC was linearized. As expression of Red-proteins had been induced at 42°C, the second homologous recombination was mediated between the both ends of the linearized BAC, in position of the segment II and III. Thus, the RSV-BAC was recirculated while all foreign sequences were removed and the point mutation remained as the only modification.

On the following day, negative selection was performed in order to distinguish bacteria colonies, in which the kanamycin-resistance gene had been removed successfully. Therefore, 12 colonies of *E.coli* were randomly chosen, and resuspended in 20 µl LB-medium, respectively. Each 10 µl of the suspension were dripped on a LB-agar plate containing chloramphenicol (25 µg/ml) and on a LB-agar plate containing both chloramphenicol (25 µg/ml) and kanamycin (50µg/ml). These colonies were each identified to enable selection. Colonies with successful removal of the kanamycin cassette were these, that were growing in the presence of chloramphenicol and not of kanamycin. Both plates were incubated at 32°C overnight and evaluated on the next day.

3.2.2.6 Extraction of BAC-DNA by mini-preparation

To ensure the successful mutagenesis of the RSV-BAC, sequencing of the segment of interest on the F-gene of RSV-BAC was executed. Therefore, a mini-preparation was performed to extract RSV-BAC DNA. Used was the "NucleoSpin Plasmid" kit by Macherey-Nagel according to its recommended protocol for isolation of low-copy plasmids. In brief, several kanamycin-sensitive colonies were picked and inoculated respectively in 5 ml LB-medium supplemented with 12.5 µl chloramphenicol stock solution, shaken overnight at 32 °C, 200 rpm. On the next morning, the saturated bacteria cultures were pelleted at 4000 x g for 10 min. As much as possible of liquid of the supernatant was discarded. The pellet was completely resuspended in 500 µl buffer A1 (resuspension buffer supplemented with RNase A). 500µl buffer A2 (lysis buffer) were added to the reaction mixture and gently mixed by inverting the tube 6-8 times. After incubation period of 5 min, 600 µl buffer A3 (neutralization buffer) were added to stop the cell lysis reaction and gently mixed again by inverting to tube 6-8 times. Lysate was then clarified by centrifugation for 10 min at 11,000 x g. To allow DNA bind to the silica-membrane of the NucleoSpin® Plasmid Column, the supernatant was loaded step-by-step onto the column and centrifuged for 1 min at 11,000 x g. Flow-through was discarded and column was washed with 600 µl buffer A4 (supplemented with ethanol) by centrifugation for 1 min at 11,000 x g. Flow-through was discarded again and the silica membrane was dried by centrifugation for 2 min at 11,000 x g. The bound DNA were eluted in 50 µl ddH_20 for 2 min at 70°C and followed by a centrifugation for 1 min at 11,000 x g. Isolated DNA was stored at 4°C until further use.

3.2.2.7 Control of successful mutagenesis by sequencing

From the isolated DNA by the mini-preparation, the region of interest on the F gen on the RSV-BAC was amplified and sequenced in order to verify the success of the mutagenesis. The component for PCR and thermal cycle conditions are shown in Table 9. After the amplification, PCR products were purified using the kit "NucleoSpin Gel and PCR clean up", eluted in 50 µl ddH_20 and checked on a 1% agarose gel. Concentration of the purified PCR product had to be adjusted to 20 - 80 ng/µl for sequencing. Subsequently, 5 µl of the adjusted PCR product and 5 µl of a suitable primer (5 pmol/µl) were mixed in a 1.5 ml tube and sent to the company GATC Biotech (Konstanz, Germany) for sequencing. Quality service chosen from GATC: Sanger sequencing- LIGHTRUN tube.

Table 9: Used components for PCR and thermal cycle conditions. PCR was performed in a total volume of 50 µl.

Component	**Volume**	**Thermal cycle conditions**			
5x ExactRun buffer	10 µl	Cycle step	Temp	Time	Cycles
dNTP's each 25 mM	0,5 µl	Initial denaturation	98°C	30 s	1
ddH_2O	33 µl	Denaturation	98°C	7s	
Primer forward	0,5 µl	Annealing	52°C	30 s	35
Primer reverse	0,5 µl	Extension	72°C	1 min	
ExactRun Polymerase	0,5 µl	Final extension	72°C	10 min	1
Template DNA	5 µl	Cool down	20°C	1 min	1
Total	**50 µl**				

3.2.2.8 Midi-preparation for transfection

As the mutagenesis had been checked by sequencing, a midi-preparation was performed to isolate a sufficient amount of BAC-DNA for transfection into BSR T7/5 cells. Isolation was performed with the kit "NucleoBond Xtra Midi" by Macherey-Nagel according to the protocol high-copy plasmid purification. Therefore, the appropriate

bacteria colony was inoculated in 100 ml LB-medium supplemented with 250 µl chloramphenicol stock solution overnight at 32°C, 200 rpm. From this overnight culture, 1 ml glycerol stock was prepared and frozen at -80°C for long-term storage. The remained bacteria were then pelleted at 4°C, 4000 x g for 15 min. The supernatant was discarded completely. The pellet was resuspended in 8 ml of the resuspension buffer RES supplemented with RNase A. In a following step, bacteria were lysed with 8 ml of the lysis buffer LYS for 5 min. During that time, the tube was gently mixed by inverting 5 times and the NucleoBond® Xtra column was equilibrated by wetting the column filter with 12 ml of equilibration buffer EQU. The lysis reaction was then stopped with 8 ml neutralization buffer NEU. Next, the lysate was load onto the column through the equilibrated filter, step-by-step. The filter held back the precipitate to prevent the column from clogging. To wash the remaining lysate out of the filter and enrich the DNA concentration, 5 ml of buffer EQU were applied carefully to the funnel shaped rim of the filter. Column filter was than discarded and column was washed with 8 ml buffer WASH. Plasmid DNA were then eluted with 5 ml elution buffer ELU and collected in a 15 ml falcon. 3.5 ml room-temperature (RT) isopropanol were added to precipitate the eluted plasmid DNA and the mixture was centrifuged at RT, 4000 x g for 30 min. Supernatant was discarded and 2 ml of RT 70% ethanol were added to the pellet and centrifuged at RT, 4000 x g for 15 min. Ethanol was removed and pellet was dried at RT for 5-10 min. Subsequently, the DNA pellet was dissolved in 100 µl ddH_20 and stored at 4°C. Concentration of DNA was determined by photometry.

3.2.2.9 Transfection of the BAC-DNA into BSR T7/5 cells and virus growth

Usually on the next day of midi-preparation, transfection was performed using the transfection reagent Lipofectamin® 2000. The following protocol were adapted from Hotard et al. 2012 and partially modified.

A day prior transfection, $4.5x10^4$ BSR T7/5 cells/well were seeded on a 6-well plate and incubated at 37°C, 5% CO2. For each RSV mutant, transfection was performed in duplicate. The following given amount is for one reaction. 4.5 µl of the Lipofectamine reagent were diluted with 250 ml Opti-MEM and incubated at RT for 5 min. In a 1.5 ml Eppendorf tube, 0.8 µg of RSV-BAC plasmid DNA and 0.4 µg of each helper plasmids in particular pA2-Lopt, pA2-Nopt, pA2-Popt and pA2-M2-1opt, were gently mixed

together and filled up to a total volume of 250 µl with Opti-MEM. 250 µl of the Lipofectamine dilution and 250 µl of plasmid DNA solution were combined and gently mixed. This transfection mixture was than incubated at RT for 20 min to allow the formation of DNA-cationic lipid complex. During this time, growth medium for BSR T7/5 cells were renewed with 2 ml of GMEM (supplemented with 5%FCS, 0.5 % P/S, 2% MEM amino acid, and 1% TPB). 500 µl of the transfection complex was dripped slowly to the well and plate was incubated at RT on a rocker set at low speed. After an incubation time of 2 h, 500 µl of GMEM was added to the well and plate was incubated at 37°C, 5% CO_2 to the next day. On the next day, transfection mixture was aspirated from the well, and replaced with 2 ml fresh GMEM. Tissue culture plate was then incubated at 37°C, 5% CO_2. Growth medium was renewed again on the next day, and on the third day cells from both transfection reactions were subcultivated into a 75 cm^2 flask. Growth medium were renewed every other days and culture was sub-passed at ratio 1:3 if necessary. Rescue of RSV can be monitored by fluorescent signal of the mKate2 protein, which gene is encoded in the RSV-BAC. As 100% of the monolayer was infected, the supernatant was collected in a tube. Incompletely budded virions were released from cell membrane by one freeze and thaw cycle of the cells layer. After thawing, the virus supernatant was used again to aspirate cells from the bottom of the flask and to collect the released virions. Subsequently, this suspension was centrifuged at 1700 rpm for 5 min to remove cell debris. The clarified supernatant was used to infect Vero cells for further virus propagation. Usually after further 2 to 3 passages, Vero cells were completely infected and the virus supernatant could be harvested in the same manner. Virus supernatant was aliquoted and frozen at -80°C for further experiments. In order to check for the presence of the desired mutation and absence of any unintended base changes emerged during the whole procedures, viral RNA was isolated from 140µl of supernatant using the “QIAamp Viral RNA Mini kit” and subsequently reverse transcribed into cDNA by the “Transcriptor First Strand cDNA Synthesis” Kit (Roche). Following, the F gene on cDNA was amplified and sequenced as describe above in section 3.2.2.7.

3.2.3 Phenotypic characterization of recombinant RSV mutants

In this work, the recombinant RSVs were characterized concerning their growth kinetics and their susceptibility to palivizumab. For these assays, the virus titer in the supernatant had to be determined previously.

3.2.3.1 Determination of virus titer as fluorescence-forming units/ml (FFU/ml)

One day prior the examination, $2x10^4$ Vero cells/well were seeded on a 96-well plate in a volume of 100 µl/well and incubated at 37°C, 5% CO_2 overnight to enable a confluent growth of cells on the bottom of the wells. For the assay, one virus aliquot was thawed at RT and a 10-fold serial dilution of the virus supernatant ranging from 10^{-1} to 10^{-6} was prepared with DMEM. 100 µl of each dilution were inoculated onto the Vero cells monolayer and incubated at 37°C, 5% CO_2 for 20-24 hours. For each dilution, 8 replicate test units were performed. After the incubation period, evaluation could be done directly by counting the fluorescence-forming units (FFU), or for later evaluation the cells could be fixed with 2% paraformaldehyde at 37°C for 10 min. For accuracy, only dilution that exhibited 10-100 FFU/well was counted. The calculation can be explained by the following example demonstrated in Figure 12. For example, at dilution 10^{-4}, each test well had an average of 23 FFU in 100 µl, or it means 230 FFU in 1 ml. And the titer of the virus stock is therefore $230x10^4$ FFU/ml or $2.3x10^6$ FFU/ml.

Because of the encoded fluorescence protein mKate2 on the RSV-BAC pSynkRSV-l19F, infection caused by virus rescued from this plasmid can be monitored directly after the inoculation period. But for the clinical strain RSV A2 that did not contained a tagged fluorescent gene in its genome, a staining to visualize viral protein had to be performed prior evaluation. Therefore, cells were fixed and permeabilized with 100 µl 80% acetone for 5 min at RT and washed subsequently twice with 100 µl PBS. Immunofluorescent staining of RSV-proteins was performed by incubation the tissue culture with 100 µl primary antibody (either with monoclonal IgG mouse antibody against RSV fusion protein or RSV nucleoprotein, dilution 1:1500 in PBS) for 2h at 37°C, 5%CO_2, or overnight at 4°C. This was followed by two washing steps, each with 100 µl PBS. The primary antibody was then allowed to react with 100 µl of the secondary antibody (Cy3-labeled goat-anti-mouse, dilution 1:300 in PBS) for 2h at

37°C, 5% CO_2. Following, the cells were washed twice with 100 µl PBS, and then wells were filled with 200 µl PBS and stored in the dark at 4°C.

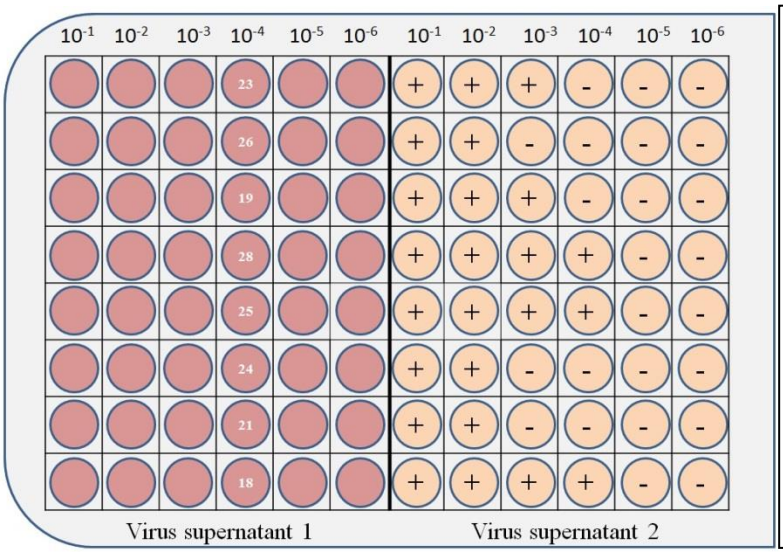

Dil.	Pos.	Cum. Pos.
10^{-2}	8/8	8/8
10^{-3}	5/8	13/8
10^{-4}	3/8	**16/8**

Calculation of $TCID_{50}$

Highest dilution giving 100% CPE
+1/2-
$\frac{\text{total number of test units showing CPE}}{\text{number of test units per dilution}}$

$= -2+1/2\ -16/8 = -3.5\ TCID_{50}$

or $10^{3.5} TCID_{50}$ in 100 µl, equal to $10^{4,5}$ $TICD_{50}$/ml or $\log TCID_{50}/ml = 4,5$

Figure 12: Illustration of plating an assay to determine virus titer as florescent-forming unit and as $TCID_{50}$. Each well was inoculated with 100 µl of the virus dilution. For the virus supernatant 1, virus titer as FFU/ml were determined 1 day after inoculation by counting the fluorescent foci in the virus dilution that exhibited 10-100 FFU per well. An average of all 8 replicate test units was calculated, for this example: in dilution 10^{-4} there was 23 FFU/100µl, is therefore $2.3x10^6$ FFU/ml. For the virus supernatant 2, virus titer as log TCID50/ml was determined by searching for positive fluorescent signal from the highest dilution giving 100% CPE (+) to the last one giving no CPE (-) and calculated as writing in the figure above.

3.2.3.2 Determination of virus titer as $TCID_{50}$ by end-point dilution assay

Another method to determine the virus titer that also used in this work was an end-point dilution assay, which was performed in the same way as described above for FFU-assay but differed in the evaluation and interpretation. Instead of counting fluorescent foci, a well was evaluated as positive, if in this well fluorescence from any single infected cells could be detected, and otherwise as negative. $TCID_{50}$, the 50% tissue culture infective dose, was than calculated with the following formula according to the Spearman (1908) Kärber (1931) method (Hierholzer and Killington 1996).

$$Highest\ dilution\ giving\ 100\%\ infected\ wells + \frac{1}{2} - \frac{total\ number\ of\ test\ unit\ with\ infected\ cells}{number\ of\ test\ units\ per\ dilution}$$

An example is demonstrated in Figure 12. In this assay, 8 replicated test units were performed per dilution. The highest dilution with all positive wells were 10^{-2} and there were 16 positive microcultures with infections ranging from 10^{-2} to 10^{-4}, which is the last dilution where positive wells could be detected. As result,

$$= -2+1/2 -16/8= -3.5\ TCID_{50}$$

$$or\ 10^{3.5} TCID_{50}\ in\ 100\ \mu l\ volume.$$

$$Therefore,\ the\ virus\ titer\ can\ be\ expressed\ as\ 10^{4,5}\ TICD_{50}/ml\ or\ logTCID_{50}/ml = 4,5$$

End-point dilution assay was used to determine titer of virus supernatant collected from growth assays.

3.2.3.3 Characterization of viral growth by multi-step growth curves

Growth assays were performed to compare growth kinetics between the recombinant RSV mutants and its parental strain RSV A2-K-line19F as well as with the clinical strain RSV A2. As RSV infection can spread very rapidly and the cell monolayers can be destructed within several days, multi-step growth assays at MOI 0.1 were performed to enable monitoring the virus growth within 6 days without massive cell destruction. For the assay, $3x10^5$ Vero/well were seeded on 6-well plates a day prior experiment to ensure adhesion of the cells to the bottom of the wells. To infect $3x10^5$ cells at MOI 0.1, $3x10^4$ FFU were needed. Therefore, frozen aliquots of virus supernatant were thawed and diluted to $3x10^4$ FFU/ml. Each well was then inoculated with 1 ml of the virus dilution and incubated for 4h at 37°C, 5% CO_2. Additionally, 1 ml of the virus input was retained and frozen at -80°C. After the incubation time, virus supernatant was removed, of which 1 ml was aliquoted and stored at -80°C.This served as sample for day 0. Wells were refilled with 2 ml growth medium/well. Virus growth was monitored for 6 days. For each day, approx. 1 ml virus supernatant was taken from a well and stored at -80°C. On the first day, samples were taken at 2 different time points and from the 2^{nd} to the 6^{th} day once a day. Each growth assay was performed in triplicate. Subsequently, log $TCID_{50}$/ml values of the collected virus supernatants were determined by end-point dilution assay as described above and plotted against the time.

3.2.3.5 Characterization of viral growth by flow cytometry

Viral growth was additionally characterized by flow cytometry due to the fact that only 5% of the progeny virus are fully budded and 95% of those remain associated with the host cell membrane (Collins et al. 2013). Furthermore, interactions between RSV and cellular actin as well as filopodia formation facilitate virus cell-to-cell spread (Ulloa et al. 1998, Mehedi et al. 2016, Mehedi et al. 2017). Hence, monitoring of only the virus titer in the supernatant is not sufficient to capture the whole growth kinetics for RSV. For this reason, an assay to measure how virus spreads in the cellular monolayer using flow cytometry was established.

3.2.3.5.1 Preparation of cell cultures for flow cytometry

To perform this assay, 1.5 x 10^5 Vero cells/well were seeded on a 6-well plate one day prior to the experiment to ensure the adherence of the cells on the bottom of the wells. Analogous to assays with multi-step growth curves, infections were monitored once a day for 6 days and for each RSV mutant three experiments were performed. On the following day, cells were infected with 1 ml viral supernatant at MOI 0.5. After 20 hours, supernatants were aspirated and replaced with 2 ml of fresh medium. The first measurement was performed at 20-24 hpi. Therefore, medium was aspirated, and cells were washed with 1 ml DPBS. Next, 500 µl of TrypLE Express were added to each well and incubated for 5 min at RT. The dissociation reaction was stopped with 500 µl of DMEM and cells were detached from the bottom of well by pipetting up and down. Cells were subsequently washed by centrifugation at 500 x rcf for 5 min and resuspended in 1ml PBS. To distinguish viable from dead cells, the cell suspensions were incubated in 2 ml PBS containing 0.8 µl fluorescein diacetate (FDA) stock solution (0.4 µg/ml) for 30 min at 37°C. Cells were than washed by centrifugation at 500 x rcf for 5 min and resuspended in 800 µl PBS. Thereafter, flow cytometry was performed with a FACS Calibur flow cytometer. Fluorescent signals were detected by using the green channel FL1 using bandpass filter 530/30 nm (excited by blue laser 488 nm) and using the red channel FL4 with bandpass filter 661/16 nm (excited by red diode laser~ 635 nm). FACS was automatically stopped as 1x10^4 viable cells passed through the detector. A negative control was prepared in parallel and treated in the same way. This negative control was used to set the photomultiplier (PMT) voltage in FL1. In contrast, PMT voltage in FL 4 was held constant.

FDA is a non-fluorescent molecule that is hydrolysed by the cell-permanent esterase to the green fluorescent fluorescein in living cell. The two acetyl groups on the xanthene backbone render the dye not only a non-fluorescent character but also a freely passive diffusion through a phospholipid bilayer possible (Boyd et al. 2008). Once hydrolysed in aqueous medium, due to a charged groups – the carbolic acid groups- in the fluorescein, this molecule cannot cross the plasma membrane anymore (Hong et al. 2013). By interacting with the intact cell membrane, this fluorescent product can be retained within the cell up to 2 h (Thermo Fisher, Figure 13). Thus, FDA can be used as viability probe to measure both enzymatic activity and cell-membrane integrity. Fluorescein has an excitation maximum at 494 nm and an emission maximum at 521 nm (Figure 14), so its fluorescence can be detected by the green channel of FACS Calibur.

The RSV-BAC harbors a gene encoding a far-red fluorescent protein - mKate2 - that enables a tracking of infection by fluorescence. mKate2 is the next generation of the reported far-red fluorescent protein mKate (Shcherbo et al. 2007, Shcherbo et al. 2009). mKate2 has an excitation maximum at 588 nm and an emission maximum at 635 nm, and is almost 3-fold brighter than its prototype and is 10-fold brighter than mPlum (Shcherbo et al. 2009). Due to the high-brightness, this protein is detectable with the red channel of FACS Calibur, although it is excited by the red diode at ~635 nm, a suboptimal excitation wavelength (Figure 14). Furthermore, the emission spectrum of fluorescein overlaps the excitation spectrum of mKate2, which means that this fluorochrome pair fluorescein/mKate2 could function as a tandem dyes and fluorescein emission can strengthen the excitation of mKate2.

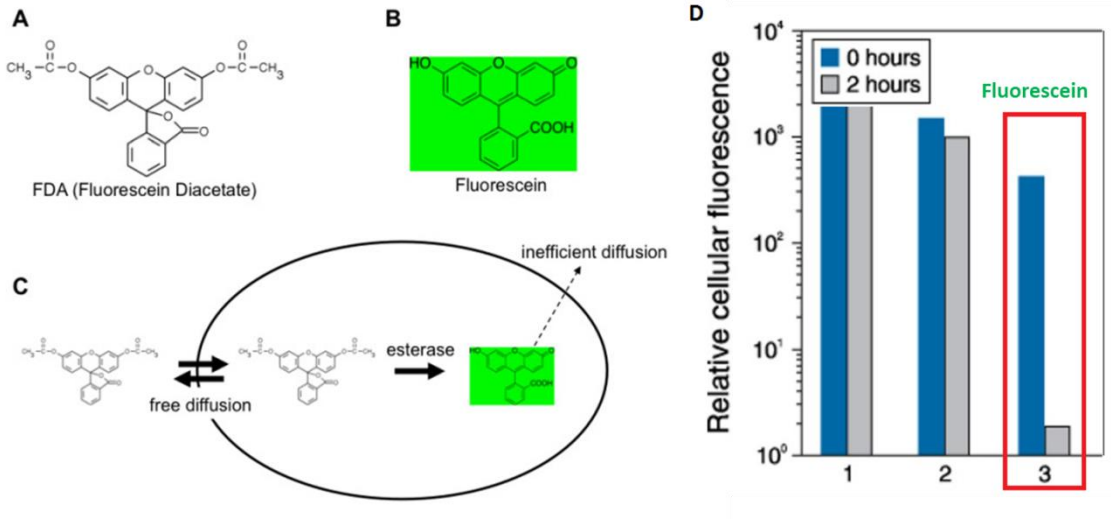

Figure 13: Mode of action and retention characteristic of fluorescein. Chemical structure FDA (A), chemical structure fluorescein (B), illustration of the chemical reaction in the cell (C), retention characteristic of fluorescein measured by flow cytometry (D) (modified figure from Hong et al. 2013 and from Thermo Fisher)

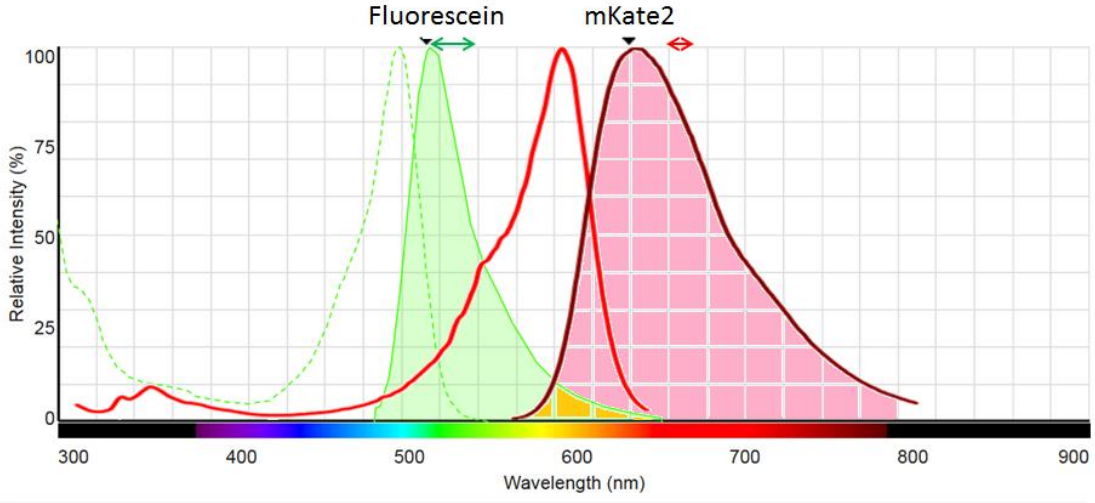

Figure 14: Excitation/emission spectra of fluorescein and mKate2. Fluorescein has an excitation maximum at 494 nm and an emission maximum at 521 nm. mKate2 has an excitation maximum at 588 nm and an emission maximum at 635 nm. The double-head arrows (green and red) indicate the wavelength characteristic of the bandpass filters in FL1 and FL4 of FACS Calibur (Evrogen and Thermo Fischer Fluorescence SpectraViewer, modified)

3.2.3.5.2 Evaluation of FACS data

Cells that were analysed by FACS as described above could be classified in 3 populations while plotting against signals for fluorescein and for mKate2: (1) UL: viable un-infected cells; (2) UR: viable infected cells; and (3) LL+LR: dead cells with low esterase activity or without cell-membrane integrity (Figure 15). Negative controls were prepared and measured to define the borders that distinguished infected from un-infected cells by the transmitted signal of mKate2, as well as living from dead cells by the signal for fluorescein (Figure 15, B). Cell death in un-infected samples were also analysed. The infection rate was defined as the proportion of all infected cells in the population and calculated as sum of UR+LL+LR. This is based on the observation that cell death was negligible in the un-infected controls, and was clearly higher in the infected samples. Furthermore, dead cells in all infected samples still exhibited slight signal for mKate2, whose intensity was stronger than that from uninfected cells but weaker that that from infected cells. Cell death and infection rates of each strain were than calculated as average of 3 independent experiments and were plotted against the time.

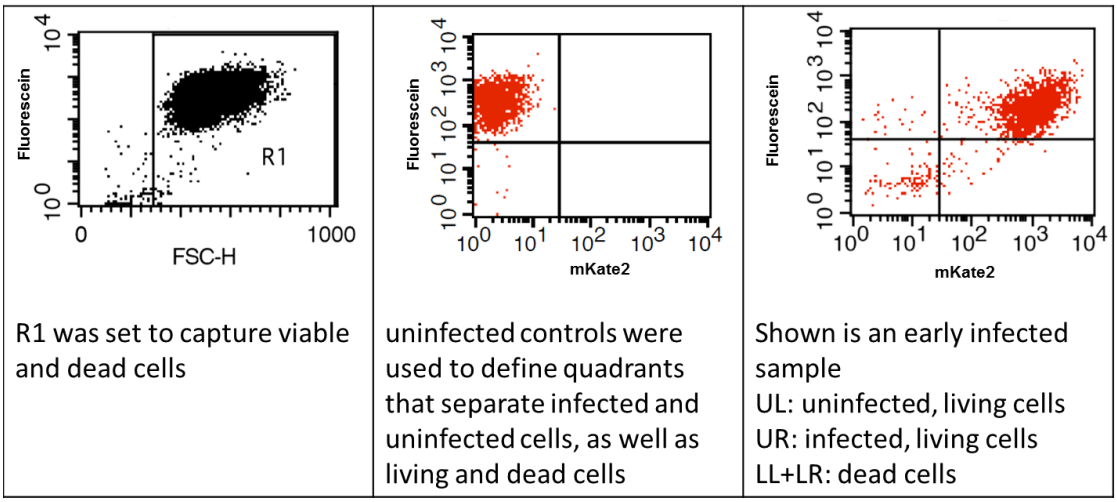

Figure 15: Gating strategy for flow cytometry. R1 was set while analysing the data to separate cells from debris by FCS signal. The cell population in R1 was then separated by their signal for fluorescein and for mKate2. Cells with positive signal for fluorescein are viable, and cells with positive signal for mKate2 are infected. Negative controls were used to set quadrants that delimit viable un-infected (UL) from infected (UR) cells as well as viable (UL+UR) from dead (LL+LR) cells.

3.2.3.4 Phenotypic characterization of recombinant RSV by PRNA

One important objective of phenotypic characterization of recombinant virus is their susceptibility again antivirals. Within the framework of this study, recombinant RSV mutants were tested against palivizumab. For this purpose, plaque-reduction neutralization assays (PRNA) were performed.

3.2.3.4.1 Performing plaque-reduction neutralization assays (PRNA)

One day prior experiment, 2 x 10^4 Vero cells/well were seeded on a 96-well plate to ensure that cells could growth to confluence on the bottom of the wells. On the day of experiment, seven 4-fold serial dilutions of palivizumab starting from 8 µg/ml were prepared. A virus stock was thawed at RT and diluted to 2000 FFU/ml. For neutralization, virus dilutions and antiviral solutions were mixed together in a ratio of 1:1 and incubated at 37°C, 5% CO_2 for 1 h. Resulting from this, the end concentrations of antiviral and of virus were reduced by half, in particular, the virus titer was 1000 FFU/ml and 4 µg/ml was the highest concentration in the 4-fold serial dilution of the drug. More details are illustrated in Figure 16. Additionally, an un-neutralized control was prepared and treated in the same way but with DMEM instead of the drug dilution (Figure 17). Later on, counted plaque numbers in this dilution were normalized to 100% in the analysis. Afterwards, growth medium was aspirated and 100 µl of the by palivizumab neutralized RSV as well as the un-neutralized RSV was added to the cell monolayers and centrifuged at 1200 rpm, 37°C for 30 min. Plating is illustrated in Figure 17. Subsequently, plate was incubated at 37°C, 5% CO2 for further 1.5 h. In the mean time, the overlay medium was prepared by mixing 2% methylcellulose (MC) in PBS with DMEM (5% FCS, 1% P/S) in ratio 1:1 and pre-warmed at 37°C. After the incubation period, 100 µl of the overlay medium were added to test wells and incubated for 4 days, at 37°C and 5%CO_2. During the incubation time, care was taken not to disturb the plate to prevent forming of uneven plaques. For each RSV strain, 4 PRNAs were performed and each as quadruplicate, with an exception that the un-neutralized control was performed in octuplicate for the purpose of a better normalization. Additionally to each test, a cell control and a virus control (w/o methylcellulose) were also prepared.

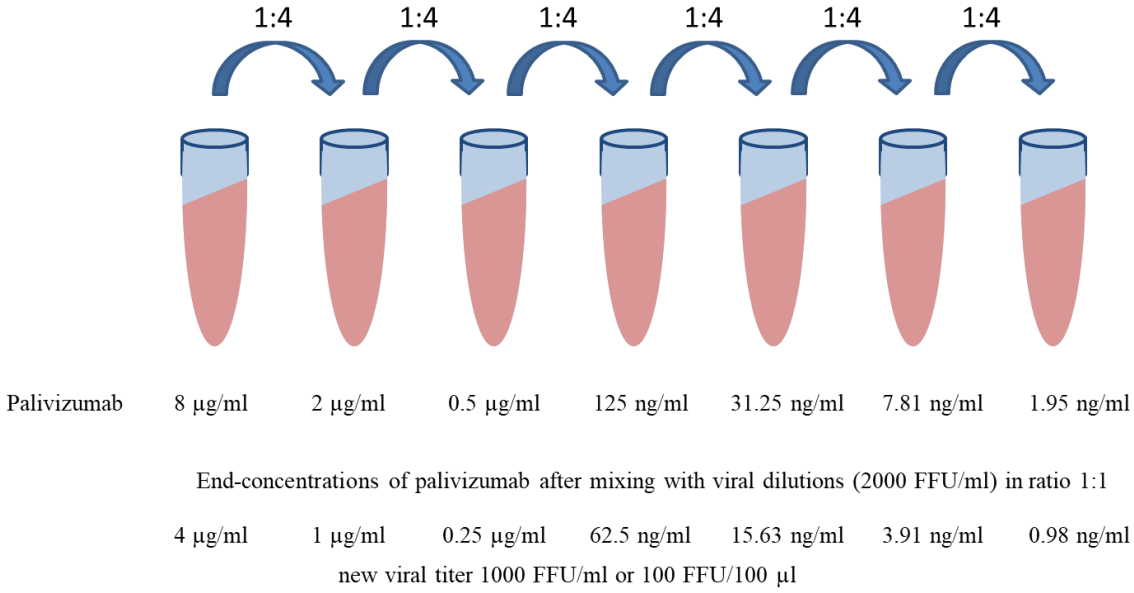

Figure 16: Preparation of palivizumab-RSV dilution for plaque-reduction neutralization assay. Viruses were neutralized at different drug concentration for 1h at 37°C, 5%CO_2. After the overall infection time of 2h, overlay medium containing 1% methylcellulose was added to testwells and plate was incubated for 4 days at 37°C, 5%CO_2. Evaluation was performed by counting the plaque number and subsequent, the IC_{50} values for each strain were calculated using the curve fitting program of GraphPad Prism 7.03.

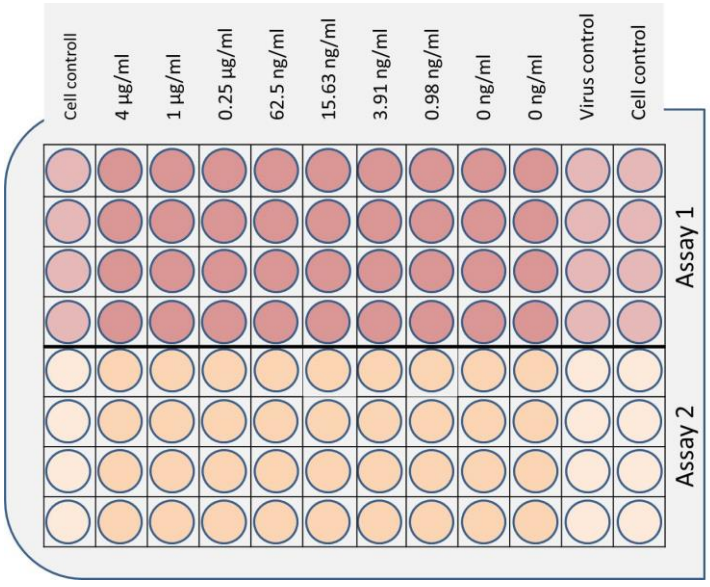

Figure 17: Illustration of sampling a plate for PRNA. For each drug dilution, test was performed in quadruplicate. Except for the un-neutralized control (w/o palivizumab), the test was performed with 8 replicas. The virus control was incubated in absence of methyl cellulose to visualize its direct effect on the spread of infection.

4 days later, plates were evaluated by counting the number of plaques in each well or fixed with 100 µl of 2%PFA for 10 min at 37°C for later evaluation. A plaque was defined as an assembly of at least 10 infected Vero cells. For the clinical strain RSV A2, viral proteins were visualized prior evaluation by immunofluorescence as described above in 3.2.3.1. IC_{50}, the concentration at which 50% of infection was inhibited, was determined using curve fitting program of GraphPad Prism 7.03. Note, for the RSV resistance control strain K272E, an additional 10-fold serial dilution of palivizumab was performed, that ranged from 10 mg/ml to 1 µg/ml (neutralizing concentration from 5 mg/ml to 0.5 µg/ml).

3.2.3.4.2 Test of a new overlay with colloidal microcrystalline cellulose

Since RSV progeny is released into the supernatant and new virions can infect surrounding uninfected cells and additionally cause undesired plaques, which bias the evaluation. Use of a high-viscosity overlay medium containing such as agarose or methylcellulose (MC) can restrict the spread of new progeny viruses to neighbouring uninfected cells. However, applying of media containing agarose or methylcellulose in 96-well culture plates is discouraging due to the high viscosity of the solution. A new low-viscosity overlay for viral plaque assays with Avicel RC/CL® was already described elsewhere (Matrosovich et al. 2006). Avicel RC/CL is originally a product brand of FMC Corporation and there are 4 types of Avicel RC/CL: RC-501, RC-581, RC-591 and CL-661 (Dell and Colliopoulus 2001). Avicel RC/CL mixtures are blends of microcrystalline cellulose (MCC) and sodium carboxymethylcellulose (NaCMC) at different ratio, whereby the fraction of NaCMC ranges from 7.1 to 18.8 % (Dell and Colliopoulus 2001, Signet Chemical Corporation 2018). A similar product to Avicel CL-661 (11.3-18.8 % NaCMC) is the colloidal microcrystalline cellulose of Sigma-Aldrich supplement with 10.0-20.0% NaCMC as stabilizer (435244 Aldrich). Like Avicel CL-661, this excipient also forms thixotropic gels and has a good thermal stability (Sigma-Alrich 2018). Thixotropic is a time dependent behaviour of an isothermal system in which the apparent viscosity decrease under mechanical stress, followed by a gradual recovery when the stress is removed (Hahn et al. 1959). Hence, a thermostable thixotropic overlay media is very attractive for experimenter, as it is easy in handling (mixing and pipetting) and likewise the virus spread can be controlled during the incubation time as the liquid becomes more viscosity while resting. For this

reason, the colloidal microcrystalline cellulose blend of Sigma-Aldrich is a promising candidate for replacement of methylcellulose in the overlay medium for PRNA. And this is to be investigated with a small test in this study.

Therefore, $2x10^4$ Vero/well that were seeded in a 96-well plate the day before, were infected with approx. 100 FFU/well in a volume of 100 µl. Subsequently, the plate was centrifuged at 1200 x g for 30 min and incubated at 37°C, 5 % CO_2 for further 1.5 h. In the meantime, overlay media with following concentration of supplement were prepared by mixing the stock solutions (colloidal MCC 3% and MC 2%) with DMEM:

- Colloidal MCC 1%, 2%, 3%

- MC 1%

All media were pre-warmed at 37°C. After the incubation period, 100 µl of each overlay media were given directly into the well without aspirating the virus supernatant. This results following concentration in the end volume:

- Colloidal MCC 0.5%, 1% and 1.5%

- MC 0.5%

On the 4^{th} of incubation at 37°C, 5% CO_2, supernatant was discarded, and cells were washed twice with 100 µl RT PBS. Following, formed plaques were evaluated under fluorescence microscopy.

4 Results

4.1 Generation of recombinant RSV with defined mutations

In this study, the following F gene mutations were identified from clinical isolates and phenotypically characterized concerning viral growth and susceptibility to palivizumab: C21G, Q34R, R49K, T100S, A103P, A518V, C550Y, and 3 mutation combinations C21G/R49K, Q34R/C550Y and T100S/A518V. Additionally, mutation K272E and N276S were also investigated. They served as palivizumab resistant and sensitive control, respectively. Mutation K272E locates within the binding epitope of palivizumab on the fusion glycoprotein F, the antigenic site A. This amino acid change was previously showed to confer stable resistance to palivizumab (Adams et al. 2010, Zhu et al. 2011, Zhu et al. 2012). Mutation N276S was firstly proposed to be responsible for a RSV breakthrough in a child under palivizumab prophylaxis by Adams et al. 2010, which was then well discussed and denied by further researchers (Zhu et al. 2011, Papenburg et al. 2012, Zhu et al. 2012, Yasui et al. 2016). Including the parental reference strain RSV A2-K-line19F that directly rescued from RSV-BAC pSynkRSV-l19F, the palivizumab resistant (K272E) and sensitive control (N276S) strain, there were in total 13 recombinant RSV variants, which were generated and characterized in this study. Furthermore, phenotype of the clinical strain RSV A2 (ATCC®VR-1540P™) was also examined using the same methods.

4.1.1 Generation of PCR-products with defined point-mutations

Mutagenesis PCR were performed as described in 3.2.2.1 and PCR-products were than separated on 1% agarose gel in order to control the success of amplifications (Figure 18). All PCR-products were approximately 1120 bp in length, of which the longest section was the positive selection marker, the kanamycin resistance gene KanR with 995 bp. This segment was flanked in both down- and upstream directions with homologous sequences (each 61-63 bp) (reference gene: RSV line 19) harboring the new nucleotide sequence (Figure 7). This resulted in that all PCR fragments were about 1120 bp in length. Lengths of all PCR fragments are listed in Table 10.

Mutation	Length [bp]
C21G	1121
Q34R	1117
R49K	1117
T100S	1117
A103P	1121
A518V	1117
C550Y	1121
K272E (resistant control)	1121
N276S (sensitive control)	1121

Table 10: Lengths of all mutagenesis PCR-fragments. The longest section in all PCR-fragments was the positive selection marker (995 bp) that was amplified from plasmid pEPkan-S (lengths of fragments were calculated with SerialCloner)

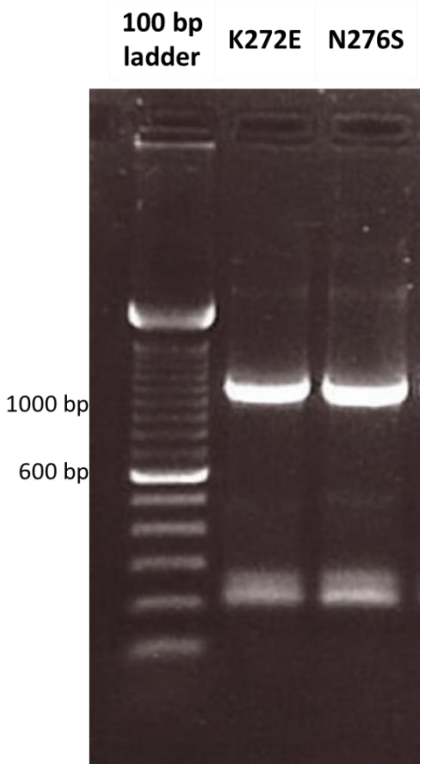

Figure 18: Separation of mutagenesis PCR-products on 1% agarose gel. PCRs for mutation K272E and N276S are shown. The extra band (~210 bp) is suggested to be primer dimer.

4.1.2 BAC-mutagenesis and sequencing of the respective regions on the fusion (F) gene

En passant mutagenesis requires that the PCR-product and the RSV-BAC pSynkRSV-l19F (Hotard et al. 2012) are both present within *E.coli* GS1783 strain. Thus, the BAC DNA was previously transformed into *E.coli* GS1783 to generate *E.coli* GS1783/pSynkRSV-l19F strain.

4.1.2.1 Generation of *E.coli* GS1783/pSynkRSV-l19F

E.coli GS1783 were prepared for electroporation by cool washing and chilling on ice. Subsequently, pSynkRSV-l19F BAC DNA was transformed into *E.coli* GS1783 by electroporation. Bacteria were then plated onto LB-agar plates containing chloramphenicol. After an incubation period of 24h, bacterial growth in the presence of chloramphenicol indicated that transformation of the BAC DNA into E.coli GS1783 was successful. Results were additionally verified by sequencing. Several glycerol stocks of *E.coli* GS1783/pSynkRSV-l19F were prepared and stored at -80°C.

4.1.2.2 BAC-mutagenesis of pSynkRSV-l19F with defined point mutation

Recombinant RSV-BACs with defined mutations were generated by *en passant* mutagenesis in *E.coli* GS1783/pSynkRSV-l19F. Each PCR product was respectively transformed into the *E.coli* GS1783/pSynkRSV-l19F by electroporation. The first recombination that was induced at 42°C resulted in the integration of the whole PCR-fragments into the RSV BAC pSynkRSV-l19F. Bacteria, in which the first recombination had been successful, exhibited resistance to chloramphenicol and kanamycin, and their colonies became visible on LB-agar plate after an incubation time of 24 h. This could be achieved for all 9 single mutations: C21G, Q34R, R49K, T100S, A103P, K272E, N276S, A518V, and C550Y. The second recombination was to remove the positive selection marker, the kanamycin resistance gene KanR. For each mutation, this step was performed with 2-4 bacterial colonies. Negative selection for loss of the KanR gene was conducted by comparing bacterial growth in the presence of either chloramphenicol or both chloramphenicol and kanamycin. Bacteria that solely grew in the presence of chloramphenicol but absence of kanamycin might contain the correct mutated RSV BAC from which the KanR gene was successfully removed. Sequencing

of the respective regions on F gene was performed to verify the success of BAC mutagenesis. Again, this was successfully performed for all 9 single mutations C21G, Q34R, R49K, T100S, A103P, K272E, N276S, A518V, and C550Y. Note, for each mutation 4-6 kanamycin sensitive bacterial colonies were selected for sequencing. Interestingly, some of them contained the sequence of the parental strain without the desired mutation. Recombinant RSV BAC with double mutations was generated by successive introduction of each mutation into the BAC. Again, this was attained for all 3 double mutations: C21R/R49K, Q34R/C550Y and T100S/A518V. Relevant sequences containing the mutations are shown in Figure 19 (for single mutations) and Figure 20 (for double mutations).

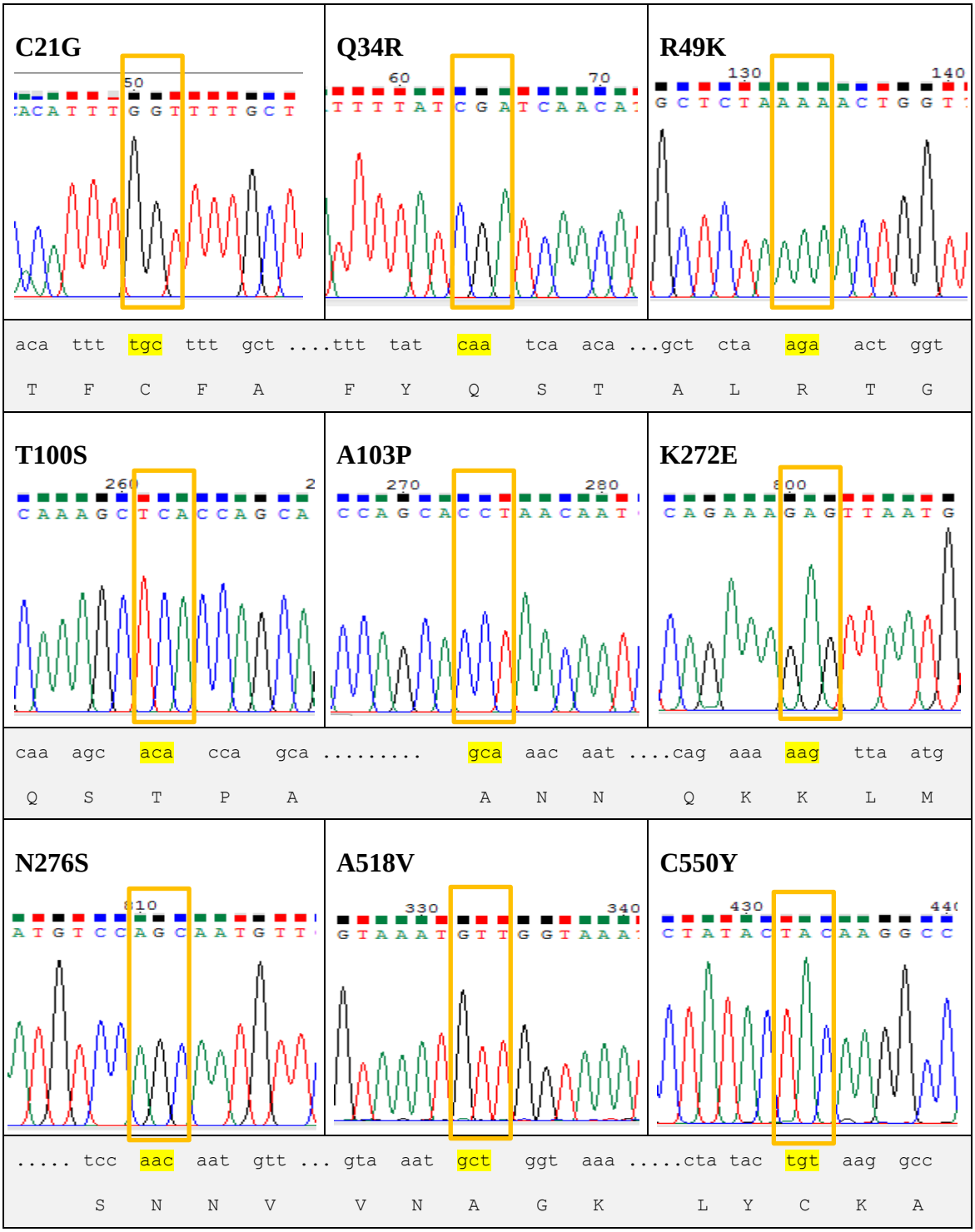

Figure 19: Sequence analysis after BAC-mutagenesis. Mutagenesis was successful conducted for all 9 single mutations C21G, Q34R, R49K, T100S, A103P, K272E, N276S, A518V, and C550Y. Chromatogram depicted regions of interest with new nucleotides. In grey: sequence of the parental strain pSynkRSV-l19F, yellow marked: target codon, orange box: the mutated codon with base substitutions.

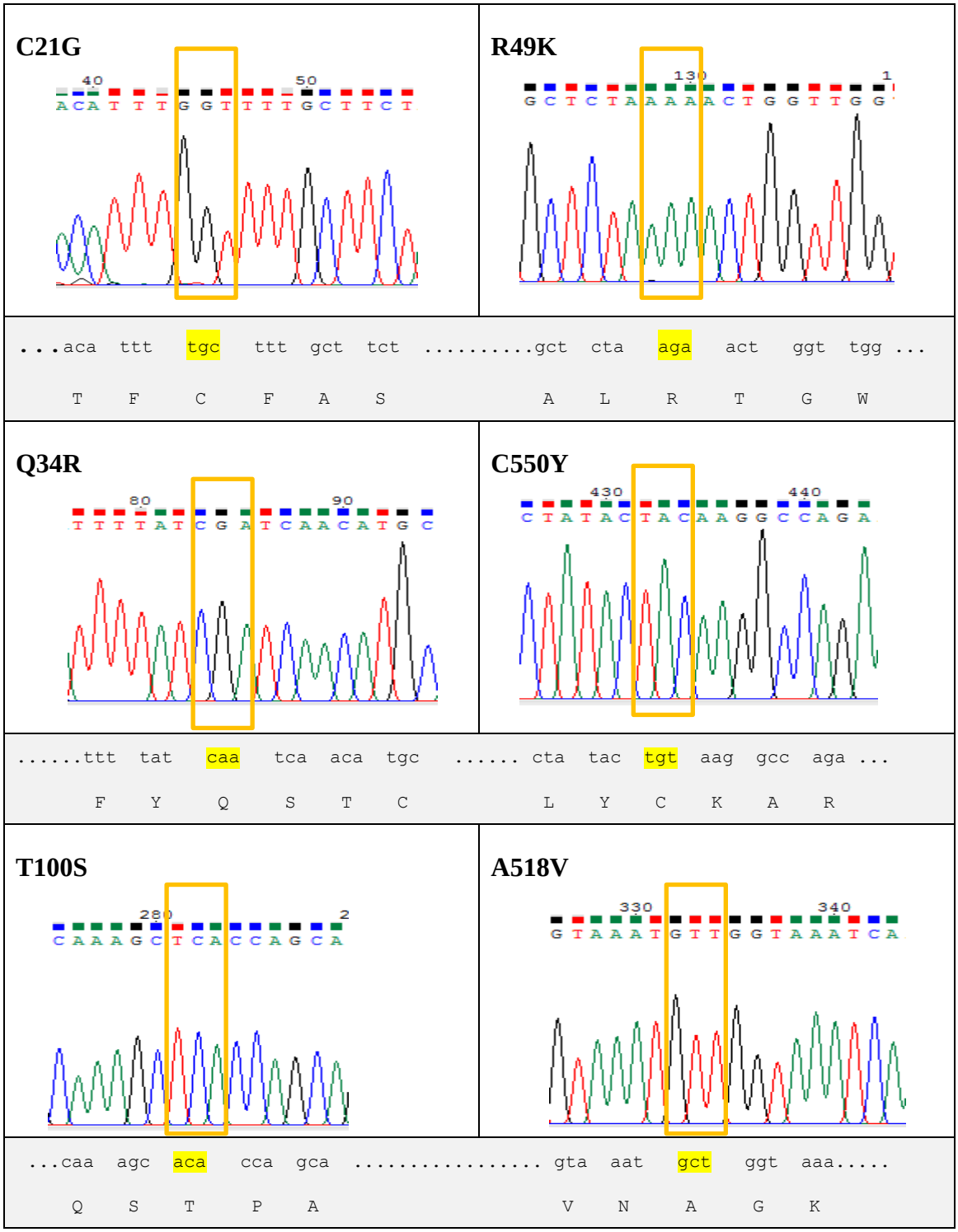

Figure 20: Sequence analysis after BAC-mutagenesis. Mutagenesis was successful for all 3 double mutations C21R/R49K, Q34R/C550Y and T100S/A518V. Chromatogram depicted regions of interest containing new nucleotides. In grey: sequence of the parental strain pSynkRSV-l19F, yellow marked: target codon, orange box: the mutated codon with base substitutions.

4.1.3 Transfection of RSV BAC DNA into BSR T7/5 and recovery of recombinant RSV

After verifying that the desired mutation had been successfully introduced into the RSV BAC pSynkRSV-l19F, recombinant BAC-DNA was isolated from bacteria by midi-preparation and its transfection into BSR T7/5 was usually performed on the following day as described in 3.2.2.9. Was the transfection successful, red fluorescence that indicated the recovery of recombinant RSV could be detected already 2 days after transfection and plaque were visible after 5 days (Figure 21). A plaque was defined as an assembly of at least 10 infected cells. Red fluorescence signalled expression of the mKate2 protein (Shcherbo et al. 2009), which is encoded on the BAC pSynkRSV-l19F (Hotard et al. 2012). Transfection of only RSV BAC DNA without helper plasmids resulted in no virus recovery. After 2-3 passages in BSRT7/5 cells, viral supernatant was harvested and enriched by one freeze-thaw cycle of the cell monolayer. Part of this supernatant was then used to infect Vero cells for further virus propagation. On Vero cells, it usually took further 3-4 passages until the cell monolayer got 100% infected. Note, one freeze-thaw cycle (5 min at -80°C) was indispensable to enrich the virus titer to a sufficient amount for infectious assays. In addition, the genome of the unmutated BAC pSynkRSV-l19F was also transfected into BSR T7/5 cells to reconstitute the parental viral strain that served as the reference strain in all phenotypic characterization assays. Transfection and virus propagation could be attained for all 13 recombinant RSV strains.

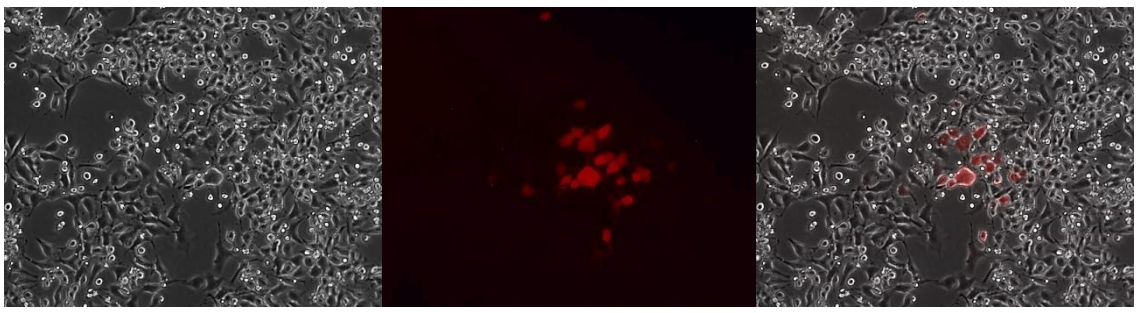

Figure 21: Reconstitution of recombinant RSV after transfection of BAC DNA into BSR T7/5. Fluorescence signal was already detectable on the 2nd day post transfection. Shown is CPE that was observed at the 5th day post transfection.

4.2 Phenotypic characterization

In this part of the study, recombinant RSV variants that recovered from RSV-BAC pSynkRSV-l19F/MUT were characterized by their growth kinetics and palivizumab susceptibility. The parental strain RSV A2-K-line19F that rescued from the unmutated BAC pSynkRSV-l19F served in all assays as the reference strain. Furthermore, differences between this parental strain and the clinical strain RSV A2 (ATCC® VR-1540P) were also investigated for a better understanding about the phenotype of this strain.

4.2.1 Characterization of viral growth by multi-step growth curves

To investigate the influence of the introduced mutations on the virus replication, multi-step growth assays were performed for each RSV variants as described in 3.2.3.3. For this assay, Vero cells were infected with RSV at MOI 0.1. Virus supernatants were then collected throughout 6 days, stored at -80°C and subsequently the log$TCID_{50}$/ml values of all supernatants were determined according to the Spearman Kärber method as described in 3.2.3.2. Each growth assay was performed as triplicate. The results are displayed below in different ways to enable the best interpretation of the data. The mean values of the virus titers are listed in Table 11. The same data were illustrated as a gradient heat map in Figure 22. Growth curves with means and SD are plotted against the time in Figure 23.

Following conclusions could be visualized from the data. In all cases, extracellular release of virus progeny could already be detected 1 day after infection. There were clearly differences in the virus titers between the first (~20 hpi) and the second sampling (~26 hpi) on the first day of infection. Thereafter, virus progenies kept accumulating in the supernatant and the virus titers increased continuously until days 3, thereupon a plateau was reached. In most of the cases, the highest virus titers within plateaus were on days 4-5 (8/14 cases, 57.1%). 3/14 (21.4%) reached the highest titers on day 3rd and 3/14 (21.4%) on day 6th. The highest virus titers could be maintained for 1-2 days and afterwards, it decreased and increased slightly again. In general, the growth curves showed insignificant variations among all tested strains and even between the single and the double mutations harboring RSV strains.

The presence of an additional gene may result in a delay of viral growth and a decrease of virus yield in vitro and as well as a reduction of plaque diameter (Bukreyev et al. 1996). Although the growth curve for the RSV strain A2 started with a lower virus titer compared to the reference strain RSV A2-K-line19F (or RSV-BAC ref), but this strain yielded higher virus titers from the 2nd day on, and reached a higher plateau on the 3rd day, 24 h earlier than the RSV-BAC ref strain. Both strains reached their plateaus on day 3-4 and showed a slight decrease of the virus titers on day 5-6. However, these differences were not significant. Indeed, the RSV-BAC ref that contained an additional gene mKate2 as an infection reporter gene grew by tendency more slowly and yielded a slightly lower titer, but these discrepancies were not significant when the standard deviations of the measurements were taken into account.

Virus recovered from RSV-BAC pSynkRSV-l19F/T100S and RSV-BAC pSynkRSV-l19F/K272E reached slightly lower plateau concentrations in comparison to others, despite both showed higher virus titers at the day of inoculation, day 0. The same observation held true for the double mutations harboring strain RSV A2-K-line19F/T100S/A518V (or RSV-BAC T100S/A518V). However, this strain was inoculated at a lower MOI. RSV A2-K-line19F/A518V showed stable growth kinetics during the whole test period of 6 days. This strain was inoculated at a moderate MOI and the virus titer started increasing from the 1st day on without any drop and reached the overall highest titer (6.8 log$TCID_{50}$/ml) on the 6th day. The same statement held true for strain RSV A2-K-line19F/A103P, which reached a lower final titer of 6.3 log$TCID_{50}$/ml on the 6th day. Calculated values for the growth curve of RSV A2-K-line19F/C21G/R49K strain showed remarkable variations within replicate measurements as well as high standard deviations compared to that of other strains.

Figure 22: Growth assays depicted as gradient heat map. The numeric data from Table 11 are transformed into a gradient heat map. The lowest value is represented in white and the highest value in dark blue. For all RSV strains, viral growth reached there plateaus after 3-4 days of. Small fluctuations in the virus titers could be observed during the plateau periods.

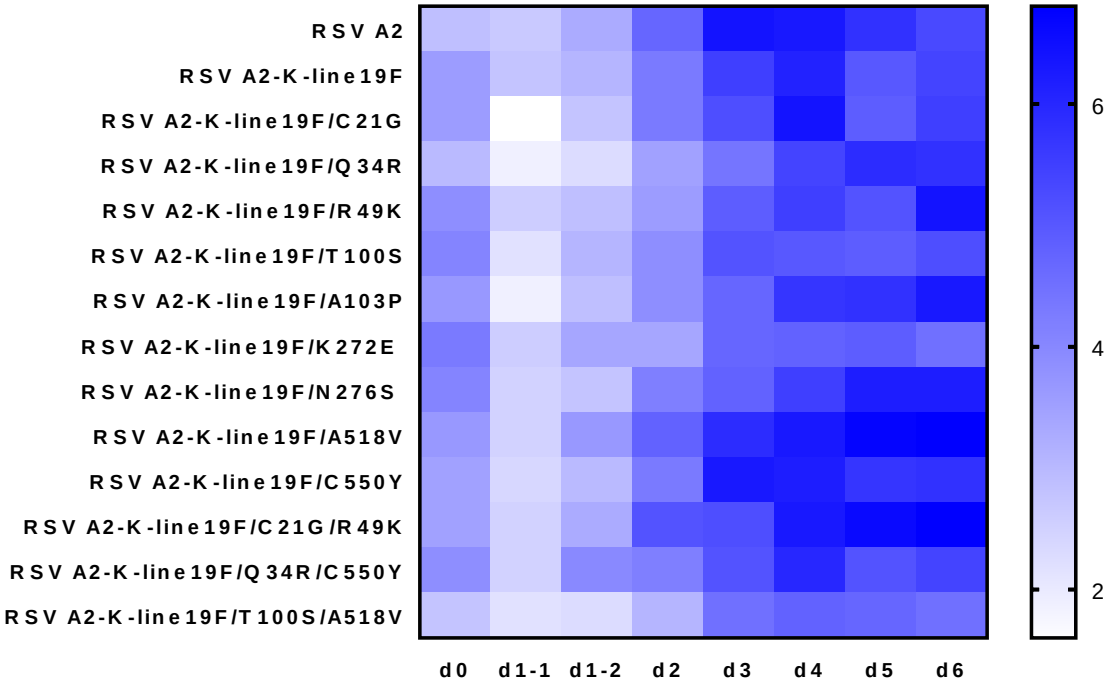

Table 11: Growth analysis of all RSV variants. The virus supernatants from infected Vero cells were collected throughout 6 days, twice on the first day, and once on 2nd to 6th days. The virus titers of these supernatants were calculated according to the Spearman Kärber method and mean values are shown below (**logTCID$_{50}$/ml)**. For each viral strain, 3 experiments were performed. The first highest peak in each growth curve is marked with dark grey.

Viruses	d0	d1[1]	d1[2]	d2	d3	d4	d5	d6
RSV A2	2.9	2.7	3.3	4.7	6.4	6.3	5.8	5.3
RSV A2-K-line19F	3.6	2.8	3.1	4.3	5.5	6.1	5.0	5.4
RSV A2-K-line19F/C21G	3.6	1.6	2.8	4.3	5.2	6.4	4.9	5.5
RSV A2-K-line19F/Q34R	3.0	1.9	2.3	3.5	4.4	5.4	5.9	5.8
RSV A2-K-line19F/R49K	3.9	2.6	2.9	3.6	4.9	5.5	5.1	6.4
RSV A2-K-line19F/T100S	4.1	2.2	3.1	3.9	5.1	5.0	4.9	5.2
RSV A2-K-line19F/A103P	3.7	1.9	2.9	3.9	4.7	5.7	5.8	6.3
RSV A2-K-line19F/K272E	4.3	2.6	3.4	3.4	4.7	4.8	4.9	4.5
RSV A2-K-line19F/N276S	4.1	2.5	2.8	4.2	4.8	5.5	6.2	6.2
RSV A2-K-line19F/A518V	3.7	2.5	3.7	4.8	5.9	6.3	6.7	6.8
RSV A2-K-line19F/C550Y	3.5	2.4	3.0	4.3	6.3	6.2	5.7	5.8
RSV A2-K-line19F/C21G/R49K	3.5	2.5	3.3	5.1	5.2	6.3	6.6	6.8
RSV A2-K-line19F/Q34R/C550Y	3.9	2.5	4.0	4.2	5.1	6.0	5.1	5.4
RSV A2-K-line19F/T100S/A518V	2.8	2.2	2.3	3.1	4.5	4.8	4.7	4.5

.

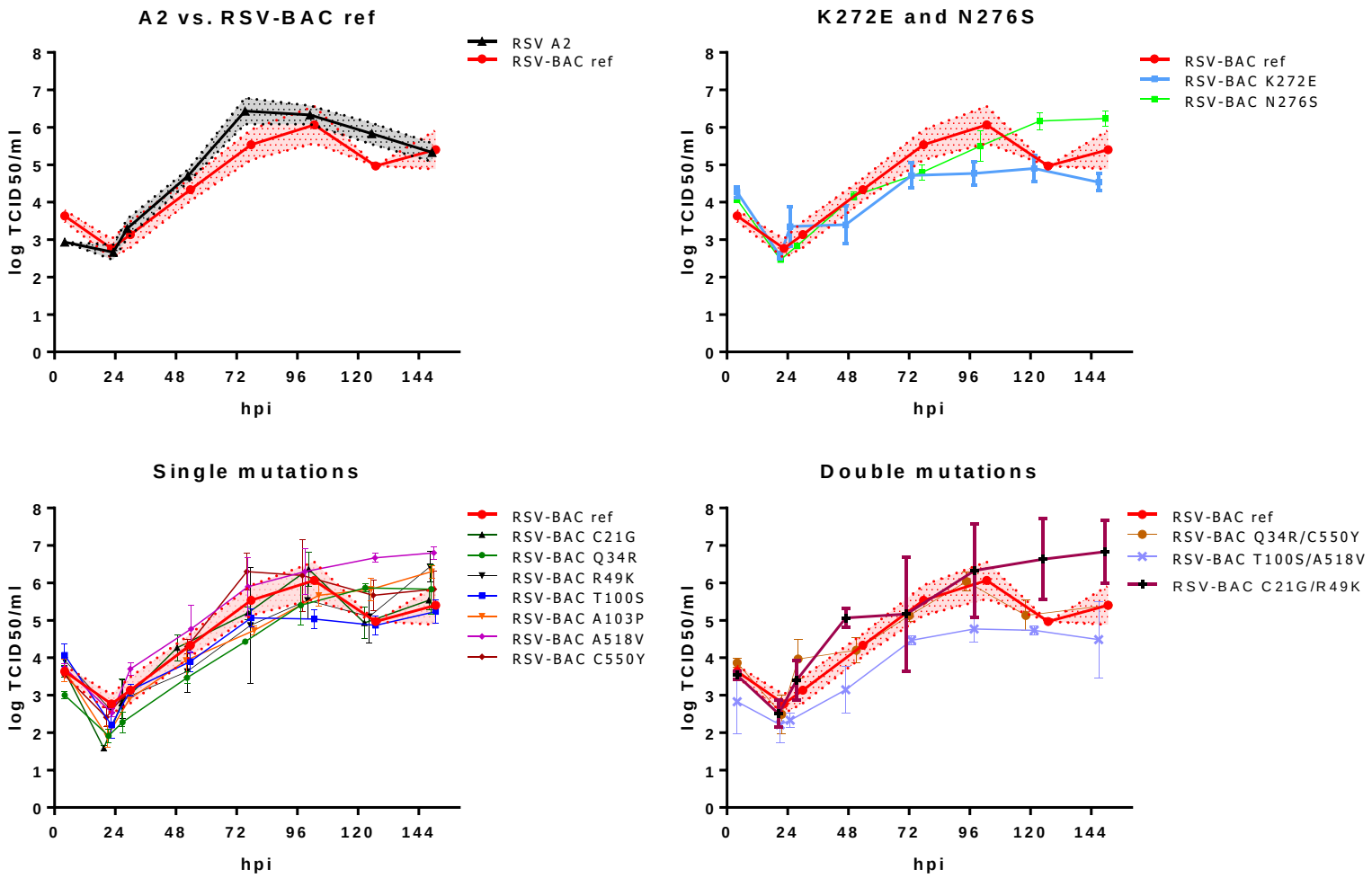

Figure 23: Multi-step growth curves. Vero cells were infected with different RSV strains at MOI 0.1, respectively. Virus supernatants were collected for 6 days and virus titers given as log $TCID_{50}$/ml (mean± SD) were calculated according to the Spearman Kärber method and plotted against the time. RSV A2 and RSV A2-K-line19F (or RSV-BAC ref) showed no significant discrepancies in their replications. RSV A2-K-line19F/K272E (or RSV-BAC K272E) yielded lower virus titers in plateau compared to the parental reference strain. Within the group of single mutations, there were no significant differences in the viral growth kinetics, which were comparable with that of the parental reference strain RSV-BAC ref. Within the group of strains with double mutations, the RSV-BAC T100/A518V reached slightly lower virus titer in plateau compared to others.

4.2.3 Characterization of viral growth by flow cytometry

This test was set-up to investigate the viral growth via spread of infection in the cell monolayer. Therefore, Vero cells were infected with RSV at MOI 0.5 and flow cytometry was performed over 6 days as described in 3.2.3.5.

Mock samples were prepared and treated in the same way to determine the fraction of dead cells in the cellular monolayer (Table 12). In the mock control, cell viability was well maintained during the first three days. Thereafter, cells became less viable. The overall highest cell death fraction observed in 6 experiments was 4.53%, which was measured on the 5th day of experiment E. Means of all 6 replicas (A-F) indicated that only a small fraction of cells died under these experimental conditions, in particular 2.5% was the highest mean value. Thus, remarkably higher cell death rates under the same experimental conditions would be linked with effects resulted from infections with the examined RSV strains, in a direct or indirect manner.

Table 12: Cell death in uninfected samples. Uninfected controls were prepared and treated in the same way as the infected samples. For this purpose, 6 experiments were prepared (named A - F).

Day	Cell death in the uninfected control (%)						
	A	B	C	D	E	F	Mean
1	0,34	0,71	0,33	0,8	0,83	0,22	0,54
2	0,35	0,23	0,32	0,8	1,48	1,86	0,84
3	0,39	0,26	1,42	1,37	1,15	1,28	0,98
4	0,49	0,85	0,57	2,3	1,05	3,1	1,39
5	2,03	0,85	2,6	4,01	**4,53**	0,96	**2,50**
6	1,68	2,19	2,55	1,24	2,03	1,59	1,88

An example of the kinetics of an RSV infection in Vero cells is shown in Figure 24. The UL quadrant depicts healthy uninfected cells, the UR viable infected cells. The LL+LR quadrants represent cells with low esterase activity or without cell-membrane integrity (indicated by the amount of intracellular fluorescein). Cells in LL+LR quadrants are considered as dead in this assay, as they showed fewer signals for the intracellular fluorescein. In all assays, the infected cell population grew within the first days of infection, and then decreased in line with the increasing dead cell population in the lower quadrants. For the infected samples, the fractions of dead cells were calculated by

adding the percentage in the LL and LR quadrants (dead cells = LL+LR) (Table 13). Compared to the uninfected control, the numbers of dead cells in infected samples were much higher and they were captured on the border between the LL and LR quadrant (Figure 24), which distinguished positive from negative signal of mKate2, a protein that indicates infection. Thus, it could be assumed that cell viability was somehow affected by an RSV infection. The infection rate describes the fraction of infected cells in a population that is at risk. To get this value, the cell fractions in UR, LL and LR quadrants were added together (infection rate = UR+LL+LR). For each RSV variant, 3 independent experiments were performed and results are listed in Table 13 and illustrated in Figure 24.

For 3 RSV strains, there were more infected cells on the first day of infection. These 3 strains are RSV A2-K-line19F (or RSV-BAC ref), RSV A2-K-line19F/R49K and RSV A2-K-line19F/C21G/R49K. Within these 3 strains, spread of infection proceeded with the same kinetics. Other strains in contrast showed small variations in their growth while starting with the same infection rate on the 1st day: A103P, Q34R/C550Y, T100S/A518V, Q34R, K272E, and A518V. The given order starts with the strain that spreads fastest and ends with the strains that spreads slowest. For all tested strains, it could be concluded that the infection spread from cell to cell with the same tendency, and that there were no significant differences between single and double mutations harboring strains. These results reflected outcomes of the multi-step growth assays.

In general, it could be observed that despite infection, Vero cells remained viable within the first 3-4 days after infection. The fractions of dead cells on the 6th day were associated with the initial infection rates on the 1st day. Samples, that showed higher infection rates at the beginning, exhibited higher cell death. RSV A2-K-line19F/R49K was an exception. This strain showed a lower death rate at day 5 and 6 compared to the reference strain RSV A2-K-line19F, although both showed the same behaviour in the courses of infection. Interestingly, this effect became less relevant as the mutation C21G get involved in, strain RSV A2-K-line19F/C21G/R49K. Note, these 3 strains showed the same progress of infection that began with a higher infection rates on the 1st day compared to other strains.

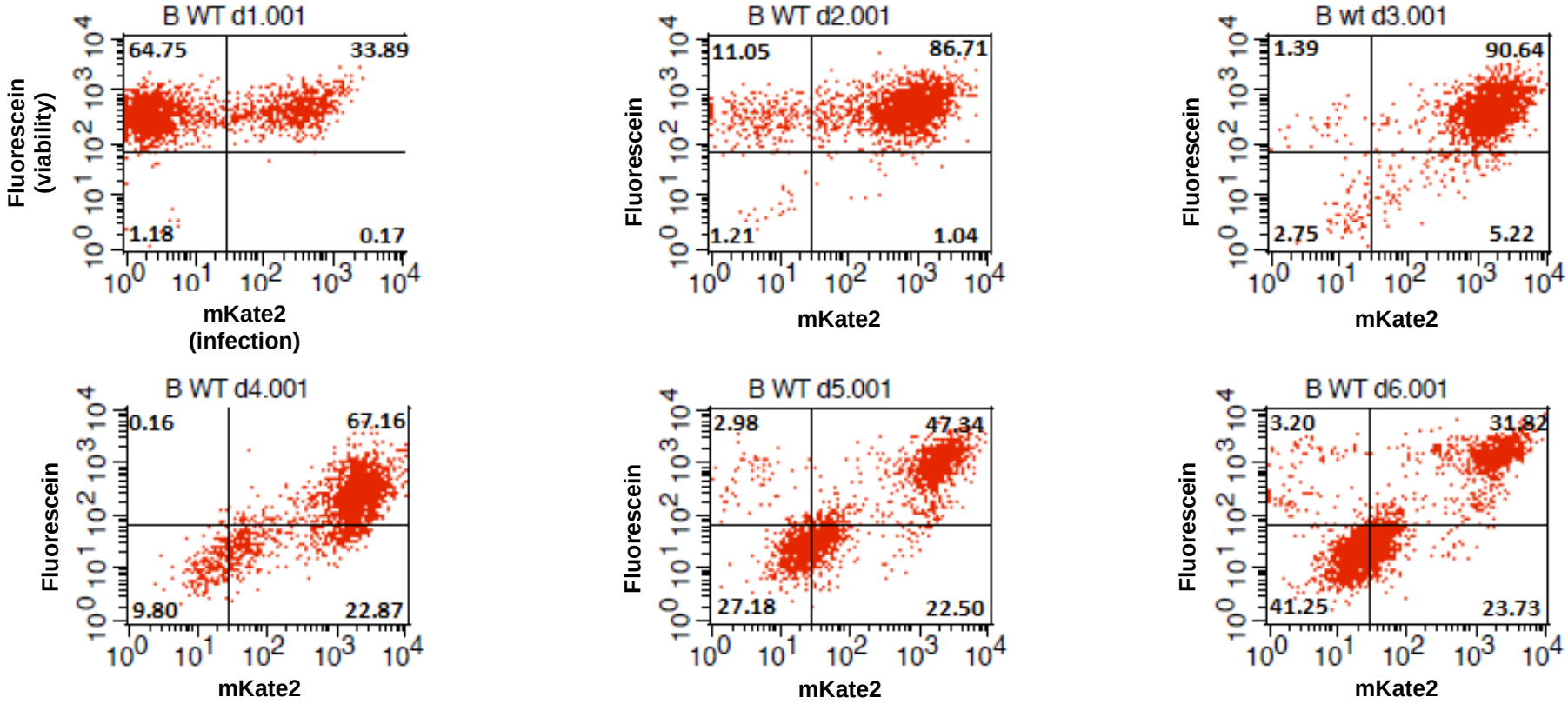

Figure 24: Results of a test for RSV A2-K-line19F. Vero cells were infected with RSV at MOI 0.5 and monitored for 6 days. Cell viability was measured by means of fluorescein and infection was traced with the on the RSV-BAC encoded mKate2 protein. The infected population grew within the first days of infection and shrank subsequently with the increasing of the less viable cell population which is presented in the lower quadrants. This kinetics was observed in all experiments.

Table 13: Cell deaths (%) and infection rates (%) within 6 days after infection. Average percentages of the dead cell populations and the infection rates for all recombinant RSV variants were calculated from 3 independent experiments. The infection rates were calculated as sum of the population in the UR and the LL+LR quadrants, and the cell death as sum of LL+LR.

	WT		C21G		Q34R		R49K		T100S		A103P		K272E	
Day	death	inf. rate	death	inf. rate	death	inf. rate	death	inf. rate	death	inf. rate	death	inf. rate	death	inf. rate
1	1.06	29.99	0.63	14.48	1.15	13.45	3.63	38.25	2.07	14.84	2.25	14.94	0.80	10.69
2	2.60	86.27	1.63	53.98	1.01	40.83	8.16	85.12	4.81	53.47	8.29	47.93	0.85	32.90
3	5.97	98.57	4.31	89.46	1.99	70.95	6.30	97.78	2.46	86.72	3.51	80.11	1.40	64.21
4	22.05	98.06	6.03	98.41	7.01	89.30	11.77	99.22	3.40	96.71	5.24	95.21	5.80	82.43
5	44.93	96.28	14.77	99.14	9.19	93.12	23.50	99.45	7.18	98.61	11.99	97.95	7.04	90.77
6	62.55	91.67	35.26	99.72	17.10	97.54	35.01	99.68	15.32	99.18	25.64	99.32	16.31	96.68

	N276S		A518V		C550Y		C21G/R49K		Q34R/C550Y		T100S/A518V	
Day	death	inf. rate	death	inf. rate	death	inf. rate	death	inf. rate	death	inf. rate	death	inf. rate
1	1.05	18.06	2.21	11.47	1.67	17.42	3.58	33.45	0.79	10.91	0.58	13.26
2	1.80	58.02	3.05	32.29	2.31	57.16	3.22	80.38	0.87	42.10	0.93	41.01
3	1.03	88.90	1.40	60.88	3.04	91.10	7.30	96.36	2.55	76.40	3.95	75.37
4	2.94	97.78	2.54	77.99	6.21	98.87	19.78	98.15	6.56	92.09	3.60	90.11
5	6.11	99.43	5.79	87.64	15.62	99.76	30.49	98.00	9.52	96.46	5.49	96.56
6	19.16	99.74	13.93	94.81	37.17	99.87	50.81	97.64	23.07	99.03	16.25	99.03

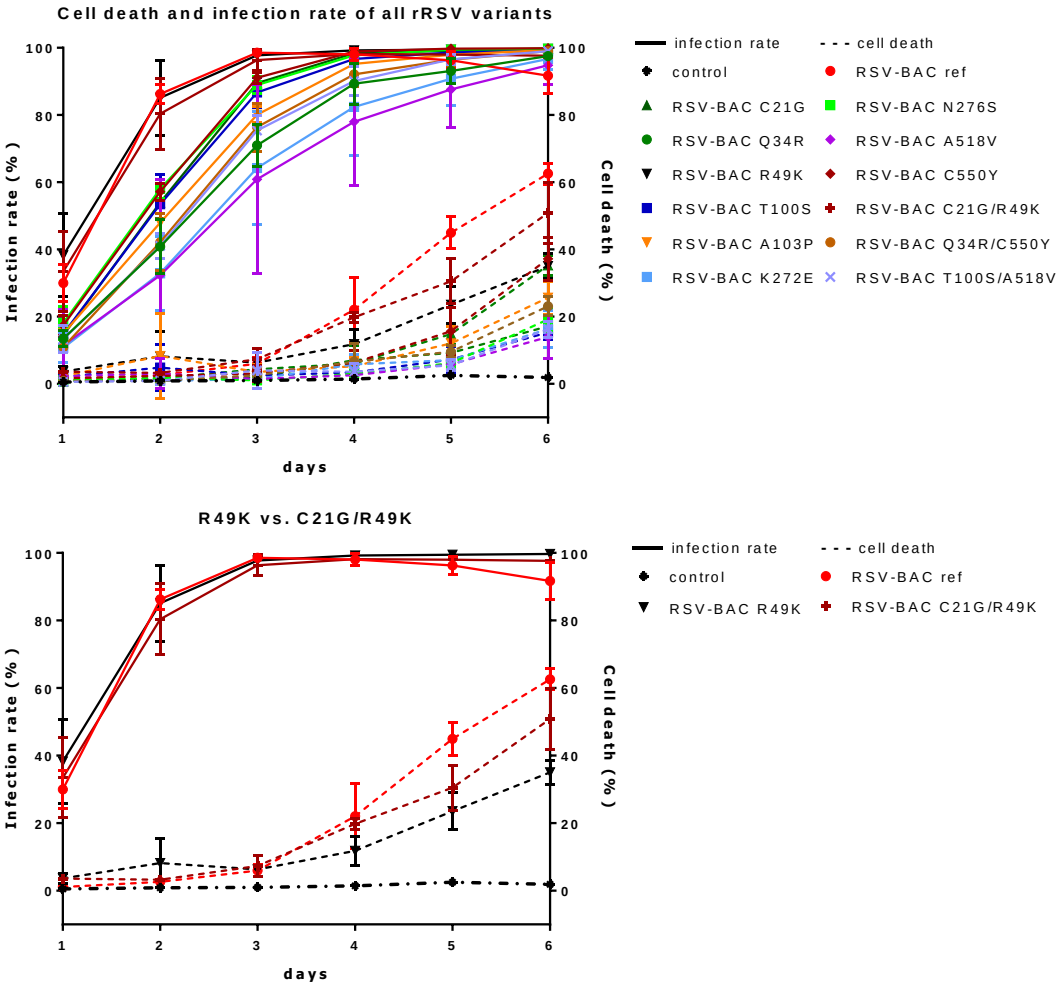

Figure 25: Infection rate and cell death in viral growth assays measured by flow cytometry. Solid lines illustrate infection rates, and dashed lines cell death, * represents the uninfected control. All recombinant RSV strains showed the same tendency in the course of infection with small variations in strains with following mutations: A103P, Q34R/C550Y, T100S/A518V, Q34R, K272E, and A518V. Note, these strains started with a similar infection rate on the 1st day. There is a correlation between the fractions of cell death (dashed lines) and the infection rate (solid lines). Despite infection, Vero cells remained viable for at least 3 days after infection. In the lower plot, strain with the mutation R49K showed a remarkable lower cell death compared to the reference strain RSV A2-K-line19F (RSV-BAC ref). This effect was minimized if both mutation C21G and R49K were present in the virus.

4.2.2 Characterization of palivizumab susceptibility by plaque-reduction neutralization assays (PRNA)

4.2.2.1 IC_{50} values (µg/ml) determined by PRNA

To investigate whether examined mutations on the F protein alters the susceptibility of the mutant variants to neutralization by palivizumab, plaque-reduction neutralization assays were performed as described in 3.2.3.4. Therefore, approx. 100 FFU RSV were neutralized for 1 hour by a 4-fold serial dilution of palivizumab ranging from 4 µg/ml to 0.98 ng/ml. Neutralized viruses were then used to infect Vero cells and incubated for 4 days at 37°C, 5% CO_2. Un-neutralized virus dilution was also prepared and treated in the same way. After 4 days of infection, plaque numbers were counted and analysed using the normalized curve fitting program of GraphPad Prism 7.03. In most of the cases, infecting the cell monolayer at this virus concentration resulted in 60-170 plaques/well in the un-neutralized control. To construct the normalized curve, the average plaque number in the un-neutralized control was defined as 100%. In the highest palivizumab concentration 4µg/ml, infection was completely inhibited and no plaque was formed, which was also defined as 0%. As these two baselines were defined, all other values were then recalculated and expressed as percentages. The program used these points to construct the normalized sigmoidal dose-response curve and calculated the IC_{50} value, the concentration by which 50% of the plaques numbers were inhibited (Figure 26). For each RSV variant, 4 PRNAs were performed. Each PRNA was performed in multiplicity (8 replicas for the un-neutralized control and 4 replicas for each drug dilution) to compensate methodical errors of biological test system (Figure 17). All IC_{50} values are listed in Table 14. Significant test was performed by one-way ANOVA multiple comparisons test of GraphPad Prism 7.03 (Table 15, Figure 27).

Following findings could be obtained from the data. Virus recovered from the RSV-BAC pSynkRSV-l19F (RSV-BAC ref: 0.035 ± 0.0138 µg/ml) had a remarkable lower IC_{50} compared to the clinical strain RSV A2 (0.12 ± 0.0179 µg/ml; 3.4x higher). RSV rescued from pSynkRSV-l19F is a chimeric strain that harbors the F protein from the RSV Line 19 while other proteins are identical to those of the RSV A2. RSV Line 19 was first isolated and identified from an infant with respiratory illness at the University of Michigan (Herlocher et al. 1999). RSV strain A2 and Line 19 are in the same subgroup A but induced different pulmonary pathology and immune responses (Lukacs

et al. 2006). Differences between the F proteins of RSV A2 and Line 19 could lead to changes in its binding interaction with palivizumab and this will be discussed in detail in section 5.2.

For the resistant control strain RSV A2-K-line19F/K272E, an additional assay with higher drug concentrations (10-fold serial dilution ranging 5 mg/ml to 0.5 µg/ml) was performed with the aims to titrate the IC_{50} value for this strain. However, as the mutation is located within the binding epitope of palivizumab, this strain with the mutation K272E escaped completely from neutralization and even test series at the highest concentration of palivizumab 5 mg/ml showed no differences compared to the un-neutralized control. The sensitive control strain RSV A2-K-line19F/N276S exhibited a similar result compared to the reference strain with an IC_{50} value of 0.048 ± 0.0108 µg/ml. It means that the sensitive and the resistant recombinant RSV, both rescued from RSV-BAC pSynkRSV-l19F/MUT, retrieved its susceptibility phenotype as in the normal RS virus. Hence, the examined BAC-based RSV rescue system and the established PRNA are suitable for phenotypic characterization of mutations in the F gene concerning antiviral susceptibility to palivizumab.

Evaluating all IC_{50} values obtained from PRNAs by one-way ANOVA multiple comparison test of GraphPad Prism 7.03 delivered following results. IC_{50} values of virus rescued from the RSV-BAC harboring following single mutations C21G, Q34R, T100S, A518V, C550Y and the double mutation T100S/A518V coincided with that of the reference strain and variations are insignificant. Therefore, these mutations could be considered as having no effect on the susceptibility of the virus against palivizumab. In contrast, virus with following mutations exhibited significant higher IC_{50} values than the RSV-BAC ref strain (Table 14, Figure 26, 27): R49K (2.3-fold), A103P (2.2-fold), Q34R/C550Y (1.86 fold) and C21G/R49K (2.8 fold). Moreover, all double mutations resulted in slightly higher IC_{50} values than the reference strain (Figure 26).

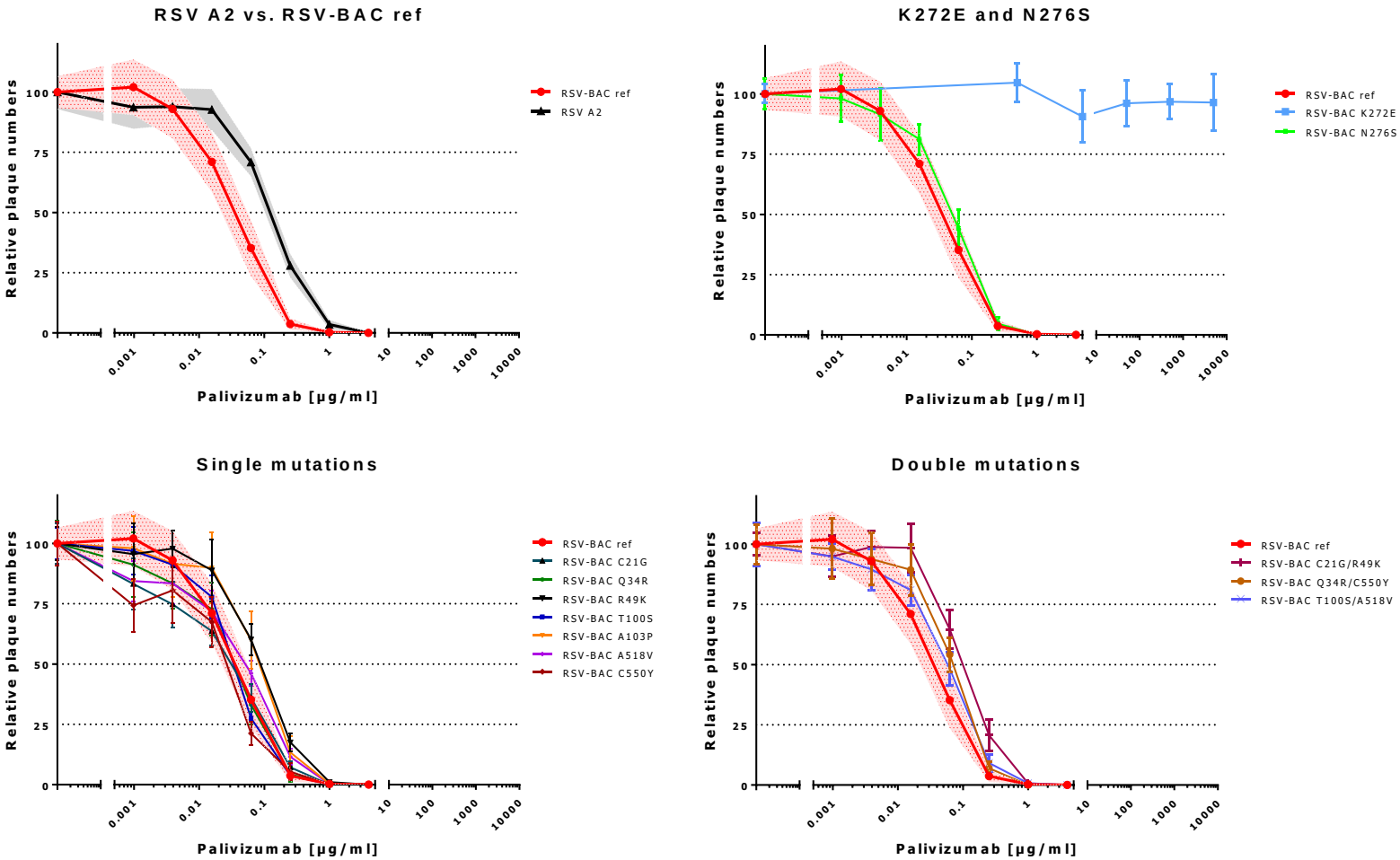

Figure 26: Determination of IC_{50} values by plaque-reduction neutralization assays. Neutralizations were performed with a 4-fold serial dilution of palivizumab for 1h. After 4 days of incubation, plaque numbers were counted. Normalized dose-response curves were constructed and analysed using the curve fitting program of GraphPad Prism 7.03. 100% were defined as the number of plaques that were formed in the absence of palivizumab. For all viral strains (except the resistant control strain K272E), infection was completely inhibited by the highest palivizumab concentration (4 µg/ml), which was normalized to 0% in the evaluation.

Table 14: IC_{50}[µg/ml] of all examined RSV variants for palivizumab. For each mutation, 4 PRNA were performed. IC_{50} values with significant differences from the RSV-BAC ref are written in **bold**. Statistics was performed by GraphPad Prism 7.03.

IC_{50} [µg/ml]	RSV A2	RSV-BAC ref	RSV-BAC C21G	RSV-BAC Q34R	RSV-BAC R49K	RSV-BAC T100S	RSV-BAC A103P	RSV-BAC N276S	RSV-BAC A518V
Assay 1	0.133	0.028	0.028	0.023	0.094	0.037	0.066	0.046	0.036
Assay 2	0.133	0.026	0.018	0.036	0.087	0.026	0.085	0.036	0.033
Assay 3	0.119	0.056	0.023	0.034	0.081	0.040	0.099	0.062	0.046
Assay 4	0.095	0.033	0.021	0.032	0.066	0.031	0.059	0.049	0.043
Mean	**0.120**	**0.035**	0.023	0.031	**0.082**	0.033	**0.077**	0.048	0.040
Std. Deviation	0.0179	0.0138	0.0041	0.0059	0.0120	0.0060	0.0182	0.0108	0.0063
Std. Error of Mean	0.0090	0.0069	0.0020	0.0029	0.0060	0.0030	0.0091	0.0054	0.0032
Lower 95% CI of mean	0.091	0.014	0.016	0.022	0.063	0.024	0.048	0.031	0.030
Upper 95% CI of mean	0.149	0.057	0.029	0.041	0.101	0.043	0.106	0.065	0.050

IC_{50} [µg/ml]	RSV-BAC C550Y	RSV-BAC C21G/R49K	RSV-BAC Q34R/C550Y	RSV -BAC T100S/A518V
Assay 1	0.009	0.112	0.065	0.047
Assay 2	0.028	0.108	0.056	0.060
Assay 3	0.021	0.088	0.067	0.049
Assay 4	0.026	0.086	0.070	0.055
Mean	0.021	**0.098**	**0.065**	0.053
Std. Deviation	0.0085	0.0131	0.0058	0.0058
Std. Error of Mean	0.0042	0.0065	0.0029	0.0029
Lower 95% CI of mean	0.007	0.078	0.055	0.043
Upper 95% CI of mean	0.034	0.119	0.074	0.062

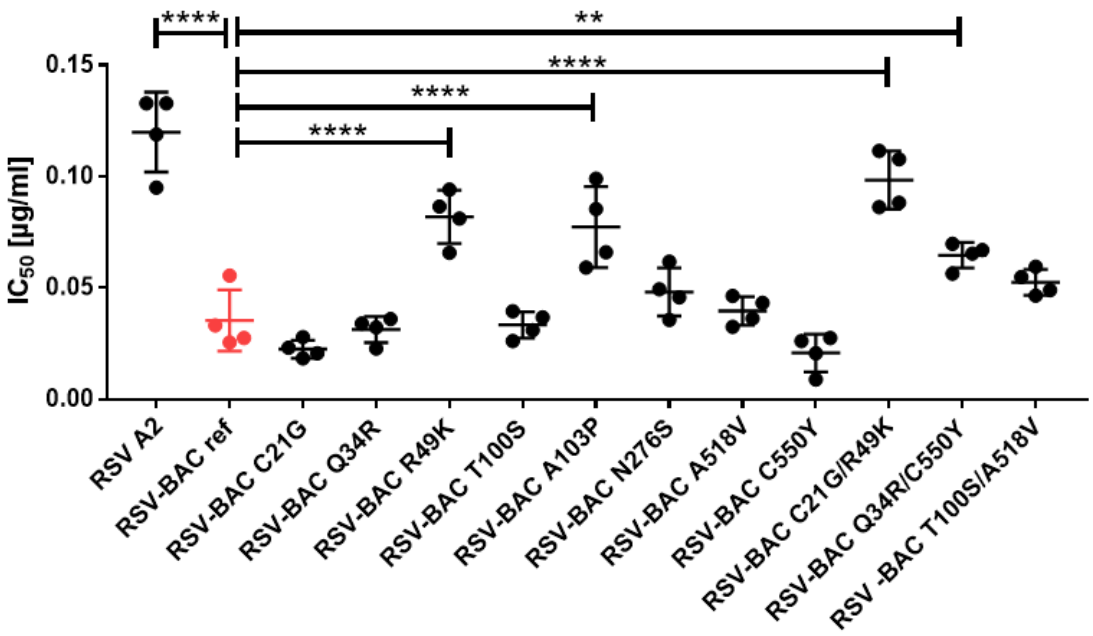

Figure 27: IC_{50}[µg/ml] for palivizumab (mean±SD). Multiple comparisons between the RSV-BAC ref strain and other viral strains were performed by one-way ANOVA test of GraphPad Prism 7.03. (* P ≤ 0.05; ** P ≤ 0.01; *** P ≤ 0.001; **** P ≤ 0.0001)

Table 15: One-way ANOVA multiple comparisons test. RSV rescued from RSV-BAC pSynkRSV-l19F served as the reference strain, to which other strains were compared. Test was performed by GraphPad Prism 7.03 (ns: not significant)

RSV-BAC ref vs.	Mean Diff.	95,00% CI of diff.	Significant?	Summary	P Value
RSV A2	**-0.08453**	**-0.1069 to -0.06218**	**Yes**	********	**0.0001**
RSV-BAC C21G	0.01291	-0.009444 to 0.03526	No	ns	0.5229
RSV-BAC Q34R	0.004115	-0.01824 to 0.02647	No	ns	0.9992
RSV-BAC R49K	**-0.04647**	**-0.06882 to -0.02412**	**Yes**	********	**0.0001**
RSV-BAC T100S	0.00207	-0.02028 to 0.02442	No	ns	0.9996
RSV-BAC A103P	**-0.04197**	**-0.06432 to -0.01961**	**Yes**	********	**0.0001**
RSV-BAC N276S	-0.01272	-0.03507 to 0.009632	No	ns	0.5400
RSV-BAC A518V	-0.004233	-0.02658 to 0.01812	No	ns	0.9991
RSV-BAC C550Y	0.01461	-0.00774 to 0.03696	No	ns	0.3775
RSV-BAC C21G/R49K	**-0.06303**	**-0.08538 to -0.04068**	**Yes**	********	**0.0001**
RSV-BAC Q34R/C550Y	**-0.02924**	**-0.05159 to -0.006886**	**Yes**	******	**0.0049**
RSV -BAC T100S/A518V	-0.01707	-0.03942 to 0.005279	No	ns	0.2166

4.2.2.2 Test of a new overlay with colloidal microcrystalline cellulose (MCC)

To investigate whether colloidal microcrystalline cellulose (MCC), a product of Sigma-Aldrich, is suitable for replacement of methylcellulose (MC) in the overlay medium used in PRNA, several media containing different concentrations of the colloidal MCC were tested as described in 3.2.3.4. Compared to MC that forms a high viscosity clear gel, colloidal MCC disperses in water and forms a low viscosity opaque gel. This property of colloidal MCC is a big advantage and could be used to simplify the preparation procedure of PRNA. After an incubation period of 4 days, plaques were evaluated under fluorescence microscope, whereby shape and size were the main parameters under study. Thanks to the translucent property of MC gel, examined microcultures could be directly microscoped while overlay media supplemented with colloidal MCC had to be removed and washed with PBS prior evaluation due to its milky appearance (Figure 28, upper section C, D, E).

Colloidal MCC is not toxic for the cells. Anny influences of colloidal MCC on cell proliferation and cell morphology were not visible under microscopy. For a complete removal of the overlay media containing colloidal MCC, the cell monolayer should be washed twice. Again, a plaque is defined as an assembly of at least 10 infected cells. In Figure 28, picture A depicted how plaques developed in the absence of a thickening agent and in B in the presence of 0.5% MC. In A, big and uneven plaques that melted in each other were observed. With 0.5% MC, plaques were formed more even with sharper border and were well distinguished from each other. Even though, some thin spines adjacent to plaques remained visible. C, D and E showed how plaques were formed in the presence of 0.5, 1 and 1.5% of colloidal MCC. In the presence of colloidal MCC, plaques were formed more isolated from its neighbours in comparison to A. With an increasing of the colloidal MCC concentration, a better plaque separation could be obtained (from C to E). By contrast with B, form and size of plaques in C, D and E were more variable and they carried more spines.

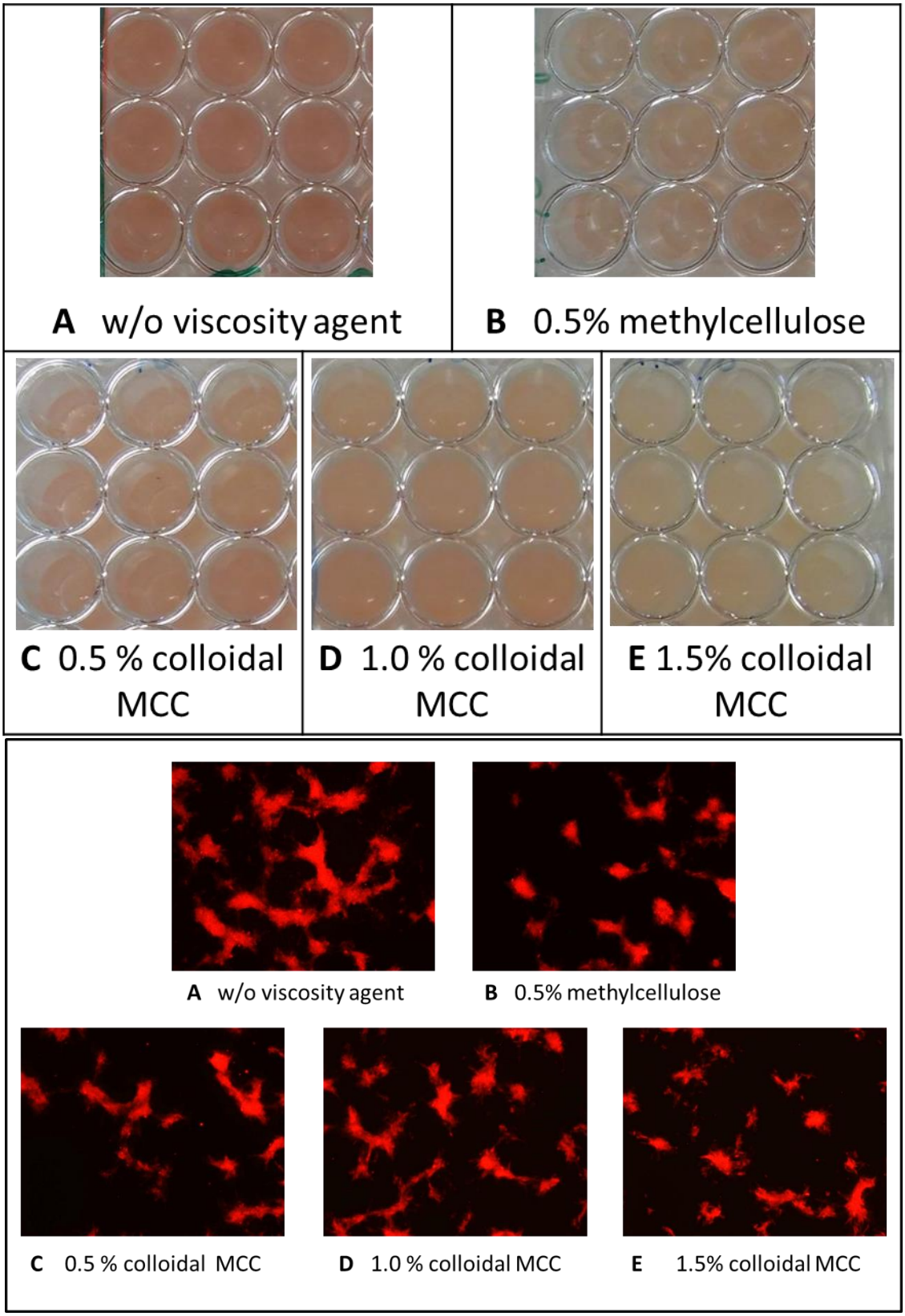

Figure 28: Test of different overlay media for plaque-reduction neutralization assay. Appearances of different overlay media are depicted in the upper section of the figure. Methyl cellulose formed a clear viscosity gel while colloidal microcrystalline cellulose (MCC) formed an opaque gel. Size and form of plaques developing in different media are pictured in the lower section.

5 Discussion

5.1 Generation of mutated RSV by *en passant* mutagenesis

During the viral replication cycle, mutations occur spontaneously and lead to development of viral quasispecies, a collection of mutants with closely related viral genome underwent a continuous process of genetic variation (Domingo et al. 2012). Competition and selection of the fittest variants in a given environment establish quasi-equilibrium of the variant proportions (Andino and Domingo 2015). In the presence of antiviral drugs, mutants with mutations that confer replication advantages overcome the selection process and become major in the mixed virus population. However, not every mutation does really confer drug-resistance or have an impact on the viral fitness, so called polymorphism. And sometimes, several mutations are required to contribute the virus replication advantages. The mistaken interpretation of mutation N276S in F gene in context with palivizumab resistance in the past is a meaningful lesson (Adams et al. 2010). Hence, newly detected mutations are needed to be examined by phenotypic characterization and reliable genotypic methods of which there is still a lack for RSV.

In this work, *en passant* mutagenesis (Tischer et al. 2006) was applied to generate mutated RSV, a method that allows for modification of the virus genome without retention of any unwanted sequences in the original BAC DNA. Thus, phenotypic alteration of the mutated virus could be than interpreted as effects elicited by the investigated mutations. The virus genome used in this work is derived from a chimeric strain RSV A2-K-line19F, and maintained in BAC pSynkRSV-l19F, that encodes furthermore a far-red fluorescence protein allowing tracking of infection through fluorescence, mKate2 (Hotard et al. 2012). BAC DNA can be well maintained and efficiently modified in bacterial cells with higher recombination frequency than in eukaryotic cells. Nowadays, several recombination systems in *E.coli* are established for simple and straightforward manipulation of BAC such as the case of *E.coli* GS1783. This strain possessed chromosomally both an I-SceI cassette and a defective λ prophage that supplies function for protection and recombination of the electroporated linear DNA in the bacterial cell (Yu et al. 2000). This prophage encodes following recombination enzymes Exo, Beta and Gam. Prophage expression is tightly controlled

by a temperature –dependent repressor and hence the recombination functions can be transiently supplied by a short temperature shift of the culture to 42°C (Yu et al. 2000). Introduction of nucleotide change into the BAC genome proceeds in two independent recombination events. The first homologous recombination facilitates insertion of the PCR-product containing the positive selection marker with the adjacent I-SceI restriction site and short-sequence duplication (Figure 9). In the second recombination, all foreign sequences were removed living the introduced mutation as the only modification in the virus genome, which represent a high advantage of this technique over former methods by which a short foreign sequence remains in the end product. Maintaining the virus genome as BAC construct allows sequence analysis of the end product to verify the presence of the investigated mutations as well as the absence of any unwanted mutation prior transfection and thus supersedes the time-consuming plaque purification. Furthermore, recombinant virus with replication disadvantages would able to propagate in such a system which would not happen in a mixed virus population with constant selective pressure during passages.

While establishing *en passant* mutagenesis on RSV BAC pSynkRSV-l19F, 12 mutated RSV strains were generated, 9 of them contain single mutations and 3 double mutations in the RSV F gene, namely C21G, Q34R, R49K, T100S, A103P, K272E, N276S, A518V, C550Y, C21G/R49K, Q34R/C550Y, T100S/A518V. These F-gene mutations were identified in clinical isolates of infants and transplant patients with respiratory infection by RSV. After both homologous recombination events, sequence analysis was performed for several bacterial colonies of each mutation to check for the presence of the desired mutation. Interestingly, not all BAC showed the expected chromatogram with the desired mutation. Some harbored the parental genotype after the second recombination event. This could be explained with existing of probably by-products resulted from partial incorporations of the PCR-product into the RSV BAC in the first recombination (Figure 29). On one hand, the PCR-product has to contain several homologous segments to enable two independent recombination events. On the other hand, these segments increased the possibility of unwanted recombination resulting in other by-products, which remains unrecognized during the positive and negative selection. In these by-products, mutation is represented either downstream or upstream of the positive selection marker. Note, correctly integrated product should harbor the mutation in both directions (Figure 9). Enter these by-products the second

recombination event, both parental and correct mutated genotype could be formed (Figure 30). Emerging possibility of by-products is suggested to depend on the bond enthalpy of the homologous sequences, which is oblique to the given nature of the parental genome, the location of interest and is limitedly modified by length variation.

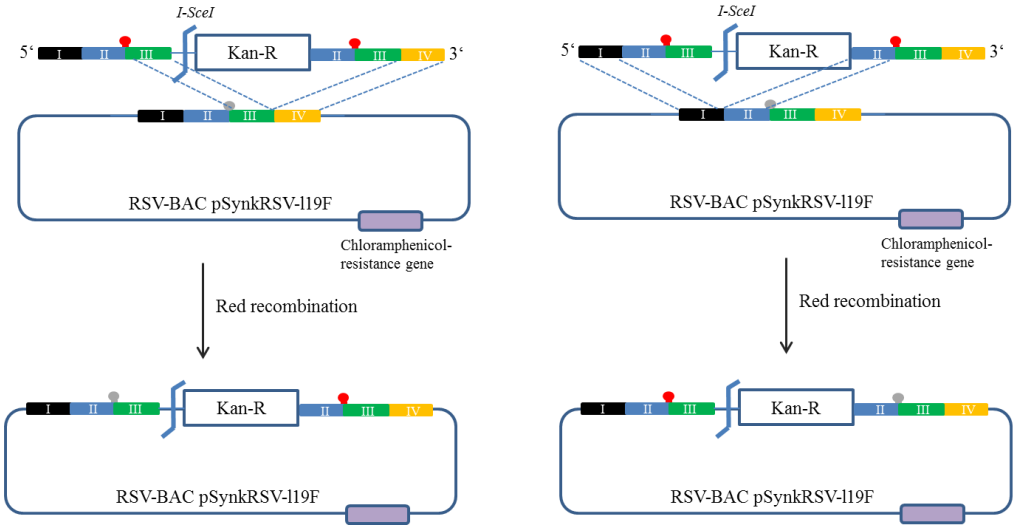

Figure 29: Possibility of by-products after the first recombination. Presence of long and different homologous sequences in the PCR-products can lead to inadequate recombination resulting in emerging of by-products. These by-products contain the desired mutation only on one side of the positive selection marker. Correctly recombined products harbor the desired mutation both on downstream and upstream direction of the positive selection marker (see Figure 9).

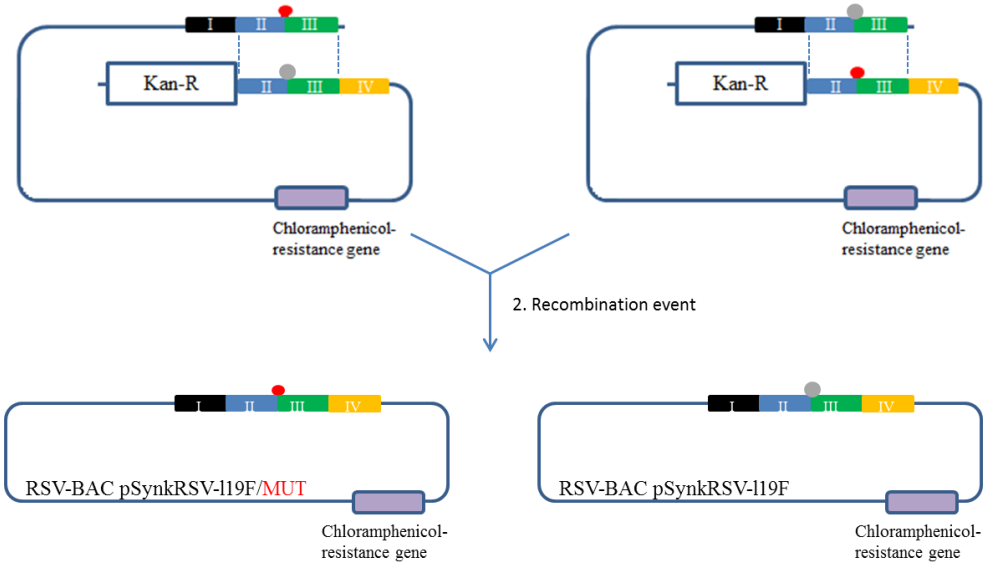

Figure 30: Possible end-products resulted from the second recombination within the by-products. Enter the by-products the second recombination event, both correct mutant and parental genotype could be formed.

5.2 Phenotypic characterization

5.2.1 Characterization of viral growth by multi-step growth curves

Growth curves display the virus titers in the supernatants throughout a defined period of time, in this work 6 days. Upon infection, the cells enter an eclipse state, where the infection cycle has already started but no infectious particle is detectable in the supernatant (Flint et al. 2009). The eclipse period of RSV is 12h after infection (Levine et al. 1977), beyond which infectious particles are released into the medium. In this work, the first samples were taken on the next day, after approx. 20h of infection, when the eclipse period is past and infectious particle releasing already started. Thereupon, the growth curves showed a continuous arising of the virus titers until reaching the plateau concentration of ~10^6 $TCID_{50}$/ml after 3-4 days of infection, when an equilibrium between releasing of new infectious particles and loss of infectivity of old virus particles is restored. It was also observed that the cell monolayer was 100% infected as the plateau was reached. Results from end-point dilution assays indicated that virus titers in the supernatant varied in some cases strongly between replicated measurements. This can be explained by a notable feature of RSV, that the virus is very unstable. The infectivity of RSV particle depends strongly on the maintenance of the meta-stable pre-fusion F conformation, which is affected by molarity of the medium, temperature and freezer-thawing. Furthermore, particles grown in vitro are mostly large filaments, and thus are morphologically unstable in handling after freeze-thawing and mixing (Collins et al. 2013). However, throughout the cycle, over 90% of the progeny virus remains associated with plasma membrane and only a few is ever released (Levine et al. 1977). But RSV is relatively non-lytic in most cell types and persistent infection was shown to be easily established for different tissue cultures (Schwarze et al. 2004). Thus, it is possible to obtain supernatants with high virus titer (~10^6 $TCID_{50}$/ml) as viable infected cells keep shedding infectious particles. The curves of a multistep growth curves depend on the capacity of the cell to produce new virus and how the infection spreads to uninfected cells. Infection spread could be facilitated in 3 different ways: (1) fusion of infected and neighbouring uninfected cells; (2) membrane associated virus could be transferred to neighbouring uninfected cells; (3) progeny virions infected further uninfected cells. Mutations on F protein could alter spread of the viral infection and thus affect growth of virus.

5.2.1.1 Multi-step growth curves of RSV strain A2 and recombinant strain RSV A2-K-line19F

Beside recombinant strains, growth curves and palivizumab susceptibility were also determined for the clinical strain RSV A2 (ATCC® VR-1540P) that was first isolated from lower respiratory tract of an infant with bronchiolitis and bronchopneumonia in Melbourne, Australia 1961. The parental recombinant strain derived from BAC pSynkRSV-l19F is a chimeric strain that contains a far-red fluorescence reporter gene mKate2, and encodes the fusion protein F of strain RSV-line19 while other protein of strain RSV A2. The resulted strain is called RSV A2-K-line19F. Different genotype possibly results in different phenotype (Vandini et al. 2017). Thus, phenotypic comparison between these two strains, RSV A2 and RSV A2-K-line19F, is necessary for a better understanding of investigated recombinant strains.

The F protein of RSV line 19 differs from that of RSV A2 in 14 amino acids (Moore et al. 2009) resulting in a variation of 2.4% in a total length of 574 aa. This chimeric strain was brought into being for displaying better pathogenesis features in mice compensating the fact that mice model are only semi-permissive for HRSV. Recombinant RSV rescued from BAC pSynkRSV-l19F contains an additional gene encoding for the fluorescence protein mKate2, which is 711bp long (Hotard et al. 2012). Previous study demonstrated that RSV genome could tolerate a foreign gene with up to 762 nucleotides in length. However, this resulted in a 10% decrease of plaque diameter, delay of viral growth and 20-fold decrease of virus yield in vitro (Bukreyev et al. 1996). The first impairment, namely smaller plaque diameter, could be qualitatively verified in this study. Likewise, growth curve comparison also showed a delay of ~24h in reaching the highest virus titer for strain RSV A2-K-line19F. However, a lower virus yield could not be verified with the results of this study, which was already demonstrated by the former group (Hotard et al. 2012).

5.2.1.2 Multi-step growth curves of recombinant strains harboring mutations

Comparing all 12 mutated strains with the parental strain, 3 strains gain the most attention for yielding a lower virus titer in the plateau phase. These strains harbor following mutation: T100S, K272E, T100S/A518V (Figure 22, 23), of which mutation K272E, the palivizumab resistant control, was additionally characterized and was not found in the patient isolates of the Institute for Medical Virology of Tuebingen.

Mutation K272E was shown to confer palivizumab resistance both in vitro and in vivo and is associated with an impaired viral fitness in cell culture (Zhu et al. 2011). Thus, it is not unexpected that recombinant RSV harboring this mutation is restricted in viral growth. However, for this finding there is no explanation until now. This amino acid position is located within the antigenic site II on F protein. Site II is well conserved between strains and even its tertiary conformation is mostly similar in pre- and post-fusion conformations (Zhu et al. 2012, Rossey et al. 2018). F is indispensable for virus attachment and entry, the first step in the infection cycle. Along with it, both pre- and post-fusion states are presented on the viral surface. It should also be emphasized that only pre-fusion conformation is able to trigger membrane fusion. Hence, the role of presenting post-F on the viral surface is an interesting question. All these facts lead to the hypothesis that this conserved region might have an important role for recognition of host structures that facilitate virus attachment or involving in the activation of refolding of pre-F for the fusion event and thus mutations in this site result in an impaired viral fitness. The former hypothesis was denied by Magro et al. in 2010 by measuring the amount of neutralized virus bound to cells and comparing with the unneutralized probes (Magro et al. 2010). The later remains an interesting research topic, since which factors trigger refolding of pre-F is still unknown up to now.

Recombinant strains harboring the single mutation T100S and the double mutations T100S/A518V also presented a slightly restricted viral growth compared to the parental strain (Figure 22 & 23). Interestingly, the effect resulted from the double mutations T100S/A518V was more remarkable. Since both strains contained mutation T100S and strain that harbored exclusively mutation A518V grew normally in cell culture, mutation T100S might be responsible for the slight retention of viral growth in vitro and an additional mutation possibly strengthen this effect. After translation, the F precursor (F0) needs to be activated by furin-like host protease to become the fully functional

mature F (Bolt et al. 2000). F0 is cleaved at 2 furin cleavage sites (FCS) at aa 109 (FCS-2) and 136 (FCS-1) (Zimmer et al. 2001). Mutants, in whom the proteolytic processing at FCS-2 is abolished, replicate in cell culture with reduced cytopathic effect and lower viral titer (Zimmer et al. 2002). In addition, Tian et al. established a FurinDB database and described 126 furin cleavage sites, which are recorded as a 20-residue motif (Tian 2009, Tian et al. 2011). It means that the amino acid at position 100 is found in the 20-residue motif of FCS-2. According to this database, T100 is located outside the binding core pocket of furin but within a flexible polar region, that might interact with the polar surface of furin and facilitate binding of the core region (Tian 2009). Hence, to some extent, this can explain how the mutation T100S causes a slight restriction of viral growth as observed in the growth curve. However, due to the relatively high standard deviation, these differences are considered as statistically insignificant. Note again, K272E was described by several researchers to clearly cause restriction in viral growth but according to results from this study, it caused a reduction but in an insignificant level. This might be an effect resulted from the recombinant virus genome and should be kept in mind while interpreting these outcomes.

5.2.2 Phenotypic characterization of viral growth by flow cytometry

Viral growth curves deliver knowledge about the number of infectious particles in the supernatant. As mentioned above, 90-95% of the progeny RS virus remains associated with the cell membrane. This means that only 5-10% of the progeny virus are visible through growth curves. Membrane associated virus could be delivered to uninfected neighbouring cells and facilitate cell fusion as well as spread of infection, a feature that is characteristic for RSV. To obtain a better understanding relating the kinetics of viral growth, a test using flow cytometry was established to evaluate the infected cell cultures throughout 6 days.

The data were evaluated by 2 parameters: (1) the infection rate (%), and (2) cell death (%). The course of infection rates described the increasing of the infected population in the cell culture for 6 days. Throughout the test period, a new cell population emerged, that exhibited lower signal intensity for intracellular fluorescein and mKate2. Fluorescein, a product from hydrolysing of fluorescein diacetate by the cellular esterase, is a probe for cell viability and membrane integrity. The protein mKate2 is expressed in infected cells and indicates an infection with recombinant RSV. This “new” population

was classified as “dead cells” because of their clearly lower signal for the viability and infection probes (fluorescein and mKate2). However, RSV infections are mostly non-lytic and RSV was described to be able to suppress cell cycle at G0/G1 as well as apoptosis. This property is preferable to produce new infectious particles. Such knowledge does not explain the emergence of this population in flow cytometry. The membrane of infected cells is widely covered by budding virus, and easily gets damage during the preparation procedures for the assays (e.g. pipetting, centrifugation, and vortex). Membrane damage leads to out flux of both fluorescein and mKate2 resulting in lower fluorescence of these two markers in the “dead” cell population. Hence, in this study, cell death is a consequence of membrane leakage and might be associated with the portion of membrane associated virus.

Results from this assay revealed that all investigated recombinant strains spread similarly in the cell monolayer. On one hand, results for some strains showed a wide distribution within repeated measurements, which were performed independently (especially, strains with mutation K272E and A518V). On the other hand, a gradient variation could be observed among following strains harboring mutation A103P, Q34R/C550Y, T100S/A518V, Q34R, K272E, and A518V, all of which interestingly started from a comparable infection rate (~15%) on the 1st after infection (Figure 25). The order is given from the fastest (A103P) to the lowest spreading strains (A518V). Since, mutation C550Y alone showed no alteration in both assays (multi-step growth curve and flow cytometry), it could be considered that the observed effect in the double mutations harboring strain Q34R/C550Y was caused by the mutation Q34R. According to these results, mutation K272E and double mutations T100S/A518V resulted in a delay of infection spread, which confirms findings of the multi-step growth curves (see 5.2.1.2). Furthermore, this gradient variation might disclose that these mutations possibly have an impact on the kinetics of infection spread but in framework of this study, it does not allow a closer interpretation relating their significance.

As mentioned above, cell death in the growth assays measured by flow cytometry is assumed to be associated with membrane instability. For most of the cases, infected cells remained viable within the first 3-4 days upon infection. Afterwards, their membrane became more and more unstable and caused cell death during the test procedure. The results displayed a relationship between rates of infection and cell death.

Viral strains that spread more slowly also caused a lower cell death or resulted in less damage on the host membrane. This correlation is easily comprehensible. The highest cell deaths were observed from 3 following strains given in descending order: the parental reference strain, strain with mutation C21G/R49K, and strain with mutation R49K (Figure 25). Paradoxically, the infection courses measured with these strains are the same. It could be thus interpreted that strain with mutation R49K possibly caused less membrane instability compared to the parental strain and strain containing the double mutations C21G/R49K. However, to causally explain this phenomenon, further experiments are required and the test should be optimized for better standardization.

5.2.3 Comparison between growth curves determining with end-point dilution assays and flow cytometry

For both growth assays determined with end-point dilution assays and flow cytometry, all variations between the mutated strains and the parental reference strain could be considered statistically insignificant due to relatively high deviations. To compensate random errors, each experiment was performed in triplicate. The means described the tendency and the standard deviations realized the variation of the data set.

F is essential for membrane fusion, which enables the virus to release its nucleocapsid into the cell cytoplasm, where the viral replication takes place. Flow cytometry detects the expression of mKate2 gene and the cell membrane integrity during the infection. According to the gene order in the viral genome, mKate2 is the first gene which is transcribed by the viral polymerase and thus indicates an early response signal to infection. End-point dilution assays detect the amount of infectious particles in the supernatant. In both, the highest viral titers or infection rate of 90-100% were obtained for most tested strains after 4-5 days of infection. It seems that the plateaus of viral titers were reached as infection is detected in 90-100% of the cells. Results of both assays indicated that mutation K272E and T100S/A518V possibly caused impairment in viral growth. Especially for the later, the effect was more clearly when both mutations T100S and A518V were present in the virus. Discordant results were observed for following mutant viruses: A103P, Q34R, and A518V. Recombinant virus harboring these mutations respectively showed a delay in spread of infection, while the viral titer resulted from these strains were comparable to the parental strains. Unfortunately, flow

cytometry results for strain A518V displayed an unusual high standard deviation and thus it is not further discussed here until additional tests are performed.

These two assays ascertained viral growth at different points within the replication cycle (Figure 31). While end-point dilution assays quantitatively examine the amount of the infectious particle in the supernatants and indirectly impart knowledge about the viral replication, flow cytometry detects how effective the infection is transmitted and spread within the cell monolayer and provide valuable hints about the effect of the mutated protein. And it seems that flow cytometry also detects minimal effects, which do not manifest in the multi-step growth curves. Hence, these results are not contradictory. They capture the same aim from different perspectives and deliver different insights. Thus it can be suggested that, mutation A103P and Q34R might result in changes in function of F protein and this needs to be verified by other experiment settings.

Of the mutations described here, the most interesting are those that may influence the function of F: Q34R, R49K, T100S and A103P. They are all located on the F2 subunit of F. This subunit is recently believed to be essential for the viral fusion event and determines the species specificity of RSV infection (Schlender et al. 2003). Most recent studies suggest the function of F2 in stabilization of pre-F or in in triggering and/or refolding of F (Bermingham et al. 2018, Hicks et al. 2018). In 2013, a mutation in amino acid position 66 was reported to be able to alter virus growth and cell fusiogenicity in vitro (Lawlor et al. 2013). Thus, despite the effects resulted from Q34R, R49K, T100S, A103P were not significant in this study, these mutations should be further investigated in other experiment settings that allow a better evaluation relating their functions on F.

Figure 31: Detection of viral fitness at different points within the viral life cycle. Two assays were established for evaluation of viral growth. The amount of infectious particles in the medium was detected by end-point dilution assays and data were present as growth curves. Infected cells expressed the fluorescent protein mKate2, whose signal was detected by flow cytometry and illustrated as courses of infection rates. mKate2 is the first protein that is expressed after infection. A cell viability and membrane integrity probe (FDA→fluorescein) was added to the flow cytometry samples. Restricted fluorescein signal indicated cell death which was assumed to be associated with the cell membrane instability resulted from incompletely budding virus.

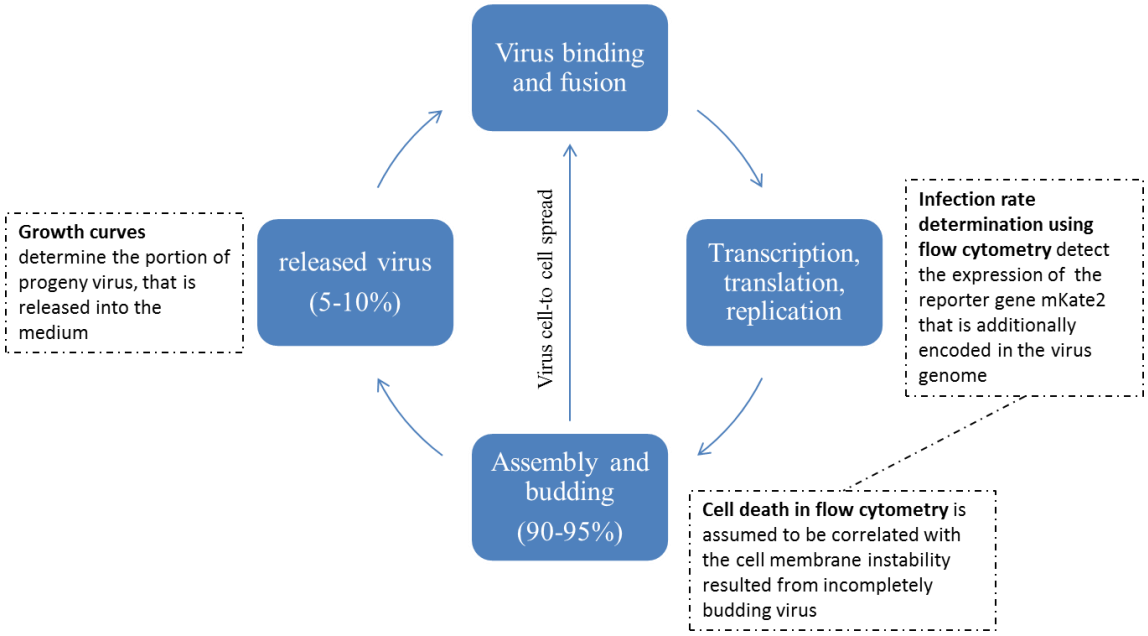

5.2.4 Palivizumab susceptibility by plaque-reduction neutralization assays (PRNA)

Palivizumab susceptibility of investigated RSV strains was determined by plaque-reduction neutralization assays. Therefore, virus was neutralized using different palivizumab concentrations prior infection of cell microcultures. After an incubation period of 4 days, the plaque numbers resulting from different neutralization concentrations were counted and IC_{50} values were calculated using the curve fitting program of GraphPad. IC_{50} is the concentration that inhibits 50% plaque formation compared to the unneutralized probe. Plaque reduction assay is a widely used method to determine drug sensitivity. However intra-assay and inter-assay precision and accuracy are known problems. Test results depend on many critical parameters such as the amount of virus, duration of neutralizing, days of cell seeding prior infection, the amount of methylcellulose used in the overlay medium, and time of incubation. Range of the tested drug dilution is also critical to enable the software performing its algorithm. Hence, PRNA was optimized for better standardization prior

implementation. Random error was minimized and accuracy of the results was improved by multiple replicas. For each viral strain, 4 PRNAs were performed. In each assay, 4 microcultures were prepared for each palivizumab dilution and for the unneutralized control the double amounts of replicas were performed for a better precision. The best fit value of IC_{50} is determined only when the plateau levels of 100% and 0% are well defined. If those plateaus are very uncertain, the same applies to the resulted IC_{50} values. This also leads to the requirement that the serial drug dilutions have to cover these two plateau levels in every assay. If not, out comes have to be interpreted with caution. This requirement was fulfilled in each assay and all calculated standard deviations were in an acceptable range.

That recombinant RSV strains with mutation R49K and C21G/R49K resulted in similar IC_{50} values in PRNA also lends reliability to the established PRNA. C21G is a mutation that is located in the signal peptide, a domain that is no longer present in the mature fusion protein F. Hence, on the viral surface presented F containing the mutation R49K and C21G/R49K are identical and these mutants are expected to be similarly susceptible to palivizumab, which was confirmed by the results of this study. Therefore, it can be concluded that the established PRNA is stable and valid.

Among all tested virus variants, strains with mutation R49K (0.063-0.101 µg/ml) and A103P (0.048-0.106 µg/ml) exhibited remarkable higher IC_{50} values (>2-fold) compared to others including the reference strain RSV A2-K-line19F (0.014-0.057 µg/ml). However, the effect is not as high as that caused by mutation K272E in the resistance control strain. K272E is located within the binding epitope of palivizumab and cause completely resistant to palivizumab even at 5 mg/ml. These results verified other findings up to now that mutations outside the palivizumab binding epitope do not confer the virus resistance to this drug. Even though, significant higher IC_{50} values for strain RSV A2-K-line19F/R49K and RSV A2-K-line19F/A103P shouldn’t be overlooked. As discussed above in 5.2.3, these mutations are located in the F2 subunit of F and caused changes in spread of infection detected by flow cytometry. In addition, they also affect neutralization of palivizumab. It means that even mutations outside the palivizumab epitope are able to alter the susceptibility of the virus against this antibody. Neutralization by antibody depends on the binding affinity between the antibody and its epitope (antigenic site II) on the target structure as well as epitope accessibility. That

R49 and A103 are located near to the antigenic site II in the tertiary structure of the protein strengthens this hypothesis (Figure 32).

Within strains containing double mutations, the largest effect was observed with mutation Q34R/C550Y. Again, this difference was not comparable with that from K272E. However, strain that respectively contains mutation Q34R or C550Y were as susceptible as the reference strain. This leads to the suggestion that accumulation of trivial mutations or polymorphisms might also affect the drug susceptibility, even when these are located outside the binding epitope of palivizumab. This explains why the IC_{50} value of the recombinant RSV-K-line19F differs much from that of strain RSV A2. F is a protein which undergoes a dramatic conformational transformation to display its function. Thus mutations that affect this process might also alter the conformation of the palivizumab binding epitope or its accessibility which lead to changes in palivizumab susceptibility.

In this study, a new thickening agent combined of microcrystalline cellulose and sodium carboxymethylcellulose (MCC) was tested for used in PRNA. MCC was examined in 3 concentrations: 0.5, 1 and 1.5% and compared to 0.5% of methylcellulose (MC). The result suggested that this cellulose blend is suitable for replacement of methylcellulose, which up to now was added to the overlay media to enhance the viscosity. MCC disperses in water to a milky fluid with lower viscosity compared to MC that forms a high-viscosity clear gel in PBS. Results indicated that supplement with 1.5% MCC was appropriate to separate plaques for assay evaluation.

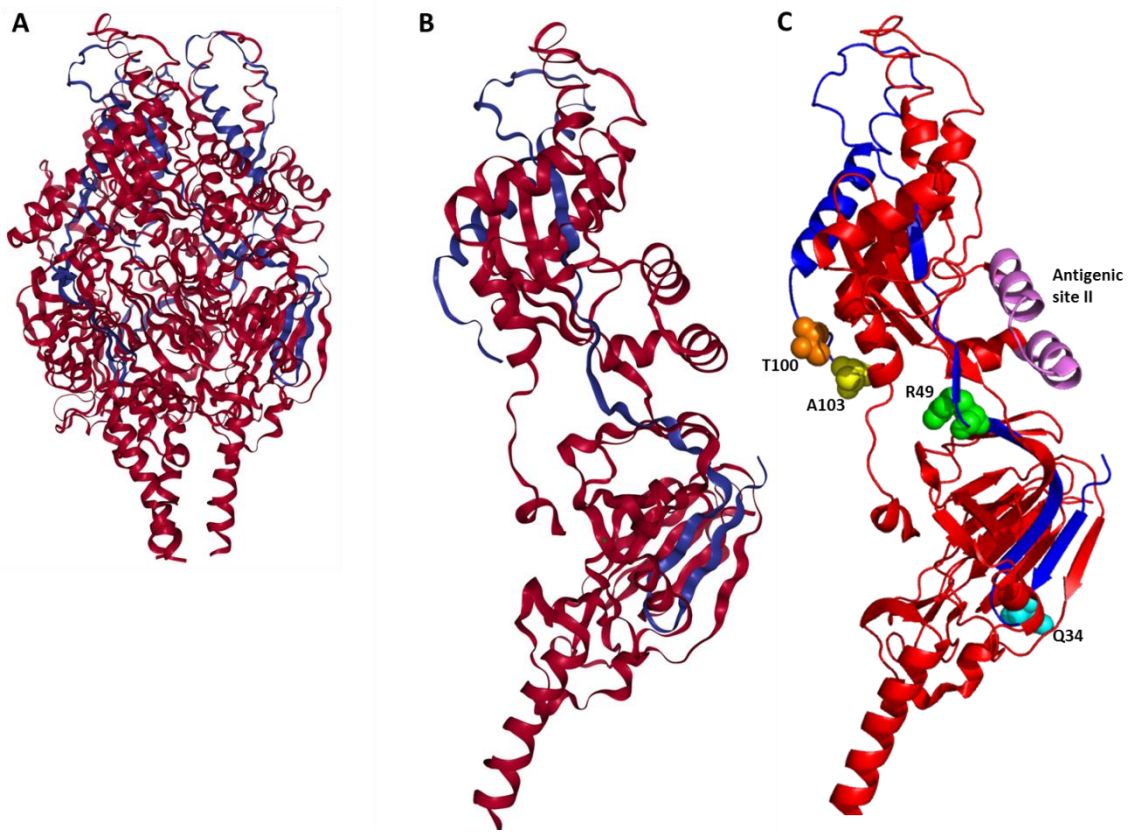

Figure 32: Structure of pre-F homotrimer, pre-F protomer and locations of identified mutations on the F2 subunit in a pre-F protomer. F1 subunit is displayed in red and F2 in blue. **A**: pre-F homotrimer, **B**: a pre-F protomer and C: amino acid positions where mutations were identified on F2 are shown as spheres; the antigenic site II is colored in pink. A and B: Cite images created with the PDB ID (4MMR) and associated publication, NGL Viewer (Rose et al. 2018) and RCSB PDB. http://www.rcsb.org/3d-view/4MMR_20.09.208. C: Image created with the educational version of PyMOL and PDB ID: 4MMR

6. Summary

Globally, respiratory syncytial virus (RSV) is a serious pathogen with high clinical significance especially for children under 5 years, the elderly and immunocompromise individuals. There are two licenced therapeutics against this pathogen: ribavirin and palivizumab. Ribavirin is administered for treatment of an active infection. But it is not recommended for routine treatment because of side effects and of a potential teratogen. Palivizumab is a monoclonal antibody that targets the fusion F protein on the RS viral surface and is used for prophylactic treatment of severe RSV infection in high-risk infants, the population that showed the most cost-benefit ratio in epidemiological studies. Another antibody derived from palivizumab is motavizumab that showed greater neutralizing activity in both vitro and in vivo. However, in clinical trials, motavizumab was shown to be non-inferior to palivizumab but with a higher potential for hypersensitivity reactions, and thus did not get approved by the FDA. Additionally, many promising antiviral candidates are now in clinical trials tested in both infants and adults. Already during the development of palivizumab, several resistance associated mutations have been identified and the same holds true for new antivirals under development.

Marker transfer analysis is a method that allows reliable characterization of newly detected mutation with unknown phenotype, a field that is now available just to a limited extent. This work engaged itself with the establishment of maker transfer analysis for RSV and standardization of in vitro assays for characterization of newly identified mutations on the RSV F gene respecting its influence on viral replication and palivizumab susceptibility. In this work, nine single mutations were characterized: C21G, Q34R, R49K, T100S, A103P, K272E, N276S, A518V, C550Y. Among which, mutation K272E and N276S were previously identified and characterized and served in this work as palivizumab resistance and sensitive control, respectively. Furthermore, the following combinations of mutations C21G/R49K, Q34R/C550Y and T100S/A518V were characterized. Investigated mutations were introduced into the bacterial artificial chromosome (BAC) pSynkRSV-l19F (BEI Resources Nr-36460) (Hottard et al. 2012) using "*en passant*" mutagenesis (Tischer et al. 2006). Viral growth was examined by growth curves using end-point dilution assays to titrate the virus titers in the

supernatants. Additionally, kinetics of infection spread within the cell monolayer was determined by flow cytometry. Palivizumab susceptibility was examined in vitro by plaque- reduction neutralization assays (PRNA).

Respecting viral fitness, all investigated mutations resulted in no significance influence on viral growth analysed by end-point dilution assays and flow cytometry. Concerning palivizumab susceptibility, all investigated mutation did not lead to a complete loss of effectiveness of palivizumab compared to mutation K272E (Zhu et al. 2011). This mutation is located within the palivizumab binding epitope and contributes to the stable resistance of the RSV to palivizumab. However, some mutants exhibit significant higher IC_{50} values compared to that of the parental reference strain RSV A2-K-line19F that directly rescued from BAC pSynkRSV-l19F harboring no mutation. IC_{50} is the drug concentration that could inhibit 50% of viral growth or plaque formation. Mutations R49K and A103P resulted in IC_{50} values, that were higher than 2 fold of the value for the parental strain. Interestingly, these mutations are located outside the palivizumab binding site. RSV variants with mutation Q34R or C550Y were similarly susceptible to palivizumab as the parental strain. Remarkably, mutants that contained both mutations Q34R and C550Y showed significant higher IC_{50} value compared to the reference strain. These results emphasize following hypothesis: (1) Even mutations outside the palivizumab binding epitope might alter susceptibility of the viral against the antibody; (2) accumulation of trivial mutations might impact the viral phenotype and thus mutation should be characterized in the context of the whole genetic background. In addition, a new thickening agent, colloidal micro crystalline cellulose was tested for replacement of methylcellulose in the overlay medium used in PRNA. A concentration of 1.5% colloidal micro crystalline cellulose was showed to be sufficient for used in PRNA.

7. Zusammenfassung

Das Respiratorische Synzytial Virus (RSV) ist weltweit ein bedeutendes Pathogen mit hoher klinischer Bedeutung für Kinder unter 5 Jahren, ältere Menschen und immungeschwächte Individuen. Es gibt zwei zugelassene Medikamente für RSV: Ribavirin und Palivizumab. Ribavirin wird angewandt zur Behandlung einer aktiven RSV Infektion. Wegen seiner Nebenwirkungen und eines möglichen teratogenen Effektes ist es nicht empfohlen für eine routinemäßige längere Anwendung. Palivizumab ist ein monoklonaler Antikörper, der das Fusion F Protein auf der Oberfläche des RS Virus bindet. Wegen der Kosten-Nutzen Bewertung wird es zur Prävention nur bei Hochrisikokindern eingesetzt. Motavizumab ist ein von Palivizumab abgeleitet Antikörper, welcher eine bessere Neutralisation-Aktivität in-vitro so wie in-vivo aufweist. In klinische Studien konnte Motavizumab eine Nicht-Unterlegenheit darlegen aber leider mit einer höheren Überempfindlichkeit, weshalb es von der FDA nicht zugelassen ist (Carbonell-Estrany et al. 2010). Viele versprechende antivirale Medikamente in der Entwicklung werden in klinischen Studien getestet. Verschiedene Palivizumab Resistenz-assoziierte Mutationen wurden bereits während der Entwicklung identifiziert. Das gleiche gilt auch für die neuen antiviralen Substanzen, welche momentan in der Entwicklung sind.

Marker Transfer Analysen erlauben eine zuverlässige Charakterisierung von neu detektierten Mutationen, deren Phänotypen noch unbekannt sind. Diese Arbeit fokussiert sich auf die Etablierung von Marker Transfer Analysen für RSV und auf die Standardisierung von in-vitro Assays, die zur Charakterisierung von neu identifizierten Mutationen in dem RSV F Gen dienen. Mutationen wurden bezüglich deren Einfluss auf die virale Replikation und Palivizumab Suszeptibilität untersucht. Analysiert wurden neun einzelne Mutationen: C21G, Q34R, R49K, T100S, A103P, K272E, N276S, A518V, C550Y. Die Mutationen K272E und N276S waren bereits charakterisiert und dienten in dieser Arbeit als Kontrollen (Zhu et al. 2011, Zhu et al. 2012). Zusätzlich wurden auch folgenden Kombinationen von Mutationen charakterisiert: C21G/R49K, Q34R/C550Y und T100S/A518V. Die zu untersuchende Mutationen wurden einzeln in bacterial artificial chromosome (BAC) pSynkRSV-l19F (BEI Resources Nr-36460) (Hottard et al. 2012) mit Hilfe der "*en passant*" Mutagenese

(Tischer et al. 2006) eingeführt. Für alle Mutanten wurden Wachstumskurven mit Hilfe von end-point dilution assays ermittelt. Die Kinetik der Infektion innerhalb des Zellmonolayers wurde mit Durchflusszytometrie bestimmt**.** Palivizumab Suszeptibilität wurde in-vitro mit Plaque-Reduktion Neutralisation Assays (PRNA) ermittelt.

Keine der untersuchten Mutationen zeigte einen Einfluss auf das Wachstumsverhalten der rekombinanten RS-Viren. Auch führte keine der getesteten Mutationen oder Kombinationen zu einen kompletten Wirkverlust gegenüber Palivizumab im Vergleich zur Mutation K272E, die einen kompletten Aktivitätsverlust verursacht (Zhu et al. 2011). Diese Mutation liegt im Bindungs-Epitop für Palivizumab und trägt zu einer Palivizumab Resistenz bei. Einige Mutationen zeigten signifikant höher IC_{50} Werte im Vergleich zu dem Referenzstamm RSV A2-K-line19F, das aus dem Wildtyp BAC pSynkRSV-l19F hergestellt wurde. IC_{50} ist die Wirkstoffkonzentration, bei der 50% des Viruswachstums bzw. der Plaquebildung gehemmt wurde. Die Mutationen R49K und A103P verursachten signifikant höher IC_{50} Werte als der des Referenzstamms (höher als 2-fach). Diese beiden Mutationen liegen interessanterweise außerhalb der Palivizumab Bindungsstelle. Rekombinante RS-Viren, die entweder die Mutation Q34R oder C550Y tragen, sind vergleichbar sensitiv gegenüber Palivizumab wie der Referenzstamm. Rekombinante RS-Viren, die sowohl die Mutation Q34R als auch C550Y haben, waren wiederum deutlich weniger sensibel gegenüber Palivizumab. Diese Erfahrungen führten zu folgenden Hypothesen: (1) die Palivizumab Suszeptibilität wird nicht nur von Mutationen in der Epitopregion beeinflusst; (2) Akkumulationen von stillen Mutationen können den viralen Phänotyp verändern, weshalb Mutationen in gesamten genetische Hintergrund betrachtet werden sollten. Darüber hinaus wurde ein neues Überschichtungsmittel, kolloidale mikrokristalline Cellulose, getestet, um die Methylcellulose in dem Overlay Medium für Plaque-Reduktion Neutralisation Assays zu ersetzen. Es konnte gezeigt werden, dass eine Konzentration von 1,5% der kolloidalen mikrokristallinen Cellulose optimal für die Anwendung in Plaque-Reduktion Neutralisation Assays war.

8. References

AAP (2014). "Updated guidance for palivizumab prophylaxis among infants and young children at increased risk of hospitalization for respiratory syncytial virus infection." Pediatrics **134**(2): e620-638.

Adams, O.; Bonzel, L.; Kovacevic, A.; Mayatepek, E.; Hoehn, T. and Vogel, M. (2010). "Palivizumab-resistant human respiratory syncytial virus infection in infancy." Clin Infect Dis **51**(2): 185-188.

Agius, G.; Dindinaud, G.; Biggar, R.J.; Peyre, R.; Vaillant, V.; Ranger, S.; Poupet, J.Y.; Cisse, M.F. and Castets, M. (1990). "An epidemic of respiratory syncytial virus in elderly people: clinical and serological findings." J Med Virol **30**(2): 117-127.

Anderson, L.J.; Hierholzer, J.C.; Tsou, C.; Hendry, R.M.; Fernie, B.F.; Stone, Y. and McIntosh, K. (1985). "Antigenic characterization of respiratory syncytial virus strains with monoclonal antibodies." J Infect Dis **151**(4): 626-633.

Andino, R. and Domingo, E. (2015). "Viral quasispecies." Virology **479-480**: 46-51.

Bachi, T. and Howe, C. (1973). "Morphogenesis and ultrastructure of respiratory syncytial virus." J Virol **12**(5): 1173-1180.

Bakker, S.E.; Duquerroy, S.; Galloux, M.; Loney, C.; Conner, E.; Eleouet, J.F.; Rey, F.A. and Bhella, D. (2013). "The respiratory syncytial virus nucleoprotein-RNA complex forms a left-handed helical nucleocapsid." J Gen Virol **94**(Pt 8): 1734-1738.

Barik, S. (2013). "Respiratory syncytial virus mechanisms to interfere with type 1 interferons." Curr Top Microbiol Immunol **372**: 173-191.

Barton, L.L.; Grant, K.L. and Lemen, R.J. (2001). "Respiratory syncytial virus immune globulin: decisions and costs." Pediatr Pulmonol **32**(1): 20-28.

Bates, J.T.; Keefer, C.J.; Slaughter, J.C.; Kulp, D.W.; Schief, W.R. and Crowe, J.E., Jr. (2014). "Escape from neutralization by the respiratory syncytial virus-specific neutralizing monoclonal antibody palivizumab is driven by changes in on-rate of binding to the fusion protein." Virology **454-455**: 139-144.

Bates, J.T.; Keefer, C.J.; Utley, T.J.; Correia, B.E.; Schief, W.R. and Crowe, J.E., Jr. (2013). "Reversion of somatic mutations of the respiratory syncytial virus-specific human monoclonal antibody Fab19 reveal a direct relationship between association rate and neutralizing potency." J Immunol **190**(7): 3732-3739.

Beeler, J.A. and van Wyke Coelingh, K. (1989). "Neutralization epitopes of the F glycoprotein of respiratory syncytial virus: effect of mutation upon fusion function." J Virol **63**(7): 2941-2950.

Belderbos, M.E.; Houben, M.L.; Wilbrink, B.; Lentjes, E.; Bloemen, E.M.; Kimpen, J.L.; Rovers, M. and Bont, L. (2011). "Cord blood vitamin D deficiency is associated with respiratory syncytial virus bronchiolitis." Pediatrics **127**(6): e1513-1520.

Bermingham, A. and Collins, P.L. (1999). "The M2-2 protein of human respiratory syncytial virus is a regulatory factor involved in the balance between RNA replication and transcription." Proc Natl Acad Sci U S A **96**(20): 11259-11264.

Bermingham, I.M.; Chappell, K.J.; Watterson, D. and Young, P.R. (2018). "The Heptad Repeat C Domain of the Respiratory Syncytial Virus Fusion Protein Plays a Key Role in Membrane Fusion." J Virol **92**(4).

Bitko, V.; Shulyayeva, O.; Mazumder, B.; Musiyenko, A.; Ramaswamy, M.; Look, D.C. and Barik, S. (2007). "Nonstructural proteins of respiratory syncytial virus suppress premature apoptosis by an NF-kappaB-dependent, interferon-independent mechanism and facilitate virus growth." J Virol **81**(4): 1786-1795.

Blanco, J.C.G.; Pletneva, L.M.; McGinnes-Cullen, L.; Otoa, R.O.; Patel, M.C.; Fernando, L.R.; Boukhvalova, M.S. and Morrison, T.G. (2018). "Efficacy of a respiratory syncytial virus vaccine candidate in a maternal immunization model." Nat Commun **9**(1): 1904.

Boivin, G.; Caouette, G.; Frenette, L.; Carbonneau, J.; Ouakki, M. and De Serres, G. (2008). "Human respiratory syncytial virus and other viral infections in infants receiving palivizumab." J Clin Virol **42**(1): 52-57.

Bolt, G.; Pedersen, L.O. and Birkeslund, H.H. (2000). "Cleavage of the respiratory syncytial virus fusion protein is required for its surface expression: role of furin." Virus Res **68**(1): 25-33.

Boyd, V.; Cholewa, O.M. and Papas, K.K. (2008). "Limitations in the Use of Fluorescein Diacetate/Propidium Iodide (FDA/PI) and Cell Permeable Nucleic Acid Stains for Viability Measurements of Isolated Islets of Langerhans." Curr Trends Biotechnol Pharm **2**(2): 66-84.

Bradley, J.P.; Bacharier, L.B.; Bonfiglio, J.; Schechtman, K.B.; Strunk, R.; Storch, G. and Castro, M. (2005). "Severity of respiratory syncytial virus bronchiolitis is affected by cigarette smoke exposure and atopy." Pediatrics **115**(1): e7-14.

Bradley, J.S.; Connor, J.D.; Compogiannis, L.S. and Eiger, L.L. (1990). "Exposure of health care workers to ribavirin during therapy for respiratory syncytial virus infections." Antimicrob Agents Chemother **34**(4): 668-670.

Branche, A.R. and Falsey, A.R. (2015). "Respiratory syncytial virus infection in older adults: an under-recognized problem." Drugs Aging **32**(4): 261-269.

Buchholz, U.J.; Finke, S. and Conzelmann, K.K. (1999). "Generation of bovine respiratory syncytial virus (BRSV) from cDNA: BRSV NS2 is not essential for virus replication in tissue culture, and the human RSV leader region acts as a functional BRSV genome promoter." J Virol **73**(1): 251-259.

Bukreyev, A.; Camargo, E. and Collins, P.L. (1996). "Recovery of infectious respiratory syncytial virus expressing an additional, foreign gene." J Virol **70**(10): 6634-6641.

Bukreyev, A.; Murphy, B.R. and Collins, P.L. (2000). "Respiratory syncytial virus can tolerate an intergenic sequence of at least 160 nucleotides with little effect on transcription or replication in vitro and in vivo." J Virol **74**(23): 11017-11026.

Bukreyev, A.; Whitehead, S.S.; Murphy, B.R. and Collins, P.L. (1997). "Recombinant respiratory syncytial virus from which the entire SH gene has been deleted grows efficiently in cell culture and exhibits site-specific attenuation in the respiratory tract of the mouse." J Virol **71**(12): 8973-8982.

Bukreyev, A.; Yang, L.; Fricke, J.; Cheng, L.; Ward, J.M.; Murphy, B.R. and Collins, P.L. (2008). "The secreted form of respiratory syncytial virus G glycoprotein helps the virus evade antibody-mediated restriction of replication by acting as an antigen decoy and through effects on Fc receptor-bearing leukocytes." J Virol **82**(24): 12191-12204.

Cameron, R.; Buck, C.; Merrill, D. and Luttick, A. (2003). "Identification of contaminating adenovirus type 1 in the ATCC reference strain of respiratory syncytial virus A2 (VR-1302)." Virus Res **92**(2): 151-156.

Capizzi, A.; Silvestri, M.; Orsi, A.; Cutrera, R.; Rossi, G.A. and Sacco, O. (2017). "The impact of the recent AAP changes in palivizumab authorization on RSV-induced bronchiolitis severity and incidence." Ital J Pediatr **43**(1): 71.

Carbonell-Estrany, X.; Simoes, E.A.; Dagan, R.; Hall, C.B.; Harris, B.; Hultquist, M.; Connor, E.M. and Losonsky, G.A. (2010). "Motavizumab for prophylaxis of respiratory syncytial virus in high-risk children: a noninferiority trial." Pediatrics **125**(1): e35-51.

Carroll, K.N.; Gebretsadik, T.; Minton, P.; Woodward, K.; Liu, Z.; Miller, E.K.; Williams, J.V.; Dupont, W.D. and Hartert, T.V. (2012). "Influence of maternal asthma on the cause and severity of infant acute respiratory tract infections." J Allergy Clin Immunol **129**(5): 1236-1242.

Carter, S.D.; Dent, K.C.; Atkins, E.; Foster, T.L.; Verow, M.; Gorny, P.; Harris, M.; Hiscox, J.A.; Ranson, N.A.; Griffin, S. and Barr, J.N. (2010). "Direct visualization of the small hydrophobic protein of human respiratory syncytial virus reveals the structural basis for membrane permeability." FEBS Lett **584**(13): 2786-2790.

Chaiwatpongsakorn, S.; Epand, R.F.; Collins, P.L.; Epand, R.M. and Peeples, M.E. (2011). "Soluble respiratory syncytial virus fusion protein in the fully cleaved, pretriggered state is triggered by exposure to low-molarity buffer." J Virol **85**(8): 3968-3977.

Chanock, R. and Finberg, L. (1957). "Recovery from infants with respiratory illness of a virus related to chimpanzee coryza agent (CCA). II. Epidemiologic aspects of infection in infants and young children." Am J Hyg **66**(3): 291-300.

Chanock, R.; Roizman, B. and Myers, R. (1957). "Recovery from infants with respiratory illness of a virus related to chimpanzee coryza agent (CCA). I. Isolation, properties and characterization." Am J Hyg **66**(3): 281-290.

Chanock, R.M.; Parrott, R.H.; Vargosko, A.J.; Kapikian, A.Z.; Knight, V. and Johnson, K.M. (1962). "Acute respiratory diseases of viral etiology. IV. Respiratory syncytial virus." Am J Public Health Nations Health **52**: 918-925.

Cheng, X.; Park, H.; Zhou, H. and Jin, H. (2005). "Overexpression of the M2-2 protein of respiratory syncytial virus inhibits viral replication." J Virol **79**(22): 13943-13952.

ClinicalTrials.gov (2018a). "A Study to Explore the Antiviral Activity, Clinical Outcomes, Safety, Tolerability, and Pharmacokinetics of JNJ-53718678 at Two Dose Levels in Non-Hospitalized Adult Participants Infected With Respiratory Syncytial Virus." Retrieved 09 aug 2018, from https://clinicaltrials.gov/ct2/show/NCT03379675?recrs=abdfgh&cond=RSV&rank=37.

ClinicalTrials.gov (2018b). "Viral Inhibition in Children for Treatment of RSV (VICTOR)." Retrieved 09 Aug 2018, 2018, from https://clinicaltrials.gov/ct2/show/NCT02654171.

ClinicalTrials.gov (2018c). "A Long-term Follow-up Study to Evaluate the Impact of Lumicitabine on the Incidence of Asthma and/or Wheezing in Infants and Children With a History of Respiratory Syncytial Virus Infection." Retrieved 09 aug, 2018, from https://clinicaltrials.gov/ct2/show/NCT03332459?recrs=abdf&cond=RSV&rank=28.

Collins, P.; Fearns, R. and Graham, B.S. (2013). Respiratory Syncytial Virus: Virology, Reverse Genetics, and Pathogenesis of Disease. Challenges and Opportunities for Respiratory Syncytial Virus Vaccines. Anderson, L. J. and Graham, B. S.

Collins, P.L.; Camargo, E. and Hill, M.G. (1999). "Support plasmids and support proteins required for recovery of recombinant respiratory syncytial virus." Virology **259**(2): 251-255.

Collins, P.L.; Hill, M.G.; Camargo, E.; Grosfeld, H.; Chanock, R.M. and Murphy, B.R. (1995). "Production of infectious human respiratory syncytial virus from cloned cDNA confirms an essential role for the transcription elongation factor from the 5' proximal open reading frame of the M2 mRNA in gene expression and provides a capability for vaccine development." Proc Natl Acad Sci U S A **92**(25): 11563-11567.

Collins, P.L.; Huang, Y.T. and Wertz, G.W. (1984). "Nucleotide sequence of the gene encoding the fusion (F) glycoprotein of human respiratory syncytial virus." Proc Natl Acad Sci U S A **81**(24): 7683-7687.

Collins, P.L. and Melero, J.A. (2011). "Progress in understanding and controlling respiratory syncytial virus: still crazy after all these years." Virus Res **162**(1-2): 80-99.

Collins, P.L. and Mottet, G. (1991). "Post-translational processing and oligomerization of the fusion glycoprotein of human respiratory syncytial virus." J Gen Virol **72 (Pt 12)**: 3095-3101.

Collins, P.L. and Mottet, G. (1992). "Oligomerization and post-translational processing of glycoprotein G of human respiratory syncytial virus: altered O-glycosylation in the presence of brefeldin A." J Gen Virol **73 (Pt 4)**: 849-863.

Collins, P.L. and Mottet, G. (1993). "Membrane orientation and oligomerization of the small hydrophobic protein of human respiratory syncytial virus." J Gen Virol **74 (Pt 7)**: 1445-1450.

Collins, P.L. and Murphy, B.R. (2007). Respiratory Syncytial Virus. Perspectives in Medical Virology. Cane, P. Amsterdam, Elsevier Science. **1st ed:** 233-277.

Connors, M.; Collins, P.L.; Firestone, C.Y. and Murphy, B.R. (1991). "Respiratory syncytial virus (RSV) F, G, M2 (22K), and N proteins each induce resistance to RSV challenge, but resistance induced by M2 and N proteins is relatively short-lived." J Virol **65**(3): 1634-1637.

Crowe, J.E.; Firestone, C.Y.; Crim, R.; Beeler, J.A.; Coelingh, K.L.; Barbas, C.F.; Burton, D.R.; Chanock, R.M. and Murphy, B.R. (1998). "Monoclonal antibody-resistant mutants selected with a respiratory syncytial virus-neutralizing human antibody fab fragment (Fab 19) define a unique epitope on the fusion (F) glycoprotein." Virology **252**(2): 373-375.

Dell, S.M. and Colliopoulus, J.A. (2001). Section 14 Avicel RC/CL, Microcrystalline Cellulose and Carboxymethylcellulose Sodium, NF, BP, FMC Corporation.

Deval, J.; Hong, J.; Wang, G.; Taylor, J.; Smith, L.K.; Fung, A.; Stevens, S.K.; Liu, H.; Jin, Z.; Dyatkina, N.; Prhavc, M.; Stoycheva, A.D.; Serebryany, V.; Liu, J.; Smith, D.B.; Tam, Y.; Zhang, Q.; Moore, M.L.; Fearns, R.; Chanda, S.M.; Blatt, L.M.; Symons, J.A. and Beigelman, L. (2015). "Molecular Basis for the Selective Inhibition of Respiratory Syncytial Virus RNA Polymerase by 2'-Fluoro-4'-Chloromethyl-Cytidine Triphosphate." PLoS Pathog **11**(6): e1004995.

DeVincenzo, J.P.; Wilkinson, T.; Vaishnaw, A.; Cehelsky, J.; Meyers, R.; Nochur, S.; Harrison, L.; Meeking, P.; Mann, A.; Moane, E.; Oxford, J.; Pareek, R.; Moore, R.; Walsh, E.; Studholme, R.; Dorsett, P.; Alvarez, R. and Lambkin-Williams, R. (2010). "Viral load drives disease in humans experimentally infected with respiratory syncytial virus." Am J Respir Crit Care Med **182**(10): 1305-1314.

Domingo, E.; Menendez-Arias, L. and Holland, J.J. (1997). "RNA virus fitness." Rev Med Virol **7**(2): 87-96.

Domingo, E.; Sheldon, J. and Perales, C. (2012). "Viral quasispecies evolution." Microbiol Mol Biol Rev **76**(2): 159-216.

Domurat, F.; Roberts, N.J., Jr.; Walsh, E.E. and Dagan, R. (1985). "Respiratory syncytial virus infection of human mononuclear leukocytes in vitro and in vivo." J Infect Dis **152**(5): 895-902.

Donalisio, M.; Rusnati, M.; Cagno, V.; Civra, A.; Bugatti, A.; Giuliani, A.; Pirri, G.; Volante, M.; Papotti, M.; Landolfo, S. and Lembo, D. (2012). "Inhibition of human respiratory syncytial virus infectivity by a dendrimeric heparan sulfate-binding peptide." Antimicrob Agents Chemother **56**(10): 5278-5288.

du Prel, J.B.; Puppe, W.; Grondahl, B.; Knuf, M.; Weigl, J.A.; Schaaff, F. and Schmitt, H.J. (2009). "Are meteorological parameters associated with acute respiratory tract infections?" Clin Infect Dis **49**(6): 861-868.

Eisenhut, M. (2006). "Extrapulmonary manifestations of severe RSV bronchiolitis." Lancet **368**(9540): 988.

Ellis, J.A. (2013). Bovine Respiratory Syncytial Virus. Mononegaviruses of Veterinary Importance. Munir, M., CABI International. **1:** 170-184.

Eshaghi, A.; Duvvuri, V.R.; Lai, R.; Nadarajah, J.T.; Li, A.; Patel, S.N.; Low, D.E. and Gubbay, J.B. (2012). "Genetic variability of human respiratory syncytial virus A strains circulating in Ontario: a novel genotype with a 72 nucleotide G gene duplication." PLoS One **7**(3): e32807.

Evangelisti, M.; Cangiano, G.; Nenna, R.; Nicolai, A.; Frassanito, A.; Papasso, S.; Alessandroni, C.; Di Mario, C.; Zambonini, V.; Di Mattia, G.; Moretto, C. and Midulla, F. (2015). "Air pollution and bronchiolitis from 2004 to 2014 in Rome." European Respiratory Journal **46**(suppl 59).

Falsey, A.R. (2007). "Respiratory syncytial virus infection in adults." Semin Respir Crit Care Med **28**(2): 171-181.

Falsey, A.R.; Hennessey, P.A.; Formica, M.A.; Cox, C. and Walsh, E.E. (2005). "Respiratory syncytial virus infection in elderly and high-risk adults." N Engl J Med **352**(17): 1749-1759.

Falsey, A.R.; McElhaney, J.E.; Beran, J.; van Essen, G.A.; Duval, X.; Esen, M.; Galtier, F.; Gervais, P.; Hwang, S.J.; Kremsner, P.; Launay, O.; Leroux-Roels, G.; McNeil, S.A.; Nowakowski, A.; Richardus, J.H.; Ruiz-Palacios, G.; St Rose, S.; Devaster, J.M.; Oostvogels, L.; Durviaux, S. and Taylor, S. (2014). "Respiratory syncytial virus and other respiratory viral infections in older adults with moderate to severe influenza-like illness." J Infect Dis **209**(12): 1873-1881.

Fearns, R. and Deval, J. (2016). "New antiviral approaches for respiratory syncytial virus and other mononegaviruses: Inhibiting the RNA polymerase." Antiviral Res **134**: 63-76.

Fearns, R.; Peeples, M.E. and Collins, P.L. (2002). "Mapping the transcription and replication promoters of respiratory syncytial virus." J Virol **76**(4): 1663-1672.

Fischer, L.; Laib Sampaio, K.; Jahn, G.; Hamprecht, K. and Gohring, K. (2013). "Generation and characterization of a GCV resistant HCMV UL97-mutation and a drug sensitive UL54-mutation." Antiviral Res **100**(3): 575-577.

Flint, S.J.; Enquist, L.W.; Racaniello, V.R. and Skalka, A.M. (2009). Principles of Virology : Molecular Biology. Washington, UNITED STATES, ASM Press.

Flynn, J.A.; Durr, E.; Swoyer, R.; Cejas, P.J.; Horton, M.S.; Galli, J.D.; Cosmi, S.A.; Espeseth, A.S.; Bett, A.J. and Zhang, L. (2016). "Stability Characterization of a Vaccine Antigen Based on the Respiratory Syncytial Virus Fusion Glycoprotein." PLoS One **11**(10): e0164789.

Forbes, M.L.; Kumar, V.R.; Yogev, R.; Wu, X.; Robbie, G.J. and Ambrose, C.S. (2014). "Serum palivizumab level is associated with decreased severity of respiratory syncytial virus disease in high-risk infants." Hum Vaccin Immunother **10**(10): 2789-2794.

Franke, G.; Freihorst, J.; Steinmuller, C.; Verhagen, W.; Hockertz, S. and Lohmann-Matthes, M.L. (1994). "Interaction of alveolar macrophages and respiratory syncytial virus." J Immunol Methods **174**(1-2): 173-184.

Fuentes, S.; Tran, K.C.; Luthra, P.; Teng, M.N. and He, B. (2007). "Function of the respiratory syncytial virus small hydrophobic protein." J Virol **81**(15): 8361-8366.

Fuller, H. and Del Mar, C. (2006). "Immunoglobulin treatment for respiratory syncytial virus infection." Cochrane Database Syst Rev(4): CD004883.

Gan, S.W.; Tan, E.; Lin, X.; Yu, D.; Wang, J.; Tan, G.M.; Vararattanavech, A.; Yeo, C.Y.; Soon, C.H.; Soong, T.W.; Pervushin, K. and Torres, J. (2012). "The small hydrophobic protein of the human respiratory syncytial virus forms pentameric ion channels." J Biol Chem **287**(29): 24671-24689.

Garcia, J.; Garcia-Barreno, B.; Vivo, A. and Melero, J.A. (1993). "Cytoplasmic inclusions of respiratory syncytial virus-infected cells: formation of inclusion bodies in transfected cells that coexpress the nucleoprotein, the phosphoprotein, and the 22K protein." Virology **195**(1): 243-247.

Geerdink, R.J.; Pillay, J.; Meyaard, L. and Bont, L. (2015). "Neutrophils in respiratory syncytial virus infection: A target for asthma prevention." J Allergy Clin Immunol **136**(4): 838-847.

Geskey, J.M.; Thomas, N.J. and Brummel, G.L. (2007). "Palivizumab: a review of its use in the protection of high risk infants against respiratory syncytial virus (RSV)." Biologics: Target and Therapy **1**: 33-43.

Ghildyal, R.; Ho, A. and Jans, D.A. (2006). "Central role of the respiratory syncytial virus matrix protein in infection." FEMS Microbiol Rev **30**(5): 692-705.

Ghildyal, R.; Mills, J.; Murray, M.; Vardaxis, N. and Meanger, J. (2002). "Respiratory syncytial virus matrix protein associates with nucleocapsids in infected cells." J Gen Virol **83**(Pt 4): 753-757.

Gilman, M.S.; Moin, S.M.; Mas, V.; Chen, M.; Patel, N.K.; Kramer, K.; Zhu, Q.; Kabeche, S.C.; Kumar, A.; Palomo, C.; Beaumont, T.; Baxa, U.; Ulbrandt, N.D.; Melero, J.A.; Graham, B.S. and McLellan, J.S. (2015). "Characterization of a Prefusion-Specific Antibody That Recognizes a Quaternary, Cleavage-Dependent Epitope on the RSV Fusion Glycoprotein." PLoS Pathog **11**(7): e1005035.

Graham, B.S.; Modjarrad, K. and McLellan, J.S. (2015). "Novel antigens for RSV vaccines." Curr Opin Immunol **35**: 30-38.

Graham, B.S.; Perkins, M.D.; Wright, P.F. and Karzon, D.T. (1988). "Primary respiratory syncytial virus infection in mice." J Med Virol **26**(2): 153-162.

Griffiths, C.; Drews, S.J. and Marchant, D.J. (2017). "Respiratory Syncytial Virus: Infection, Detection, and New Options for Prevention and Treatment." Clin Microbiol Rev **30**(1): 277-319.

Groskreutz, D.J.; Monick, M.M.; Babor, E.C.; Nyunoya, T.; Varga, S.M.; Look, D.C. and Hunninghake, G.W. (2009). "Cigarette smoke alters respiratory syncytial virus-induced apoptosis and replication." Am J Respir Cell Mol Biol **41**(2): 189-198.

Gupta, C.K.; Leszczynski, J.; Gupta, R.K. and Siber, G.R. (1996). "Stabilization of respiratory syncytial virus (RSV) against thermal inactivation and freeze-thaw cycles for development and control of RSV vaccines and immune globulin." Vaccine **14**(15): 1417-1420.

Gutfraind, A.; Galvani, A.P. and Meyers, L.A. (2015). "Efficacy and optimization of palivizumab injection regimens against respiratory syncytial virus infection." JAMA Pediatr **169**(4): 341-348.

Haber, N. (2018). "Respiratory syncytial virus infection in elderly adults." Med Mal Infect **48**(6): 377-382.

Hahn, S.J.; Ree, T. and Eyring, H. (1959). "Flow Mechanism of Thixotropic Substances." Industrial & Engineering Chemistry **51**(7): 856-857.

Hallak, L.K.; Kwilas, S.A. and Peeples, M.E. (2007). "Interaction between respiratory syncytial virus and glycosaminoglycans, including heparan sulfate." Methods Mol Biol **379**: 15-34.

Hallak, L.K.; Spillmann, D.; Collins, P.L. and Peeples, M.E. (2000). "Glycosaminoglycan sulfation requirements for respiratory syncytial virus infection." J Virol **74**(22): 10508-10513.

Han, L.L.; Alexander, J.P. and Anderson, L.J. (1999). "Respiratory syncytial virus pneumonia among the elderly: an assessment of disease burden." J Infect Dis **179**(1): 25-30.

Herlocher, M.L.; Ewasyshyn, M.; Sambhara, S.; Gharaee-Kermani, M.; Cho, D.; Lai, J.; Klein, M. and Maassab, H.F. (1999). "Immunological properties of plaque purified strains of live attenuated respiratory syncytial virus (RSV) for human vaccine." Vaccine **17**(2): 172-181.

Hewitt, R.; Farne, H.; Ritchie, A.; Luke, E.; Johnston, S.L. and Mallia, P. (2016). "The role of viral infections in exacerbations of chronic obstructive pulmonary disease and asthma." Ther Adv Respir Dis **10**(2): 158-174.

Hicks, S.N.; Chaiwatpongsakorn, S.; Costello, H.M.; McLellan, J.S.; Ray, W. and Peeples, M.E. (2018). "Five Residues in the Apical Loop of the Respiratory Syncytial Virus Fusion Protein F2 Subunit Are Critical for Its Fusion Activity." J Virol **92**(15).

Hierholzer, J.C. and Killington, R.A. (1996). Virus isolation and quantification. Virology Methods Manual, Academic Press. Ltd**:** 37.

Hong, D.; Lee, G.; Jung, N.C. and Jeon, M. (2013). "Fast automated yeast cell counting algorithm using bright-field and fluorescence microscopic images." Biol Proced Online **15**(1): 13.

Hotard, A.L.; Shaikh, F.Y.; Lee, S.; Yan, D.; Teng, M.N.; Plemper, R.K.; Crowe, J.E., Jr. and Moore, M.L. (2012). "A stabilized respiratory syncytial virus reverse genetics system amenable to recombination-mediated mutagenesis." Virology **434**(1): 129-136.

ICTV (2018). "Genus: *Orthopneumovirus*." Retrieved 05 July 2018, 2018, from https://talk.ictvonline.org/ictv-reports/ictv_online_report/negative-sense-rna-viruses/mononegavirales/w/pneumoviridae/738/genus-orthopneumovirus.

Israel, S.; Rusch, S.; DeVincenzo, J.; Boyers, A.; Fok-Seang, J.; Huntjens, D.; Lounis, N.; Mariën, K.; Stevens, M. and Verloes, R. (2016). "Effect of Oral JNJ-53718678 (JNJ-678) on Disease Severity in Healthy Adult Volunteers Experimentally Inoculated With Live Respiratory Syncytial Virus (RSV): A Placebo-Controlled Challenge Study." Open Forum Infectious Diseases **3**(suppl_1): 650-650.

Johnson, J.E.; Gonzales, R.A.; Olson, S.J.; Wright, P.F. and Graham, B.S. (2007). "The histopathology of fatal untreated human respiratory syncytial virus infection." Mod Pathol **20**(1): 108-119.

Johnson, P.R.; Spriggs, M.K.; Olmsted, R.A. and Collins, P.L. (1987). "The G glycoprotein of human respiratory syncytial viruses of subgroups A and B: extensive sequence divergence between antigenically related proteins." Proc Natl Acad Sci U S A **84**(16): 5625-5629.

Johnson, S.; Oliver, C.; Prince, G.A.; Hemming, V.G.; Pfarr, D.S.; Wang, S.C.; Dormitzer, M.; O'Grady, J.; Koenig, S.; Tamura, J.K.; Woods, R.; Bansal, G.; Couchenour, D.; Tsao, E.; Hall, W.C. and Young, J.F. (1997). "Development of a humanized monoclonal antibody (MEDI-493) with potent in vitro and in vivo activity against respiratory syncytial virus." J Infect Dis **176**(5): 1215-1224.

Johnson, T.R.; McLellan, J.S. and Graham, B.S. (2012). "Respiratory syncytial virus glycoprotein G interacts with DC-SIGN and L-SIGN to activate ERK1 and ERK2." J Virol **86**(3): 1339-1347.

Kapikian, A.Z.; Mitchell, R.H.; Chanock, R.M.; Shvedoff, R.A. and Stewart, C.E. (1969). "An epidemiologic study of altered clinical reactivity to respiratory syncytial

(RS) virus infection in children previously vaccinated with an inactivated RS virus vaccine." Am J Epidemiol **89**(4): 405-421.

Karr, C.J.; Rudra, C.B.; Miller, K.A.; Gould, T.R.; Larson, T.; Sathyanarayana, S. and Koenig, J.Q. (2009). "Infant exposure to fine particulate matter and traffic and risk of hospitalization for RSV bronchiolitis in a region with lower ambient air pollution." Environ Res **109**(3): 321-327.

Karron, R.A.; Buonagurio, D.A.; Georgiu, A.F.; Whitehead, S.S.; Adamus, J.E.; Clements-Mann, M.L.; Harris, D.O.; Randolph, V.B.; Udem, S.A.; Murphy, B.R. and Sidhu, M.S. (1997). "Respiratory syncytial virus (RSV) SH and G proteins are not essential for viral replication in vitro: clinical evaluation and molecular characterization of a cold-passaged, attenuated RSV subgroup B mutant." Proc Natl Acad Sci U S A **94**(25): 13961-13966.

Khanna, N.; Widmer, A.F.; Decker, M.; Steffen, I.; Halter, J.; Heim, D.; Weisser, M.; Gratwohl, A.; Fluckiger, U. and Hirsch, H.H. (2008). "Respiratory syncytial virus infection in patients with hematological diseases: single-center study and review of the literature." Clin Infect Dis **46**(3): 402-412.

Kim, H.W.; Canchola, J.G.; Brandt, C.D.; Pyles, G.; Chanock, R.M.; Jensen, K. and Parrott, R.H. (1969). "Respiratory syncytial virus disease in infants despite prior administration of antigenic inactivated vaccine." Am J Epidemiol **89**(4): 422-434.

Kwakkenbos, M.J.; Diehl, S.A.; Yasuda, E.; Bakker, A.Q.; van Geelen, C.M.; Lukens, M.V.; van Bleek, G.M.; Widjojoatmodjo, M.N.; Bogers, W.M.; Mei, H.; Radbruch, A.; Scheeren, F.A.; Spits, H. and Beaumont, T. (2010). "Generation of stable monoclonal antibody-producing B cell receptor-positive human memory B cells by genetic programming." Nat Med **16**(1): 123-128.

Kwon, Y.S.; Park, S.H.; Kim, M.A.; Kim, H.J.; Park, J.S.; Lee, M.Y.; Lee, C.W.; Dauti, S. and Choi, W.I. (2017). "Risk of mortality associated with respiratory syncytial virus and influenza infection in adults." BMC Infect Dis **17**(1): 785.

Lai, C.; Fischer, T. and Munroe, E. (2015). "Homologous recombination using bacterial artificial chromosomes." Cold Spring Harb Protoc **2015**(2): 180-190.

Langedijk, J.P.; de Groot, B.L.; Berendsen, H.J. and van Oirschot, J.T. (1998). "Structural homology of the central conserved region of the attachment protein G of respiratory syncytial virus with the fourth subdomain of 55-kDa tumor necrosis factor receptor." Virology **243**(2): 293-302.

Lapena, S.; Robles, M.B.; Castanon, L.; Martinez, J.P.; Reguero, S.; Alonso, M.P. and Fernandez, I. (2005). "Climatic factors and lower respiratory tract infection due to respiratory syncytial virus in hospitalised infants in northern Spain." Eur J Epidemiol **20**(3): 271-276.

Larios Mora, A.; Detalle, L.; Gallup, J.M.; Van Geelen, A.; Stohr, T.; Duprez, L. and Ackermann, M.R. (2018). "Delivery of ALX-0171 by inhalation greatly reduces respiratory syncytial virus disease in newborn lambs." MAbs **10**(5): 778-795.

Lavoie, P.M.; Solimano, A.; Taylor, R.; Kwan, E.; Claydon, J.; Turvey, S.E. and Marr, N. (2016). "Outcomes of Respiratory Syncytial Virus Immunoprophylaxis in Infants Using an Abbreviated Dosing Regimen of Palivizumab." JAMA Pediatr **170**(2): 174-176.

Lawlor, H.A.; Schickli, J.H. and Tang, R.S. (2013). "A single amino acid in the F2 subunit of respiratory syncytial virus fusion protein alters growth and fusogenicity." J Gen Virol **94**(Pt 12): 2627-2635.

Levine, S.; Peeples, M. and Hamilton, R. (1977). "Effect of respiratory syncytial virus infection of HeLa-cell macromolecular synthesis." J Gen Virol **37**(1): 53-63.

Lewis FA et al. (1961). " A syncytial virus associated with epidemic disease of the lower respiratory tract in infants and young children." Med. J. Aust. **2**: 932-933.

Liesman, R.M.; Buchholz, U.J.; Luongo, C.L.; Yang, L.; Proia, A.D.; DeVincenzo, J.P.; Collins, P.L. and Pickles, R.J. (2014). "RSV-encoded NS2 promotes epithelial cell shedding and distal airway obstruction." J Clin Invest **124**(5): 2219-2233.

Lifland, A.W.; Jung, J.; Alonas, E.; Zurla, C.; Crowe, J.E., Jr. and Santangelo, P.J. (2012). "Human respiratory syncytial virus nucleoprotein and inclusion bodies antagonize the innate immune response mediated by MDA5 and MAVS." J Virol **86**(15): 8245-8258.

Liljeroos, L.; Krzyzaniak, M.A.; Helenius, A. and Butcher, S.J. (2013). "Architecture of respiratory syncytial virus revealed by electron cryotomography." Proc Natl Acad Sci U S A **110**(27): 11133-11138.

Linn, W.S.; Gong, H., Jr.; Anderson, K.R.; Clark, K.W. and Shamoo, D.A. (1995). "Exposures of health-care workers to ribavirin aerosol: a pharmacokinetic study." Arch Environ Health **50**(6): 445-451.

Lopez, J.A.; Bustos, R.; Orvell, C.; Berois, M.; Arbiza, J.; Garcia-Barreno, B. and Melero, J.A. (1998). "Antigenic structure of human respiratory syncytial virus fusion glycoprotein." J Virol **72**(8): 6922-6928.

Lukacs, N.W.; Moore, M.L.; Rudd, B.D.; Berlin, A.A.; Collins, R.D.; Olson, S.J.; Ho, S.B. and Peebles, R.S., Jr. (2006). "Differential immune responses and pulmonary pathophysiology are induced by two different strains of respiratory syncytial virus." Am J Pathol **169**(3): 977-986.

Magro, M.; Andreu, D.; Gomez-Puertas, P.; Melero, J.A. and Palomo, C. (2010). "Neutralization of human respiratory syncytial virus infectivity by antibodies and low-molecular-weight compounds targeted against the fusion glycoprotein." J Virol **84**(16): 7970-7982.

Magro, M.; Mas, V.; Chappell, K.; Vazquez, M.; Cano, O.; Luque, D.; Terron, M.C.; Melero, J.A. and Palomo, C. (2012). "Neutralizing antibodies against the preactive form of respiratory syncytial virus fusion protein offer unique possibilities for clinical intervention." Proc Natl Acad Sci U S A **109**(8): 3089-3094.

Malhotra, R.; Ward, M.; Bright, H.; Priest, R.; Foster, M.R.; Hurle, M.; Blair, E. and Bird, M. (2003). "Isolation and characterisation of potential respiratory syncytial virus receptor(s) on epithelial cells." Microbes Infect **5**(2): 123-133.

Marr, N. and Turvey, S.E. (2012). "Role of human TLR4 in respiratory syncytial virus-induced NF-kappaB activation, viral entry and replication." Innate Immun **18**(6): 856-865.

Matrosovich, M.; Matrosovich, T.; Garten, W. and Klenk, H.D. (2006). "New low-viscosity overlay medium for viral plaque assays." Virol J **3**: 63.

Mazur, N.I.; Higgins, D.; Nunes, M.C.; Melero, J.A.; Langedijk, A.C.; Horsley, N.; Buchholz, U.J.; Openshaw, P.J.; McLellan, J.S.; Englund, J.A.; Mejias, A.; Karron, R.A.; Simoes, E.A.; Knezevic, I.; Ramilo, O.; Piedra, P.A.; Chu, H.Y.; Falsey, A.R.; Nair, H.; Kragten-Tabatabaie, L.; Greenough, A.; Baraldi, E.; Papadopoulos, N.G.; Vekemans, J.; Polack, F.P.; Powell, M.; Satav, A.; Walsh, E.E.; Stein, R.T.; Graham, B.S.; Bont, L.J. and Respiratory Syncytial Virus Network, F. (2018). "The respiratory syncytial virus vaccine landscape: lessons from the graveyard and promising candidates." Lancet Infect Dis.

McKimm-Breschkin, J.L.; Jiang, S.; Hui, D.S.; Beigel, J.H.; Govorkova, E.A. and Lee, N. (2018). "Prevention and treatment of respiratory viral infections: Presentations on antivirals, traditional therapies and host-directed interventions at the 5th ISIRV Antiviral Group conference." Antiviral Res **149**: 118-142.

McLellan, J.S. (2015). "Neutralizing epitopes on the respiratory syncytial virus fusion glycoprotein." Curr Opin Virol **11**: 70-75.

McLellan, J.S.; Chen, M.; Leung, S.; Graepel, K.W.; Du, X.; Yang, Y.; Zhou, T.; Baxa, U.; Yasuda, E.; Beaumont, T.; Kumar, A.; Modjarrad, K.; Zheng, Z.; Zhao, M.; Xia, N.; Kwong, P.D. and Graham, B.S. (2013). "Structure of RSV fusion glycoprotein trimer bound to a prefusion-specific neutralizing antibody." Science **340**(6136): 1113-1117.

McLellan, J.S.; Ray, W.C. and Peeples, M.E. (2013). "Structure and function of respiratory syncytial virus surface glycoproteins." Curr Top Microbiol Immunol **372**: 83-104.

McLellan, J.S.; Yang, Y.; Graham, B.S. and Kwong, P.D. (2011). "Structure of respiratory syncytial virus fusion glycoprotein in the postfusion conformation reveals preservation of neutralizing epitopes." J Virol **85**(15): 7788-7796.

Mehedi, M.; Collins, P.L. and Buchholz, U.J. (2017). "A novel host factor for human respiratory syncytial virus." Commun Integr Biol **10**(3): e1319025.

Mehedi, M.; McCarty, T.; Martin, S.E.; Le Nouen, C.; Buehler, E.; Chen, Y.C.; Smelkinson, M.; Ganesan, S.; Fischer, E.R.; Brock, L.G.; Liang, B.; Munir, S.; Collins, P.L. and Buchholz, U.J. (2016). "Actin-Related Protein 2 (ARP2) and Virus-Induced Filopodia Facilitate Human Respiratory Syncytial Virus Spread." PLoS Pathog **12**(12): e1006062.

Mehta, J.; Walsh, E.E.; Mahadevia, P.J. and Falsey, A.R. (2013). "Risk factors for respiratory syncytial virus illness among patients with chronic obstructive pulmonary disease." COPD **10**(3): 293-299.

Melero, J.A. (2007). Molecular Biology of Human Respiratory Syncytial Virus. Respiratory Syncytial Virus. Cane, P., Elsevier. **14:** 1-42.

Melero, J.A. and Moore, M.L. (2013). "Influence of respiratory syncytial virus strain differences on pathogenesis and immunity." Curr Top Microbiol Immunol **372**: 59-82.

Mitra, R.; Baviskar, P.; Duncan-Decocq, R.R.; Patel, D. and Oomens, A.G. (2012). "The human respiratory syncytial virus matrix protein is required for maturation of viral filaments." J Virol **86**(8): 4432-4443.

Miyairi, I. and DeVincenzo, J.P. (2008). "Human genetic factors and respiratory syncytial virus disease severity." Clin Microbiol Rev **21**(4): 686-703.

Moore, M.L.; Chi, M.H.; Luongo, C.; Lukacs, N.W.; Polosukhin, V.V.; Huckabee, M.M.; Newcomb, D.C.; Buchholz, U.J.; Crowe, J.E., Jr.; Goleniewska, K.; Williams, J.V.; Collins, P.L. and Peebles, R.S., Jr. (2009). "A chimeric A2 strain of respiratory syncytial virus (RSV) with the fusion protein of RSV strain line 19 exhibits enhanced viral load, mucus, and airway dysfunction." J Virol **83**(9): 4185-4194.

Morales, F.; Calder, M.A.; Inglis, J.M.; Murdoch, P.S. and Williamson, J. (1983). "A study of respiratory infections in the elderly to assess the role of respiratory syncytial virus." J Infect **7**(3): 236-247.

Morris, J.A.; Blount, R.E. and Savage, R.E. (1956). "Recovery of Cytopathogenic Agent from Chimpanzees with Goryza." Experimental Biology and Medicine **92**(3): 544-549.

Mousa, J.J.; Kose, N.; Matta, P.; Gilchuk, P. and Crowe, J.E., Jr. (2017). "A novel pre-fusion conformation-specific neutralizing epitope on the respiratory syncytial virus fusion protein." Nat Microbiol **2**: 16271.

Mousa, J.J.; Sauer, M.F.; Sevy, A.M.; Finn, J.A.; Bates, J.T.; Alvarado, G.; King, H.G.; Loerinc, L.B.; Fong, R.H.; Doranz, B.J.; Correia, B.E.; Kalyuzhniy, O.; Wen, X.; Jardetzky, T.S.; Schief, W.R.; Ohi, M.D.; Meiler, J. and Crowe, J.E., Jr. (2016). "Structural basis for nonneutralizing antibody competition at antigenic site II of the respiratory syncytial virus fusion protein." Proc Natl Acad Sci U S A **113**(44): E6849-e6858.

Nair, H.; Nokes, D.J.; Gessner, B.D.; Dherani, M.; Madhi, S.A.; Singleton, R.J.; O'Brien, K.L.; Roca, A.; Wright, P.F.; Bruce, N.; Chandran, A.; Theodoratou, E.; Sutanto, A.; Sedyaningsih, E.R.; Ngama, M.; Munywoki, P.K.; Kartasasmita, C.; Simoes, E.A.; Rudan, I.; Weber, M.W. and Campbell, H. (2010). "Global burden of acute lower respiratory infections due to respiratory syncytial virus in young children: a systematic review and meta-analysis." Lancet **375**(9725): 1545-1555.

Noyola, D.E. and Mandeville, P.B. (2008). "Effect of climatological factors on respiratory syncytial virus epidemics." Epidemiol Infect **136**(10): 1328-1332.

Oertel, M.D. (1996). "RespiGam: an RSV immune globulin." Pediatr Nurs **22**(6): 525-528.

Okiro, E.A.; Ngama, M.; Bett, A.; Cane, P.A.; Medley, G.F. and James Nokes, D. (2008). "Factors associated with increased risk of progression to respiratory syncytial virus-associated pneumonia in young Kenyan children." Trop Med Int Health **13**(7): 914-926.

Olchanski, N.; Hansen, R.N.; Pope, E.; D'Cruz, B.; Fergie, J.; Goldstein, M.; Krilov, L.R.; McLaurin, K.K.; Nabrit-Stephens, B.; Oster, G.; Schaecher, K.; Shaya, F.T.; Neumann, P.J. and Sullivan, S.D. (2018). "Palivizumab Prophylaxis for Respiratory Syncytial Virus: Examining the Evidence Around Value." Open Forum Infect Dis **5**(3): ofy031.

Openshaw, P.J. (2013). "The mouse model of respiratory syncytial virus disease." Curr Top Microbiol Immunol **372**: 359-369.

Pangesti, K.N.A.; Abd El Ghany, M.; Walsh, M.G.; Kesson, A.M. and Hill-Cawthorne, G.A. (2018). "Molecular epidemiology of respiratory syncytial virus." Rev Med Virol **28**(2).

Papenburg, J.; Carbonneau, J.; Hamelin, M.E.; Isabel, S.; Bouhy, X.; Ohoumanne, N.; Dery, P.; Paes, B.A.; Corbeil, J.; Bergeron, M.G.; De Serres, G. and Boivin, G. (2012). "Molecular evolution of respiratory syncytial virus fusion gene, Canada, 2006-2010." Emerg Infect Dis **18**(1): 120-124.

PATH (2018). "RSV Vaccine and mAb Snapshot." Retrieved 03 Aug. 2018, 2018, from https://vaccineresources.org/details.php?i=1562.

Peret, T.C.; Hall, C.B.; Schnabel, K.C.; Golub, J.A. and Anderson, L.J. (1998). "Circulation patterns of genetically distinct group A and B strains of human respiratory syncytial virus in a community." J Gen Virol **79 (Pt 9)**: 2221-2229.

Polack, F.P.; Irusta, P.M.; Hoffman, S.J.; Schiatti, M.P.; Melendi, G.A.; Delgado, M.F.; Laham, F.R.; Thumar, B.; Hendry, R.M.; Melero, J.A.; Karron, R.A.; Collins, P.L. and Kleeberger, S.R. (2005). "The cysteine-rich region of respiratory syncytial virus attachment protein inhibits innate immunity elicited by the virus and endotoxin." Proc Natl Acad Sci U S A **102**(25): 8996-9001.

Prince, G.A.; Horswood, R.L.; Berndt, J.; Suffin, S.C. and Chanock, R.M. (1979). "Respiratory syncytial virus infection in inbred mice." Infect Immun **26**(2): 764-766.

Ramaswamy, M.; Groskreutz, D.J. and Look, D.C. (2009). "Recognizing the importance of respiratory syncytial virus in chronic obstructive pulmonary disease." COPD **6**(1): 64-75.

Resch, B. (2012). "Burden of respiratory syncytial virus infection in young children." World J Clin Pediatr **1**(3): 8-12.

Resch, B. (2014). "Respiratory Syncytial Virus Infection in High-risk Infants - an Update on Palivizumab Prophylaxis." Open Microbiol J **8**: 71-77.

Resch, B. (2017). "Product review on the monoclonal antibody palivizumab for prevention of respiratory syncytial virus infection." Hum Vaccin Immunother **13**(9): 2138-2149.

Rima, B.; Collins, P.; Easton, A.; Fouchier, R.; Kurath, G.; Lamb, R.A.; Lee, B.; Maisner, A.; Rota, P.; Wang, L. and Ictv Report, C. (2017). "ICTV Virus Taxonomy Profile: Pneumoviridae." J Gen Virol **98**(12): 2912-2913.

Rincheval, V.; Lelek, M.; Gault, E.; Bouillier, C.; Sitterlin, D.; Blouquit-Laye, S.; Galloux, M.; Zimmer, C.; Eleouet, J.F. and Rameix-Welti, M.A. (2017). "Functional organization of cytoplasmic inclusion bodies in cells infected by respiratory syncytial virus." Nat Commun **8**(1): 563.

Roberts, S.R.; Compans, R.W. and Wertz, G.W. (1995). "Respiratory syncytial virus matures at the apical surfaces of polarized epithelial cells." J Virol **69**(4): 2667-2673.

Romero, J.R. (2003). "Palivizumab prophylaxis of respiratory syncytial virus disease from 1998 to 2002: results from four years of palivizumab usage." Pediatr Infect Dis J **22**(2 Suppl): S46-54.

Rose, A.S.; Bradley, A.R.; Valasatava, Y.; Duarte, J.M.; Prlić, A. and Rose, P.W. (2018). "NGL viewer: web-based molecular graphics for large complexes." Bioinformatics: bty419-bty419.

Rossey, I.; Gilman, M.S.; Kabeche, S.C.; Sedeyn, K.; Wrapp, D.; Kanekiyo, M.; Chen, M.; Mas, V.; Spitaels, J.; Melero, J.A.; Graham, B.S.; Schepens, B.;

McLellan, J.S. and Saelens, X. (2017). "Potent single-domain antibodies that arrest respiratory syncytial virus fusion protein in its prefusion state." Nat Commun **8**: 14158.

Rossey, I.; McLellan, J.S.; Saelens, X. and Schepens, B. (2018). "Clinical Potential of Prefusion RSV F-specific Antibodies." Trends Microbiol **26**(3): 209-219.

Roymans, D.; Alnajjar, S.S.; Battles, M.B.; Sitthicharoenchai, P.; Furmanova-Hollenstein, P.; Rigaux, P.; Berg, J.V.D.; Kwanten, L.; Ginderen, M.V.; Verheyen, N.; Vranckx, L.; Jaensch, S.; Arnoult, E.; Voorzaat, R.; Gallup, J.M.; Larios-Mora, A.; Crabbe, M.; Huntjens, D.; Raboisson, P.; Langedijk, J.P.; Ackermann, M.R.; McLellan, J.S.; Vendeville, S. and Koul, A. (2017). "Therapeutic efficacy of a respiratory syncytial virus fusion inhibitor." Nat Commun **8**(1): 167.

Ruckwardt, T.J.; Morabito, K.M. and Graham, B.S. (2016). "Determinants of early life immune responses to RSV infection." Curr Opin Virol **16**: 151-157.

Sastre, P.; Melero, J.A.; Garcia-Barreno, B. and Palomo, C. (2005). "Comparison of affinity chromatography and adsorption to vaccinia virus recombinant infected cells for depletion of antibodies directed against respiratory syncytial virus glycoproteins present in a human immunoglobulin preparation." J Med Virol **76**(2): 248-255.

Schlender, J.; Zimmer, G.; Herrler, G. and Conzelmann, K.K. (2003). "Respiratory syncytial virus (RSV) fusion protein subunit F2, not attachment protein G, determines the specificity of RSV infection." J Virol **77**(8): 4609-4616.

Schobel, S.A.; Stucker, K.M.; Moore, M.L.; Anderson, L.J.; Larkin, E.K.; Shankar, J.; Bera, J.; Puri, V.; Shilts, M.H.; Rosas-Salazar, C.; Halpin, R.A.; Fedorova, N.; Shrivastava, S.; Stockwell, T.B.; Peebles, R.S.; Hartert, T.V. and Das, S.R. (2016). "Respiratory Syncytial Virus whole-genome sequencing identifies convergent evolution of sequence duplication in the C-terminus of the G gene." Sci Rep **6**: 26311.

Schwarze, J.; O'Donnell, D.R.; Rohwedder, A. and Openshaw, P.J. (2004). "Latency and persistence of respiratory syncytial virus despite T cell immunity." Am J Respir Crit Care Med **169**(7): 801-805.

Schweitzer, J.W. and Justice, N.A. (2018). "Respiratory Syncytial Virus Infection (RSV)." from https://www.ncbi.nlm.nih.gov/books/NBK459215/.

Shaikh, F.Y. and Crowe, J.E., Jr. (2013). "Molecular mechanisms driving respiratory syncytial virus assembly." Future Microbiol **8**(1): 123-131.

Shcherbo, D.; Merzlyak, E.M.; Chepurnykh, T.V.; Fradkov, A.F.; Ermakova, G.V.; Solovieva, E.A.; Lukyanov, K.A.; Bogdanova, E.A.; Zaraisky, A.G.; Lukyanov, S. and Chudakov, D.M. (2007). "Bright far-red fluorescent protein for whole-body imaging." Nat Methods **4**(9): 741-746.

Shcherbo, D.; Murphy, C.S.; Ermakova, G.V.; Solovieva, E.A.; Chepurnykh, T.V.; Shcheglov, A.S.; Verkhusha, V.V.; Pletnev, V.Z.; Hazelwood, K.L.; Roche, P.M.; Lukyanov, S.; Zaraisky, A.G.; Davidson, M.W. and Chudakov, D.M. (2009). "Far-red fluorescent tags for protein imaging in living tissues." Biochem J **418**(3): 567-574.

Shi, T.; McAllister, D.A.; O'Brien, K.L.; Simoes, E.A.F.; Madhi, S.A.; Gessner, B.D.; Polack, F.P.; Balsells, E.; Acacio, S.; Aguayo, C.; Alassani, I.; Ali, A.; Antonio, M.; Awasthi, S.; Awori, J.O.; Azziz-Baumgartner, E.; Baggett, H.C.; Baillie, V.L.; Balmaseda, A.; Barahona, A.; Basnet, S.; Bassat, Q.; Basualdo, W.; Bigogo, G.; Bont, L.; Breiman, R.F.; Brooks, W.A.; Broor, S.; Bruce, N.; Bruden, D.; Buchy, P.;

Campbell, S.; Carosone-Link, P.; Chadha, M.; Chipeta, J.; Chou, M.; Clara, W.; Cohen, C.; de Cuellar, E.; Dang, D.A.; Dash-Yandag, B.; Deloria-Knoll, M.; Dherani, M.; Eap, T.; Ebruke, B.E.; Echavarria, M.; de Freitas Lazaro Emediato, C.C.; Fasce, R.A.; Feikin, D.R.; Feng, L.; Gentile, A.; Gordon, A.; Goswami, D.; Goyet, S.; Groome, M.; Halasa, N.; Hirve, S.; Homaira, N.; Howie, S.R.C.; Jara, J.; Jroundi, I.; Kartasasmita, C.B.; Khuri-Bulos, N.; Kotloff, K.L.; Krishnan, A.; Libster, R.; Lopez, O.; Lucero, M.G.; Lucion, F.; Lupisan, S.P.; Marcone, D.N.; McCracken, J.P.; Mejia, M.; Moisi, J.C.; Montgomery, J.M.; Moore, D.P.; Moraleda, C.; Moyes, J.; Munywoki, P.; Mutyara, K.; Nicol, M.P.; Nokes, D.J.; Nymadawa, P.; da Costa Oliveira, M.T.; Oshitani, H.; Pandey, N.; Paranhos-Baccala, G.; Phillips, L.N.; Picot, V.S.; Rahman, M.; Rakoto-Andrianarivelo, M.; Rasmussen, Z.A.; Rath, B.A.; Robinson, A.; Romero, C.; Russomando, G.; Salimi, V.; Sawatwong, P.; Scheltema, N.; Schweiger, B.; Scott, J.A.G.; Seidenberg, P.; Shen, K.; Singleton, R.; Sotomayor, V.; Strand, T.A.; Sutanto, A.; Sylla, M.; Tapia, M.D.; Thamthitiwat, S.; Thomas, E.D.; Tokarz, R.; Turner, C.; Venter, M.; Waicharoen, S.; Wang, J.; Watthanaworawit, W.; Yoshida, L.M.; Yu, H.; Zar, H.J.; Campbell, H.; Nair, H. and Network, R.S.V.G.E. (2017). "Global, regional, and national disease burden estimates of acute lower respiratory infections due to respiratory syncytial virus in young children in 2015: a systematic review and modelling study." Lancet **390**(10098): 946-958.

Sigma-Alrich (2018). "Cellulose colloidal, microcrystalline 435244." Retrieved 25 May, 2018, from https://www.sigmaaldrich.com/catalog/product/aldrich/435244?lang=de&region=DE&gclid=EAIaIQobChMIxN-X1vag2wIVCZzVCh0TDAtHEAAYASAAEgIrePD_BwE.

Signet Chemical Corporation (2018). "AVICEL RC / CL, Microcrystalline Cellulose and Carboxymethylcellulose Sodium USP/NF, EP, JPE ". Retrieved 24 May, 2018, from http://www.signetchem.com/product.aspx?prdid=7.

Sirimi, N.; Miligkos, M.; Koutouzi, F.; Petridou, E.; Siahanidou, T. and Michos, A. (2016). "Respiratory syncytial virus activity and climate parameters during a 12-year period." J Med Virol **88**(6): 931-937.

Sommer, C.; Resch, B. and Simoes, E.A. (2011). "Risk factors for severe respiratory syncytial virus lower respiratory tract infection." Open Microbiol J **5**: 144-154.

Sorvillo, F.J.; Huie, S.F.; Strassburg, M.A.; Butsumyo, A.; Shandera, W.X. and Fannin, S.L. (1984). "An outbreak of respiratory syncytial virus pneumonia in a nursing home for the elderly." J Infect **9**(3): 252-256.

Stevens, M.; Rusch, S.; DeVincenzo, J.; Kim, Y.I.; Harrison, L.; Meals, E.A.; Boyers, A.; Fok-Seang, J.; Huntjens, D.; Lounis, N.; Mari, N.K.; Remmerie, B.; Roymans, D.; Koul, A. and Verloes, R. (2018). "Antiviral Activity of Oral JNJ-53718678 in Healthy Adult Volunteers Challenged With Respiratory Syncytial Virus: A Placebo-Controlled Study." J Infect Dis **218**(5): 748-756.

Stobart, C.C.; Hotard, A.L.; Meng, J. and Moore, M.L. (2016). Reverse Genetics of Respiratory Syncytial Virus. Human Respiratory Syncytial Virus: Methods and Protocols. Tripp, R. A. and Jorquera, P. A. New York, NY, Springer New York**:** 141-153.

Stobart, C.C. and Moore, M.L. (2014). "RNA virus reverse genetics and vaccine design." Viruses **6**(7): 2531-2550.

Subramanian, K.N.; Weisman, L.E.; Rhodes, T.; Ariagno, R.; Sanchez, P.J.; Steichen, J.; Givner, L.B.; Jennings, T.L.; Top, F.H., Jr.; Carlin, D. and Connor, E. (1998). "Safety, tolerance and pharmacokinetics of a humanized monoclonal antibody to respiratory syncytial virus in premature infants and infants with bronchopulmonary dysplasia. MEDI-493 Study Group." Pediatr Infect Dis J **17**(2): 110-115.

Sudo, K.; Watanabe, W.; Mori, S.; Konno, K.; Shigeta, S. and Yokota, T. (1999). "Mouse model of respiratory syncytial virus infection to evaluate antiviral activity in vivo." Antivir Chem Chemother **10**(3): 135-139.

Swanson, K.A.; Settembre, E.C.; Shaw, C.A.; Dey, A.K.; Rappuoli, R.; Mandl, C.W.; Dormitzer, P.R. and Carfi, A. (2011). "Structural basis for immunization with postfusion respiratory syncytial virus fusion F glycoprotein (RSV F) to elicit high neutralizing antibody titers." Proc Natl Acad Sci U S A **108**(23): 9619-9624.

Tabatabai, J.; Prifert, C.; Pfeil, J.; Grulich-Henn, J. and Schnitzler, P. (2014). "Novel respiratory syncytial virus (RSV) genotype ON1 predominates in Germany during winter season 2012-13." PLoS One **9**(10): e109191.

Taleb, S.A.; Al Thani, A.A.; Al Ansari, K. and Yassine, H.M. (2018). "Human respiratory syncytial virus: pathogenesis, immune responses, and current vaccine approaches." Eur J Clin Microbiol Infect Dis.

Tan, B.J. (1998). "Respiratory syncytial virus immune globulin intravenous." Paediatr Child Health **3**(1): 11-14.

Tayyari, F.; Marchant, D.; Moraes, T.J.; Duan, W.; Mastrangelo, P. and Hegele, R.G. (2011). "Identification of nucleolin as a cellular receptor for human respiratory syncytial virus." Nat Med **17**(9): 1132-1135.

Techaarpornkul, S.; Barretto, N. and Peeples, M.E. (2001). "Functional analysis of recombinant respiratory syncytial virus deletion mutants lacking the small hydrophobic and/or attachment glycoprotein gene." J Virol **75**(15): 6825-6834.

Techaarpornkul, S.; Collins, P.L. and Peeples, M.E. (2002). "Respiratory syncytial virus with the fusion protein as its only viral glycoprotein is less dependent on cellular glycosaminoglycans for attachment than complete virus." Virology **294**(2): 296-304.

The IMpact-RSV Study Group (1998). "Palivizumab, a humanized respiratory syncytial virus monoclonal antibody, reduces hospitalization from respiratory syncytial virus infection in high-risk infants. The IMpact-RSV Study Group." Pediatrics **102**(3 Pt 1): 531-537.

Tian, S. (2009). "A 20 Residues Motif Delineates the Furin Cleavage Site and its Physical Properties May Influence Viral Fusion." Biochemistry Insights **2**: BCI.S2049.

Tian, S.; Huang, Q.; Fang, Y. and Wu, J. (2011). "FurinDB: A database of 20-residue furin cleavage site motifs, substrates and their associated drugs." Int J Mol Sci **12**(2): 1060-1065.

Tischer, B.K.; Smith, G.A. and Osterrieder, N. (2010). "En passant mutagenesis: a two step markerless red recombination system." Methods Mol Biol **634**: 421-430.

Tischer, B.K.; von Einem, J.; Kaufer, B. and Osterrieder, N. (2006). "Two-step red-mediated recombination for versatile high-efficiency markerless DNA manipulation in Escherichia coli." Biotechniques **40**(2): 191-197.

Tripp, R.A.; Jones, L.P.; Haynes, L.M.; Zheng, H.; Murphy, P.M. and Anderson, L.J. (2001). "CX3C chemokine mimicry by respiratory syncytial virus G glycoprotein." Nat Immunol **2**(8): 732-738.

Turner, T.L.; Kopp, B.T.; Paul, G.; Landgrave, L.C.; Hayes, D., Jr. and Thompson, R. (2014). "Respiratory syncytial virus: current and emerging treatment options." Clinicoecon Outcomes Res **6**: 217-225.

Ulloa, L.; Serra, R.; Asenjo, A. and Villanueva, N. (1998). "Interactions between cellular actin and human respiratory syncytial virus (HRSV)." Virus Res **53**(1): 13-25.

Utokaparch, S.; Marchant, D.; Gosselink, J.V.; McDonough, J.E.; Thomas, E.E.; Hogg, J.C. and Hegele, R.G. (2011). "The relationship between respiratory viral loads and diagnosis in children presenting to a pediatric hospital emergency department." Pediatr Infect Dis J **30**(2): e18-23.

van Drunen Littel-van den Hurk, S. and Watkiss, E.R. (2012). "Pathogenesis of respiratory syncytial virus." Curr Opin Virol **2**(3): 300-305.

Van Heeke, G.; Allosery, K.; De Brabandere, V.; De Smedt, T.; Detalle, L. and de Fougerolles, A. (2017). "Nanobodies(R) as inhaled biotherapeutics for lung diseases." Pharmacol Ther **169**: 47-56.

Vandini, S.; Biagi, C. and Lanari, M. (2017). "Respiratory Syncytial Virus: The Influence of Serotype and Genotype Variability on Clinical Course of Infection." Int J Mol Sci **18**(8).

Varga, S.M. and Braciale, T.J. (2013). The Adaptive Immune Response to Respiratory Syncytial Virus. Challenges and Opportunities for Respiratory Syncytial Virus Vaccines. Anderson, L. J. and Graham, B. S. **372:** 155-172.

Volling, C.; Hassan, K.; Mazzulli, T.; Green, K.; Al-Den, A.; Hunter, P.; Mangat, R.; Ng, J. and McGeer, A. (2014). "Respiratory syncytial virus infection-associated hospitalization in adults: a retrospective cohort study." BMC Infect Dis **14**(1): 665.

Wang, G.; Deval, J.; Hong, J.; Dyatkina, N.; Prhavc, M.; Taylor, J.; Fung, A.; Jin, Z.; Stevens, S.K.; Serebryany, V.; Liu, J.; Zhang, Q.; Tam, Y.; Chanda, S.M.; Smith, D.B.; Symons, J.A.; Blatt, L.M. and Beigelman, L. (2015). "Discovery of 4'-chloromethyl-2'-deoxy-3',5'-di-O-isobutyryl-2'-fluorocytidine (ALS-8176), a first-in-class RSV polymerase inhibitor for treatment of human respiratory syncytial virus infection." J Med Chem **58**(4): 1862-1878.

Ward, C.; Maselko, M.; Lupfer, C.; Prescott, M. and Pastey, M.K. (2017). "Interaction of the Human Respiratory Syncytial Virus matrix protein with cellular adaptor protein complex 3 plays a critical role in trafficking." PLoS One **12**(10): e0184629.

Wasserman, R.L.; Greener, B.N. and Mond, J. (2017). "RI-002, an intravenous immunoglobulin containing high titer neutralizing antibody to RSV and other respiratory viruses for use in primary immunodeficiency disease and other immune compromised populations." Expert Rev Clin Immunol **13**(12): 1107-1119.

Wasserman, R.L.; Lumry, W.; Harris, J., 3rd; Levy, R.; Stein, M.; Forbes, L.; Cunningham-Rundles, C.; Melamed, I.; Kobayashi, A.L.; Du, W. and Kobayashi, R. (2016). "Efficacy, Safety, and Pharmacokinetics of a New 10 % Liquid Intravenous Immunoglobulin Containing High Titer Neutralizing Antibody to RSV and Other

Respiratory Viruses in Subjects with Primary Immunodeficiency Disease." J Clin Immunol **36**(6): 590-599.

Weber, M.W.; Milligan, P.; Hilton, S.; Lahai, G.; Whittle, H.; Mulholland, E.K. and Greenwood, B.M. (1999). "Risk factors for severe respiratory syncytial virus infection leading to hospital admission in children in the Western Region of The Gambia." Int J Epidemiol **28**(1): 157-162.

Weinberger, D.M.; Warren, J.L.; Steiner, C.A.; Charu, V.; Viboud, C. and Pitzer, V.E. (2015). "Reduced-Dose Schedule of Prophylaxis Based on Local Data Provides Near-Optimal Protection Against Respiratory Syncytial Virus." Clin Infect Dis **61**(4): 506-514.

Welliver, R.C., Sr.; Checchia, P.A.; Bauman, J.H.; Fernandes, A.W.; Mahadevia, P.J. and Hall, C.B. (2010). "Fatality rates in published reports of RSV hospitalizations among high-risk and otherwise healthy children." Curr Med Res Opin **26**(9): 2175-2181.

Welliver, T.P.; Reed, J.L. and Welliver, R.C., Sr. (2008). "Respiratory syncytial virus and influenza virus infections: observations from tissues of fatal infant cases." Pediatr Infect Dis J **27**(10 Suppl): S92-96.

Widjaja, I.; Rigter, A.; Jacobino, S.; van Kuppeveld, F.J.; Leenhouts, K.; Palomo, C.; Melero, J.A.; Leusen, J.H.; Haijema, B.J.; Rottier, P.J. and de Haan, C.A. (2015). "Recombinant Soluble Respiratory Syncytial Virus F Protein That Lacks Heptad Repeat B, Contains a GCN4 Trimerization Motif and Is Not Cleaved Displays Prefusion-Like Characteristics." PLoS One **10**(6): e0130829.

Wright, M. and Piedimonte, G. (2011). "Respiratory syncytial virus prevention and therapy: past, present, and future." Pediatr Pulmonol **46**(4): 324-347.

Wu, S.J.; Schmidt, A.; Beil, E.J.; Day, N.D.; Branigan, P.J.; Liu, C.; Gutshall, L.L.; Palomo, C.; Furze, J.; Taylor, G.; Melero, J.A.; Tsui, P.; Del Vecchio, A.M. and Kruszynski, M. (2007). "Characterization of the epitope for anti-human respiratory syncytial virus F protein monoclonal antibody 101F using synthetic peptides and genetic approaches." J Gen Virol **88**(Pt 10): 2719-2723.

Wu, W.; Munday, D.C.; Howell, G.; Platt, G.; Barr, J.N. and Hiscox, J.A. (2011). "Characterization of the interaction between human respiratory syncytial virus and the cell cycle in continuous cell culture and primary human airway epithelial cells." J Virol **85**(19): 10300-10309.

Xia, Q.; Zhou, L.; Peng, C.; Hao, R.; Ni, K.; Zang, N.; Ren, L.; Deng, Y.; Xie, X.; He, L.; Tian, D.; Wang, L.; Huang, A.; Zhao, Y.; Zhao, X.; Fu, Z.; Tu, W. and Liu, E. (2014). "Detection of respiratory syncytial virus fusion protein variants between 2009 and 2012 in China." Arch Virol **159**(5): 1089-1098.

Xin, Y.; Weng, W.; Murray, B.P.; Eisenberg, E.J.; Chien, J.W.; Ling, J. and Silverman, J.A. (2018). "The Drug-Drug Interaction Profile of Presatovir." J Clin Pharmacol **58**(6): 771-780.

Yasui, Y.; Yamaji, Y.; Sawada, A.; Ito, T. and Nakayama, T. (2016). "Cell fusion assay by expression of respiratory syncytial virus (RSV) fusion protein to analyze the mutation of palivizumab-resistant strains." J Virol Methods **231**: 48-55.

Young, J. (2002). "Development of a potent respiratory syncytial virus-specific monoclonal antibody for the prevention of serious lower respiratory tract disease in infants." Respir Med **96 Suppl B**: S31-35.

Yu, D.; Ellis, H.M.; Lee, E.C.; Jenkins, N.A.; Copeland, N.G. and Court, D.L. (2000). "An efficient recombination system for chromosome engineering in Escherichia coli." Proc Natl Acad Sci U S A **97**(11): 5978-5983.

Yunus, A.S.; Jackson, T.P.; Crisafi, K.; Burimski, I.; Kilgore, N.R.; Zoumplis, D.; Allaway, G.P.; Wild, C.T. and Salzwedel, K. (2010). "Elevated temperature triggers human respiratory syncytial virus F protein six-helix bundle formation." Virology **396**(2): 226-237.

Zhang, L.; Peeples, M.E.; Boucher, R.C.; Collins, P.L. and Pickles, R.J. (2002). "Respiratory syncytial virus infection of human airway epithelial cells is polarized, specific to ciliated cells, and without obvious cytopathology." J Virol **76**(11): 5654-5666.

Zhang, X.L.; Shao, X.J.; Wang, J. and Guo, W.L. (2013). "Temporal characteristics of respiratory syncytial virus infection in children and its correlation with climatic factors at a public pediatric hospital in Suzhou." J Clin Virol **58**(4): 666-670.

Zhao, X.; Chen, F.P.; Megaw, A.G. and Sullender, W.M. (2004). "Variable resistance to palivizumab in cotton rats by respiratory syncytial virus mutants." J Infect Dis **190**(11): 1941-1946.

Zhao, X.; Chen, F.P. and Sullender, W.M. (2004). "Respiratory syncytial virus escape mutant derived in vitro resists palivizumab prophylaxis in cotton rats." Virology **318**(2): 608-612.

Zhao, X.; Liu, E.; Chen, F.P. and Sullender, W.M. (2006). "In vitro and in vivo fitness of respiratory syncytial virus monoclonal antibody escape mutants." J Virol **80**(23): 11651-11657.

Zhu, Q.; McAuliffe, J.M.; Patel, N.K.; Palmer-Hill, F.J.; Yang, C.F.; Liang, B.; Su, L.; Zhu, W.; Wachter, L.; Wilson, S.; MacGill, R.S.; Krishnan, S.; McCarthy, M.P.; Losonsky, G.A. and Suzich, J.A. (2011). "Analysis of respiratory syncytial virus preclinical and clinical variants resistant to neutralization by monoclonal antibodies palivizumab and/or motavizumab." J Infect Dis **203**(5): 674-682.

Zhu, Q.; McLellan, J.S.; Kallewaard, N.L.; Ulbrandt, N.D.; Palaszynski, S.; Zhang, J.; Moldt, B.; Khan, A.; Svabek, C.; McAuliffe, J.M.; Wrapp, D.; Patel, N.K.; Cook, K.E.; Richter, B.W.M.; Ryan, P.C.; Yuan, A.Q. and Suzich, J.A. (2017). "A highly potent extended half-life antibody as a potential RSV vaccine surrogate for all infants." Sci Transl Med **9**(388).

Zhu, Q.; Patel, N.K.; McAuliffe, J.M.; Zhu, W.; Wachter, L.; McCarthy, M.P. and Suzich, J.A. (2012). "Natural polymorphisms and resistance-associated mutations in the fusion protein of respiratory syncytial virus (RSV): effects on RSV susceptibility to palivizumab." J Infect Dis **205**(4): 635-638.

Zimmer, G.; Budz, L. and Herrler, G. (2001). "Proteolytic activation of respiratory syncytial virus fusion protein. Cleavage at two furin consensus sequences." J Biol Chem **276**(34): 31642-31650.

Zimmer, G.; Conzelmann, K.K. and Herrler, G. (2002). "Cleavage at the furin consensus sequence RAR/KR(109) and presence of the intervening peptide of the

respiratory syncytial virus fusion protein are dispensable for virus replication in cell culture." J Virol **76**(18): 9218-9224.

Zimmer, G.; Trotz, I. and Herrler, G. (2001). "N-glycans of F protein differentially affect fusion activity of human respiratory syncytial virus." J Virol **75**(10): 4744-4751.

Appendix 1: The F-sequence on the bacterial artificial chromosome pSynkRSV-l19F is depicted. All mutations that were characterized in this work are highlighted in yellow for those that were identified in clinical isolates and in pink for those that served as resistant and sensitive control. Primers used for sequencing are illustrated with black arrows. Since the annealing position of the reverse primer 2R is located downstream of the stop codon in F, this primer is not presented here.

```
   Part of primer 1F
  ---------->
atg gag ttg cca atc ctc aaa gca aat gca att acc aca atc ctc gct gca gtc aca ttt  < 60
M   E   L   P   I   L   K   A   N   A   I   T   T   I   L   A   A   V   T   F     20
            10          20          30          40          50
C21G                                            Q34R
tgc ttt gct tct agt caa aac atc act gaa gaa ttt tat caa tca aca tgc agt gca gtt  <120
C   F   A   S   S   Q   N   I   T   E   E   F   Y   Q   S   T   C   S   A   V     40
            70          80          90          100         110
                                R49K
agc aaa ggc tat ctt agt gct cta aga act ggt tgg tat act agt gtt ata act ata gaa  <180
S   K   G   Y   L   S   A   L   R   T   G   W   Y   T   S   V   I   T   I   E     60
            130         140         150         160         170

tta agt aat atc aag aaa aat aag tgt aat gga aca gat gct aag gta aaa ttg atg aaa  <240
L   S   N   I   K   K   N   K   C   N   G   T   D   A   K   V   K   L   M   K     80
            190         200         210         220         230
                                                                    T100S
caa gaa tta gat aaa tat aaa aat gct gta aca gaa ttg cag ttg ctc atg caa agc aca  <300
Q   E   L   D   K   Y   K   N   A   V   T   E   L   Q   L   L   M   Q   S   T     100
            250         260         270         280         290
        A103P
cca gca gca aac aat cga gcc aga aga gaa cta cca agg ttt atg aat tat aca ctc aac  <360
P   A   A   N   N   R   A   R   R   E   L   P   R   F   M   N   Y   T   L   N     120
            310         320         330         340         350

aat acc aaa aaa acc aat gta aca tta agc aag aaa agg aaa aga aga ttt ctt ggt ttt  <420
N   T   K   K   T   N   V   T   L   S   K   K   R   K   R   R   F   L   G   F     140
            370         380         390         400         410

ttg tta ggt gtt gga tct gca atc gcc agt ggc att gct gta tct aag gtc ctg cac tta  <480
L   L   G   V   G   S   A   I   A   S   G   I   A   V   S   K   V   L   H   L     160
            430         440         450         460         470

gaa gga gaa gtg aac aag atc aaa agt gct cta cta tcc aca aac aag gcc gta gtc agc  <540
E   G   E   V   N   K   I   K   S   A   L   L   S   T   N   K   A   V   V   S     180
            490         500         510         520         530
                      primer 190R     primer 4F
tta tca aat gga gtt agt gtc tta acc agc aga gtg tta gac ctc aaa aac tat ata gat  <600
L   S   N   G   V   S   V   L   T   S   R   V   L   D   L   K   N   Y   I   D     200
            550         560         570         580         590
  <----------                        ---------->
aaa caa ttg tta cct att gtg aat aag caa agc tgc aga ata tca aat ata gaa act gtg  <660
K   Q   L   L   P   I   V   N   K   Q   S   C   R   I   S   N   I   E   T   V     220
            610         620         630         640         650

ata gag ttc caa caa aag aac aac aga cta cta gag att acc agg gaa ttt agt gtt aat  <720
I   E   F   Q   Q   K   N   N   R   L   L   E   I   T   R   E   F   S   V   N     240
            670         680         690         700         710

gca ggt gta act aca cct gta agc act tac atg tta act aat agt gaa tta ttg tca tta  <780
A   G   V   T   T   P   V   S   T   Y   M   L   T   N   S   E   L   L   S   L     260
            730         740         750         760         770
```

```
                                                K272E                   N276S
atc aat gat atg cct ata aca aat gat cag aaa aag tta atg tcc aac aat gtt caa ata  <840
I   N   D   M   P   I   T   N   D   Q   K   K   L   M   S   N   N   V   Q   I    280
            790         800         810         820         830

gtt aga cag caa agt tac tct atc atg tcc ata ata aaa gag gaa gtc tta gca tat gta  <900
V   R   Q   Q   S   Y   S   I   M   S   I   I   K   E   E   V   L   A   Y   V    300
            850         860         870         880         890

gta caa tta cca cta tat ggt gtg ata gat aca cct tgt tgg aaa tta cac aca tcc cct  <960
V   Q   L   P   L   Y   G   V   I   D   T   P   C   W   K   L   H   T   S   P    320
            910         920         930         940         950

cta tgt aca acc aac aca aaa gaa ggg tca aac atc tgt tta aca aga act gac aga gga  <1020
L   C   T   T   N   T   K   E   G   S   N   I   C   L   T   R   T   D   R   G    340
            970         980         990         1000        1010

tgg tac tgt gac aat gca gga tca gta tct ttc ttc cca caa gct gaa aaa tgt aaa gtt  <1080
W   Y   C   D   N   A   G   S   V   S   F   F   P   Q   A   E   K   C   K   V    360
            1030        1040        1050        1060        1070

caa tcg aat cga gta ttt tgt gac aca atg tac agt tta aca tta cca agt gaa gta aat  <1140
Q   S   N   R   V   F   C   D   T   M   Y   S   L   T   L   P   S   E   V   N    380
            1090        1100        1110        1120        1130
                                                                primer 5F
ctc tgc aat gtt gac ata ttc aat ccc aaa tat gat tgt aaa att atg act tca aaa aca  <1200
L   C   N   V   D   I   F   N   P   K   Y   D   C   K   I   M   T   S   K   T    400
            1150        1160        1170        1180        1190

gat gta agc agc tcc gtt atc aca tct cta gga gcc att gtg tca tgc tat ggc aaa act  <1260
D   V   S   S   S   V   I   T   S   L   G   A   I   V   S   C   Y   G   K   T    420
            1210        1220        1230        1240        1250

aaa tgt aca gca tcc aat aaa aat cgt gga atc ata aag aca ttt tct aac ggg tgt gat  <1320
K   C   T   A   S   N   K   N   R   G   I   I   K   T   F   S   N   G   C   D    440
            1270        1280        1290        1300        1310

tat gta tca aat aaa ggg gtg gac act gtg tct gta ggt aac aca tta tat tat gta aat  <1380
Y   V   S   N   K   G   V   D   T   V   S   V   G   N   T   L   Y   Y   V   N    460
            1330        1340        1350        1360        1370

aag caa gaa ggc aaa agt ctc tat gta aaa ggt gaa cca ata ata aat ttc tat gac cca  <1440
K   Q   E   G   K   S   L   Y   V   K   G   E   P   I   I   N   F   Y   D   P    480
            1390        1400        1410        1420        1430

tta gta ttc ccc tct gat gaa ttt gat gca tca ata tct caa gtc aat gag aag att aac  <1500
L   V   F   P   S   D   E   F   D   A   S   I   S   Q   V   N   E   K   I   N    500
            1450        1460        1470        1480        1490
                                                            A518V
cag agt tta gca ttt att cgt aaa tcc gat gaa tta tta cat aat gta aat gct ggt aaa  <1560
Q   S   L   A   F   I   R   K   S   D   E   L   L   H   N   V   N   A   G   K    520
            1510        1520        1530        1540        1550

tca acc aca aat atc atg ata act act ata att ata gtg att ata gta ata ttg tta tca  <1620
S   T   T   N   I   M   I   T   T   I   I   I   V   I   I   V   I   L   L   S    540
            1570        1580        1590        1600        1610
                                    C550Y
tta att gct gtt gga ctg ctc cta tac tgt aag gcc aga agc aca cca atc aca cta agc  <1680
L   I   A   V   G   L   L   L   Y   C   K   A   R   S   T   P   I   T   L   S    560
            1630        1640        1650        1660        1670

aag gat caa ctg agt ggt ata aat aat att gca ttt agt aac tga  < 1725
K   D   Q   L   S   G   I   N   N   I   A   F   S   N   *
            1690        1700        1710        1720
```